Stratigraphic architecture of a Paleoproterozoic iron formation depositional system: the Gunflint, Mesabi and Cuyuna iron ranges

by

Peir Kenneth Pufahl ©

A thesis submitted in partial
fulfillment of the requirements for
the degree of Masters of Science

Lakehead University, Thunder Bay, Ont.

November, 1996

ABSTRACT

Understanding iron formation depositional processes has been hindered by the lack of precise modern analogues. However, by combining a regional basin analysis of sedimentary and volcanic rocks surrounding an iron formation with detailed examination of sedimentary structures and lithic associations within an iron formation, the depositional setting and physical processes of sedimentation can be inferred (Fralick and Barrett, 1995). This technique departs significantly from previous methods used for interpreting iron formation sedimentological environments. Instead of focusing on their mineralogy, the description of iron-bearing formations and members, and the erection of stratotypes the basis of this method is the application of Walther's Law and the facies model concept to large scale depositional tracts, up to and including the entire basin (Miall, 1984).

Three Paleoprotoerozoic iron formations from the Lake Superior region were investigated using this approach. The Gunflint, Biwabik, and Trommald iron formations are correlative ferruginous units from the Animikie and North Range Groups along the north shore of Lake Superior in Ontario and Minnesota. Two clastic, two volcaniclastic, nine chemical sedimentary, and two cryptalgal facies are present: clast and matrix supported pebble conglomerate, massive quartz sandstone, slate, lapilli tuff, massive and/or cross stratified chert-carbonate grainstone, massive and/or cross stratified hematite-rich grainstone, massive chert-carbonate grainstone with rip up clasts, flaser bedded chert-carbonate grainstone, wavy bedded chert-carbonate grainstone, hummocky cross-stratified chert grainstone, parallel and wavy laminated chemical slate interbedded with chert grainstone, parallel and wavy laminated chemical slate, stromatolites, and oncolites. Chemical sedimentary facies may be grouped into associations comprising seven informal stratigraphic members.

Lateral and vertical facies transitions within these members are similar to many Phanerozoic marine shelf systems. Like sediments accumulating along the margins of modern oceans, the chemical sedimentary rocks in Ontario and Minnesota also form a sedimentary wedge which fines and thickens from coarse wave reworked, nearshore deposits of the foreshore and shoreface to parallel laminated mudstones of the outer shelf and slope break. One important difference is the absence of a mud dominated inner shelf. This may be the result of the development of "grainstone factories" below fairweather wave base. Grainstone factories are thought to have formed in proximal offshore areas where iron oxide and silica gel actively precipitated, and where currents could rework these chemical precipitates into rip-up grains. They are broadly similar to modern "subtidal carbonate factories". Stratigraphic data also indicates that iron-bearing members are diachronous and that their deposition was governed by five changes in relative sea level and three pulses of volcanism. The final volcanic episode marks the cessation of iron formation accumulation as the depositional system was rapidly overwhelmed with volcaniclastics.

ACKNOWLEDGEMENTS

I would like to thank the staff who assisted me from the drill core repositories in Thunder Bay Ontario, Hibbing Minnesota, Madison Wisconsin, and Marquette Michigan. Without you I couldn't have done it. Thanks also go to Dr. G. Morey and Dr. D. Southwick for allowing me access to drill core housed at the Minnesota Geological Survey.

A special thanks and appreciation are due to Dr. Phil Fralick. His encouragement, time, and enthusiasm were indispensable in the completion of this thesis. Many thanks also go to the professors in the Geology department at Lakehead University for their guidance over the years.

The assistance of Sam Spivak, Reino Viitala, Anne Hammond and Wendy Bourke is much appreciated. Sam provided technical advice when drafting, Anne and Reino prepared countless thin sections, and Wendy always had the key to the computer room.

I would also like to thank Dr. Denver Stone, a good friend to whom I am truly indebted. Denver, thanks for giving a young kid a chance.

Last, but certainly not least, I would like to thank my family and wife Christa. Mom, Dad and Meagan you've always supported me with love and encouragement. Christa you stood behind me with love and reassurance, and pushed me when I needed it. I couldn't have done it without you.

TABLE OF CONTENTS

LIST OF FIGURES

LIST OF TABLES

CHAPTER 1: INTRODUCTION

1.1 Introduction

Paleoproterozoic iron formations host most of the world's iron ore and many other important mineral deposits (Simonson, 1985). Consequently they have been the focus of hundreds of mineralogical, geochemical and sedimentological investigations. However, in spite of this immense amount of data no consensus has ever been reached as to their origins. Some of this controversy stems from a poor understanding of the sedimentological environments in which they accumulated (Simonson, 1985). They were deposited during a unique interval of earth history when grossly different atmospheric and hydrologic conditions prevailed (Cloud, 1973), and therefore lack precise modern analogues (Simonson, 1985; Fralick and Barrett, 1995). Modern subaqueous hot-spring activity has provided clues to understanding the precipitation of iron-rich sediments, but the mineralogy and areal extent of modern deposits is not comparable to the large Paleoproterozoic iron formations deposited during the Earth's early history (Fralick and Barrett, 1995). Detailed petrographic investigations of iron formations have contributed to interpreting the paragenesis of syndepositional, diagenetic and metamorphic mineral assemblages, but they have done little to provide detailed, reliable information regarding iron formation depositional processes. Minerals and textures are commonly altered to secondary assemblages, and when primary

minerals are present theoretical chemical modelling has been limited in its ability to explain their genesis (Fralick and Barrett, 1995). Paleoenvironmental inferences from grain-size distributions in iron formations are also plagued with uncertainty because they are commonly indurated, diagenetically altered, and frequently fine-grained (Simonson, 1985).

Fortunately, these problems can be overcome by combining a regional basin analysis of clastic and volcanic rocks surrounding iron formations with detailed examination of vertical and lateral facies trends within chemical sedimentary successions (Fralick and Barrett, 1995). Associated sedimentary and volcanic rocks provide data on depositional settings. Sedimentary structures and lithic associations within iron formations give information on physical sedimentary processes, and regional basin analysis provides a framework within which to view iron formation genesis (Fralick and Barrett, 1995). Combining these techniques makes paleogeographic reconstruction and depositional modelling possible (Fralick and Barrett, 1995). This is the same approach used by sedimentologists and stratigraphers to reconstruct clastic depositional systems.

The purpose of this thesis is to use these techniques to re-examine the stratigraphy and sedimentology of the Paleoproterozoic iron formations of the Gunflint, Mesabi and Cuyuna iron ranges in Ontario and Minnesota (Fig. 1) in order to gain insight into iron formation depositional processes. Although a great deal of

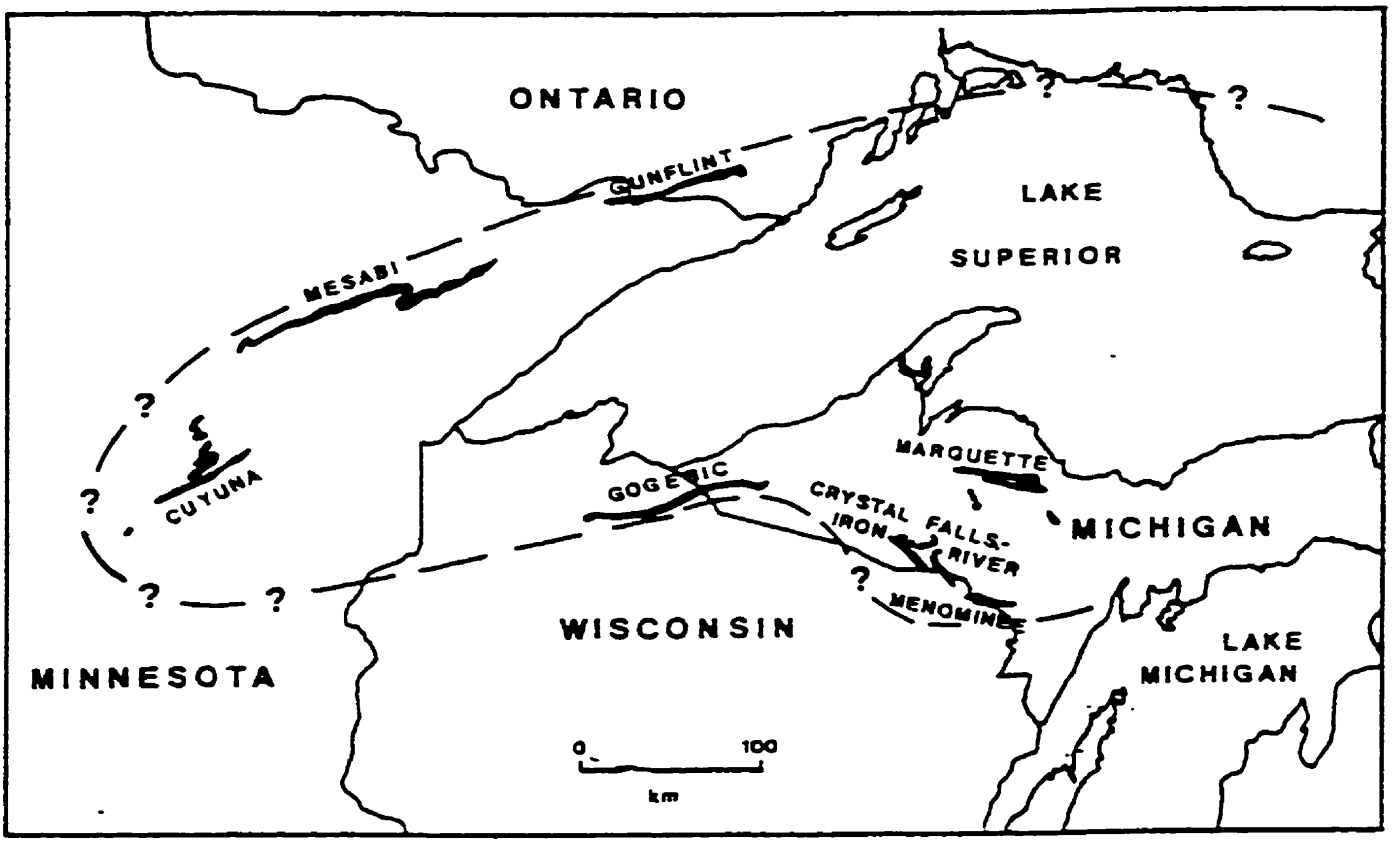

Fig. 1. Generalized geologic map showing location of iron ranges (black) of the Lake Superior region. Dashed line shows out crop area of rocks deposited in the Animikie Basin. From Ojakangas (1983).

stratigraphic and structural data has been amassed for these chemical sedimentary rocks a comprehensive investigation using modern basin analysis techniques can provide important information on how system tracts responsible for their genesis are organized. This region is especially well suited for a detailed investigation because there is an abundance of drill hole data, stratigraphic relations are well known, and the majority of strata are generally flat lying and structurally uncomplicated.

Four conceptually unified ideas are the focus of this study: 1) to develop a facies nomenclature for iron formations in Ontario and Minnesota (Chapter 2), 2) use this facies categorization for a detailed stratigraphic and sedimentological investigation of the Gunflint iron formation in Ontario (Chapters 3 and 4), 3) apply knowledge gained on iron formation depositional processes from this detailed study to re-evaluate the stratigraphy and sedimentology of iron formations in the Mesabi and Cuyuna iron ranges (Chapters 5 and 6), and 4) to use this information to acquire insight into the stratigraphic architecture of Paleoproterozoic, iron formation depositional systems in the Lake Superior region (Chapter 7).

1.2 Location

The Paleoproterozoic iron formations in the seven iron ranges of the Lake

Superior region crop out in east-central and northern Minnesota, adjacent areas in Ontario, northern Wisconsin, and the Upper Peninsula of Michigan as an oval shaped region encompassing 220 000 km^2 (Fig. 1) (Morey, 1983). The term "range" refers to the presence of iron formation within each region. Their deposition occurred in the Animikie Basin (Trendall, 1968), which is located at a major crustal boundary between the Late Archean crust of the Superior province of the Canadian Shield and the approximately penecontemporaneous crust assembled during the Penokean orogeny (Goldich, 1960), 1.85 Ga, in northern Wisconsin and the Upper Peninsula of Michigan. Only detailed descriptions of the Gunflint, Mesabi and Cuyuna iron ranges are given below as these are the only iron ranges considered in this study.

The main portion of the Gunflint iron range extends 170 km northeast from the United States, at Gunflint Lake, to Loon Lake, Ontario (Fig. 2). In Minnesota the Gunflint forms a narrow belt 20 km long which is truncated to the southwest by the Duluth Complex. Erosional remnants 98 km northeast of Thunder Bay at Schreiber, Ontario, suggest a pre-erosional continuation of the chemical sedimentary rocks to the east.

The Mesabi range lies northwest of Lake Superior (Fig. 2). It crops out as a narrow belt 0.40 to 4.8 km wide, that extends east-northeast for 193 km from eastern Cass county through Itasca county to Birch Lake in St. Louis county in

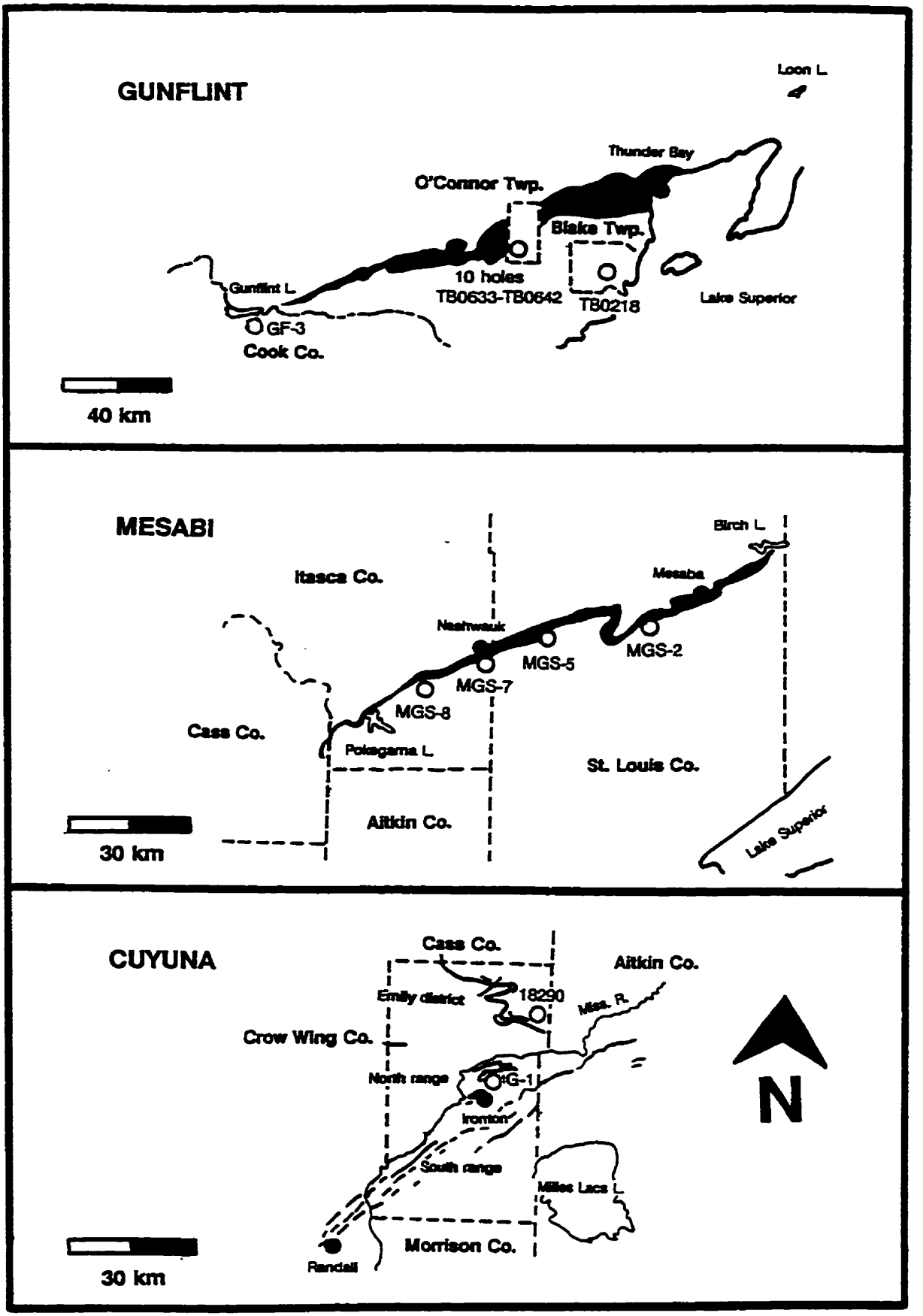

Fig. 2. Detailed location maps of Gunflint, Mesabi, and Cuyuna iron ranges with location of cored drill holes used for stratigraphic correlation.

northern Minnesota (Morey, 1993). The name refers to the preglacial outcrop of the Biwabik iron formation. The eastern end of the Mesabi is truncated by the Duluth complex; the western end is covered by thick glacial deposits (White, 1954). For convenience White (1954) divided the Mesabi into four parts: the "East Mesabi" is between Birch Lake and Mesaba; the "Main Mesabi" extends from Mesaba westward to Nashwauk; the "West Mesabi" extends from Nashwauk to Pokegama Lake; and the "Westernmost Mesabi" extends from Pokegama Lake to a point in eastern Cass County.

The Cuyuna iron range is about 160 km southwest of Duluth, Minnesota in Aitkin, Cass, Crow Wing and Morrison Counties (east-central Minnesota) (Fig. 2) (Morey *et al.*, 1991). It has traditionally been divided into three districts; the Emily district, the North range and the South range (Morey *et al.*, 1991). The Emily district extends from the Mississippi River northward through Crow Wing County and into Southern Cass County (Morey *et al.*, 1991). The North range is near the cities of Crosby and Ironton in Crow Wing County (Morey *et al.*, 1991). The South range comprises an area of northeast trending, generally parallel belts of iron formation extending from near Randall in Morrison County northeast for approximately 100 km (Morey *et al.*, 1991).

1.3 Geologic setting

The Precambrian rocks of the Lake Superior region include; (1) the southern part of the Archean Superior Province, (2) Paleoproterozoic rocks of the Animikie Basin, (3) the Penokean orogenic belt, and the (4) Mesoproterozoic rocks related to the Midcontinental rift system (Fig. 3).

Superior Province

The Superior province consists of northern and southern high-grade gneiss subprovinces and a central region of subparallel, east-west trending, subduction related, metavolcanic, plutonic and metasedimentary terranes that were accreted from north to south during the interval 3.0 to 2.6 Ga (Card, 1990). It is a remnant of a more extensive Archean craton now surrounded and truncated by Paleoproterozoic orogens; the Trans-Hudson and Grenville orogens in the west, north, and southeast and the Penokean and New Quebec orogens in the south and east (Card, 1990).

In the Lake Superior region the southern margin of the Superior Province consists of the Wawa subprovince, a Late Archean island arc terrane (Hoffman, 1989), and the Minnesota River Valley gneisses, an Early Archean high-grade, gneiss terrane (Morey, 1983). The two are juxtaposed along a Late Archean suture, currently named the Great Lakes Tectonic Zone (Sims *et al.*, 1980, Gibbs *et*

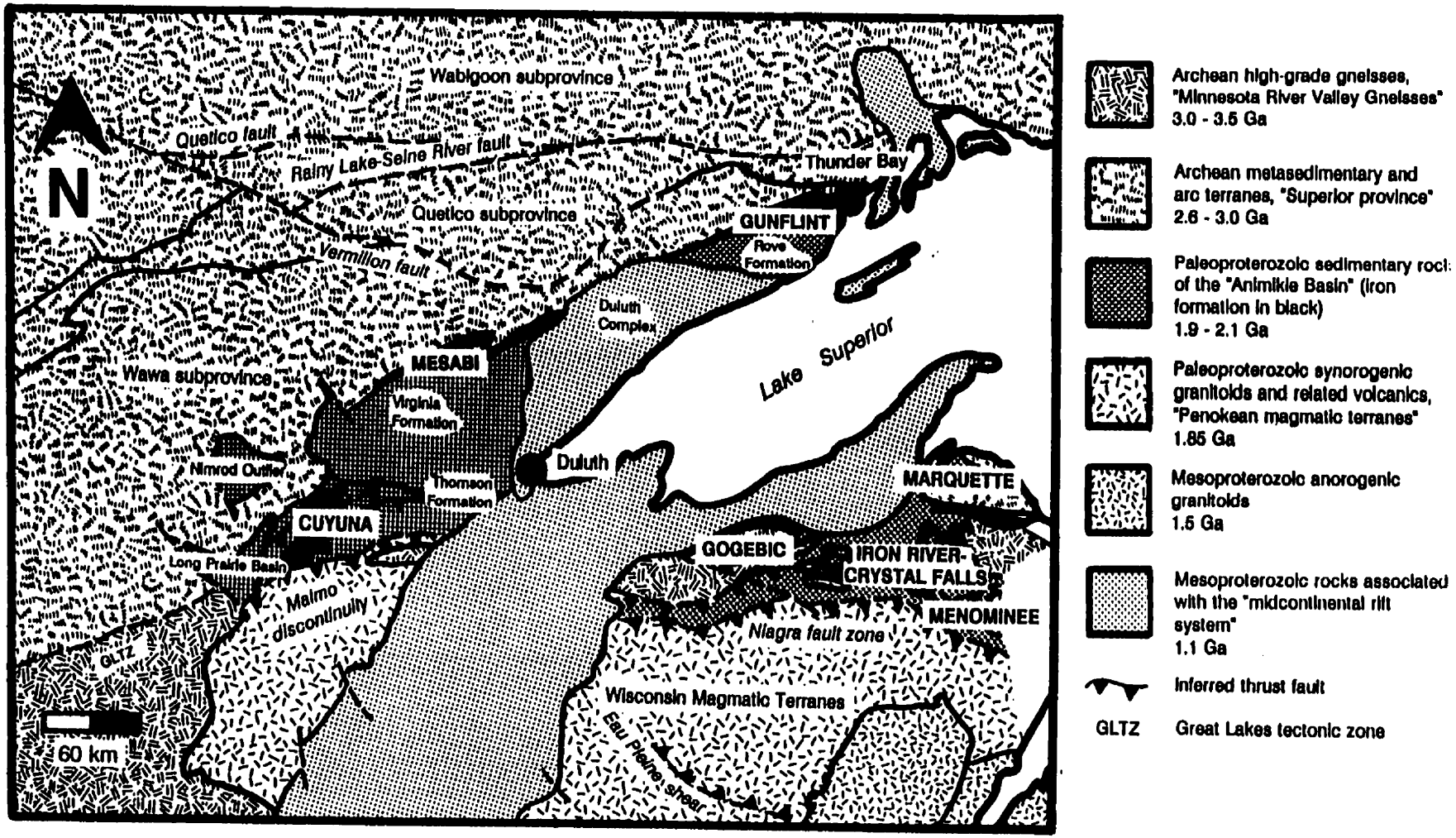

Fig. 3. Generalized geological map of Lake Superior region as well as location of iron ranges and place names mentioned in text.

al., 1984). The Wawa subprovince is separated in the north from the Quetico subprovince by the Vermilion Fault. The Quetico is an accretionary prism comprised of symmetrically metamorphosed, deformed turbidites (Hoffman, 1989). It is separated along its northern margin from the Wabigoon subprovince, an east-west trending arc terrane (Hoffman, 1989), by the Rainy Lake-Seine River and Quetico Faults.

Animikie Basin

The Paleoproterozoic sedimentary rocks deposited in the Animikie Basin form a southward-thickening wedge covering the southern margin of the Superior province, which is truncated in east-central Minnesota and northern Wisconsin by the "Penokean" magmatic terranes". Sedimentation began approximately 2.1 Ga ago and ceased roughly 1.85 Ga ago (Morey, 1983), prior to or during the Penokean orogeny of Goldich *et al.* (1961). The nature of the sediment varies considerably, ranging from volcanic and clastic to the chemical precipitates which form the thick successions of iron formation. The termination of the Penokean orogeny marked the onset of an intrusive igneous phase which emplaced subduction related tonalitic and granitic plutons into the Animikie sediments and the arc related volcanics of the Wisconsin magmatic terranes. The present form of the basin was achieved around 1.1 Ga ago (Silver and Green, 1972; Hanson, 1975; Wanless and Lovebridge, 1978) when a north-northwest trending branch of the Midcontinental Rift System (King and Zietz, 1971) separated the Animikie

sediments into a northwestern and southeastern segment (Morey, 1983).

In the most recent stratigraphic synthesis (Morey and Van Schmus, 1988) the Animikie Group of the northwestern segment is correlated with the Menominee and Baraga groups comprising the Marquette Range Supergroup of the southeastern segment (Fig. 4). The northwestern segment of the Animikie Group unconformably overlays the Superior Province and consists of a basal sandstone-siltstone (Pokegama Quartzite, Mahnomen Formation), iron formation (Gunflint, Biwabik, Trommald iron formations), and a thick, upper, shale-siltstone sequence (Rove, Virginia and Rabbit Lake Formations). In east-central Minnesota the Thomson Formation (Figs. 3 and 5), which has similar lithology to the Rove, Virginia and Rabbit Lake Formations, has also been considered correlative to the Animikie Group (Morey and Ojakangas, 1970). However, recent structural interpretations have complicated the correlation of these units (Ojakangas, 1995); northward thrusting during the Penokean Orogeny has juxtaposed units of differing Early Proterozoic ages in east-central Minnesota (Southwick *et al.*, 1988; Southwick and Morey, 1991; Hemming, 1994). Similar structural complexities also hinder correlation within the southeastern segment in northern Wisconsin and the Upper Peninsula of Michigan (Klasner *et al.*, 1991; Gregg 1993).

Southwick *et al.* (1988) have identified two shale-siltstone successions west and southwest of the Mesabi range; the Nimrod outlier and Long Prairie basin (Figs.

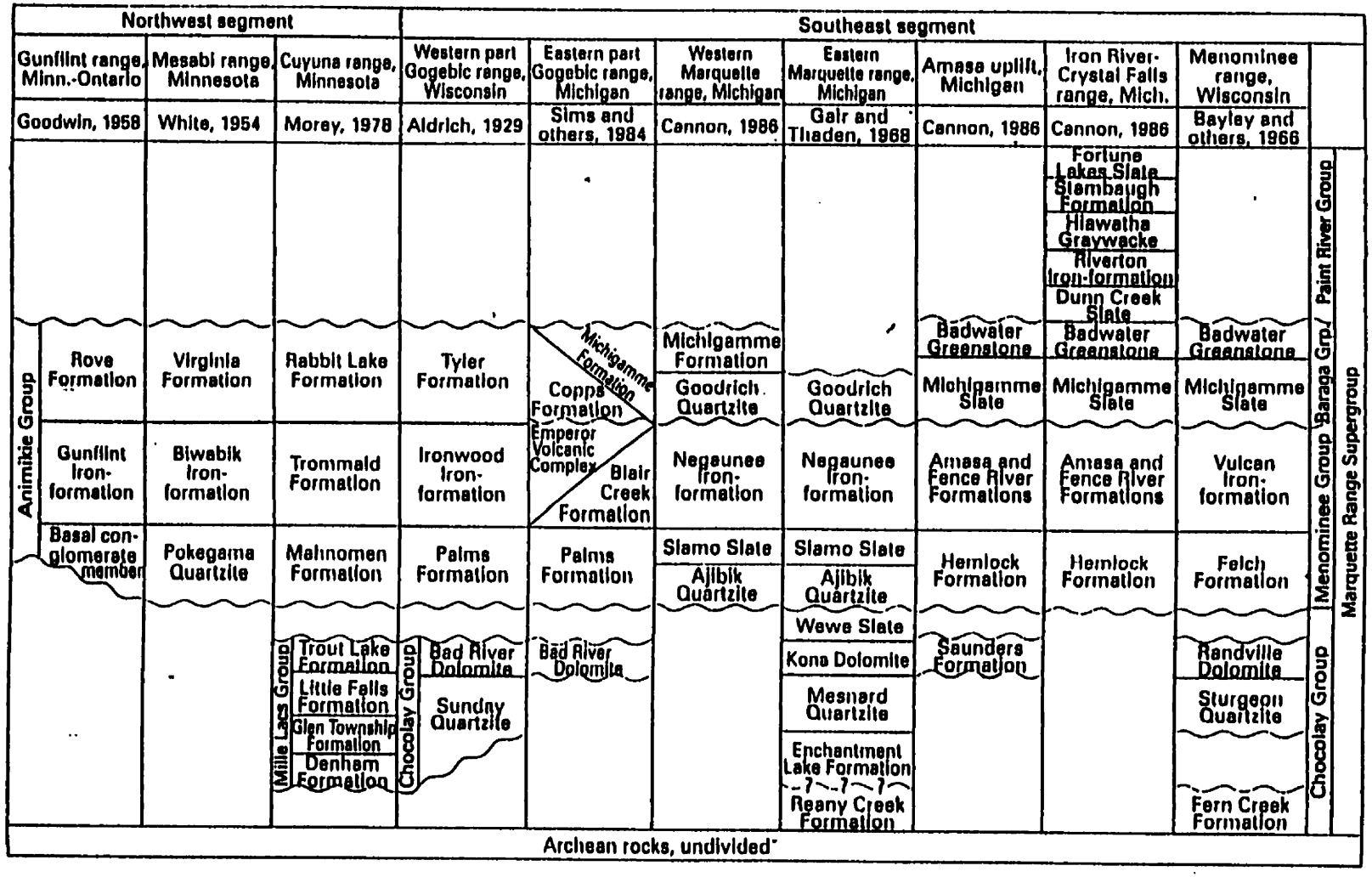

Fig. 4. Correlation chart for sedimentary and volcanic rock units of Early Proterozoic age in the Animikie Basin. From Morey and Van Schmus (1988).

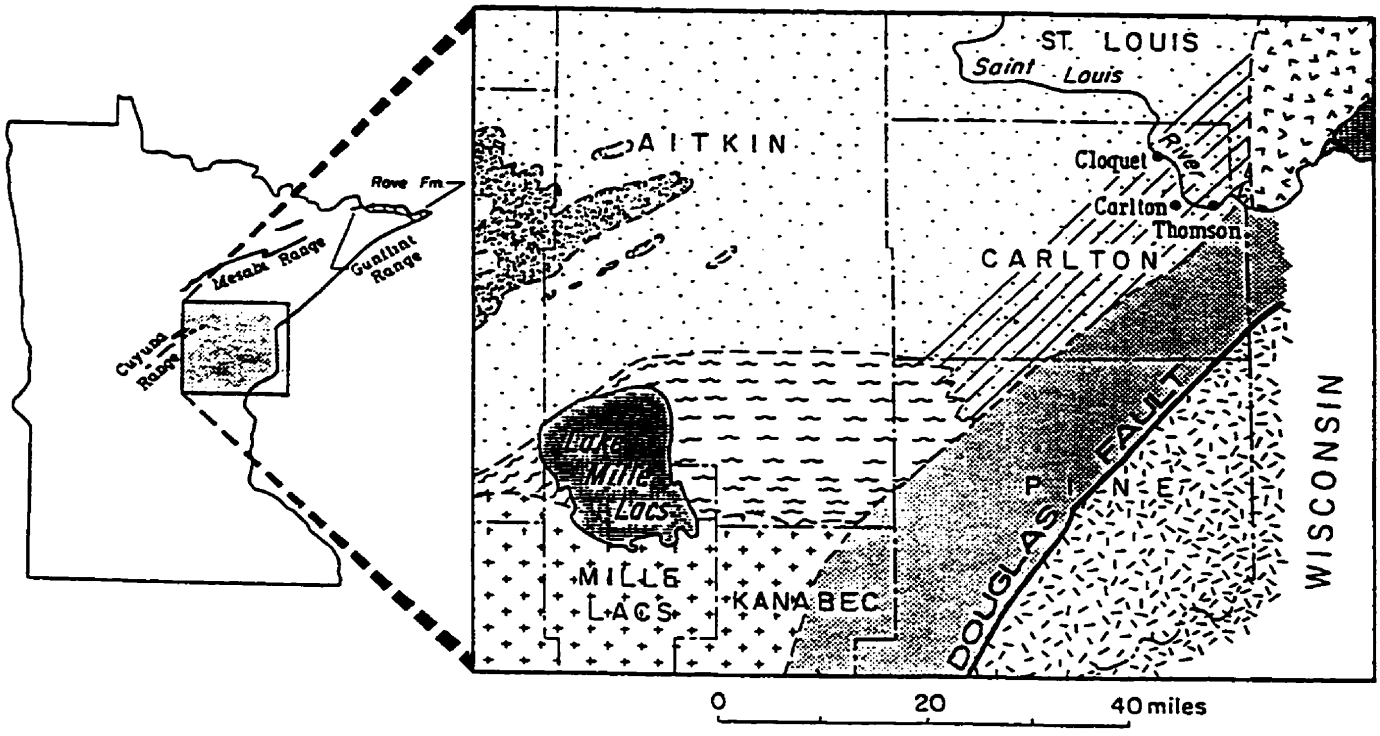

Fig. 5. Generalized geologic map of east-central Minnesota. The inferred distribution of the Thomson Formation and correlative rocks is shown by stippled pattern; diagonal lined pattern outlines the area where bedrock is exposed at the surface. From Morey and Ojakangas (1970).

3 and 6). Like the Thomson Formation they too are similar to the Virginia and Rove Formations and may be correlative (Southwick *et al.*, 1988).

Penokean Orogenic Belt

The Penokean orogeny is a zone of deformed and metamorphosed Paleoproterozoic and Archean rocks along the southern margin of the Superior Province (Sims, 1991). It is thought to have occurred between 1.9 and 1.76 Ga (Van Schmus, 1976; Van Schmus and Bickford, 1985). In the Great Lakes region it forms the transition between the Late Archean crust of the Superior Province and the Paleoproterozoic continental crust of the Mazatzal and Yavapai provinces of the southwestern United States (Sims and Peterman, 1986; Hoffman, 1989; Barovich *et al.*, 1989). Deformation along this tectonic front involved thrusting and development of basement gneiss domes (Southwick *et al.*, 1988). Rocks of the orogeny are exposed in east-central Minnesota, northern Wisconsin and the Upper Peninsula of Michigan.

The orogeny consists of a northern zone of deformed Animikie strata and a southern assemblage of arc-related volcanics and synorogenic, calc-alkaline plutonic rocks of the Wisconsin magmatic terranes, separated by the Niagra Fault Zone in northern Wisconsin and the Upper Peninsula of Michigan (Sims *et al.*, 1989) and by the Malmo Discontinuity in east-central Minnesota (Southwick and Morey, 1991). The Wisconsin magmatic terranes are comprised of a northern

Pembine-Wausau terrane and a southern Marshfield terrane, separated by the Eau Pleine suture zone (Hoffman, 1989). The Pembine-Wausau terrane consists of Proterozoic, deformed volcanic and derived sedimentary rocks, and coeval 1.89 to 1.84 Ga gabbroic through granitic plutons (Hoffman, 1989). Nd isotopic data indicate derivation of the terrane from Paleoproterozoic crust, or alternatively, from juvenile crust with a minor Archean component (Hoffman, 1989). The Marshfield terrane has an Archean basement, which is overlain by terrigenous sediments and 1.86 Ga felsic to mafic volcanics, and intruded by 1.89 to 1.84 Ga tonalitic, mafic, and granitic plutons (Hoffman, 1989).

Southwick *et al.* (1988) and Southwick and Morey (1991) have recognized, based on map-view geophysical discordances, four major structural discontinuities in the southern part of the orogeny in east-central Minnesota. These discontinuities are interpreted as shallow, southward dipping, brittle-ductile thrust faults which bound three structural terranes of differing rock type, metamorphic grade and structural style; the McGrath-Little Falls, Moose Lake-Glen Township, Cuyuna South Range, and Cuyuna North Range terranes (Fig. 6). The McGrath-Little falls terrane is south of the Malmo Discontinuity and contains several types of gneiss, amphibolite facies metasedimentary rocks and a variety of synorogenic granitic and tonalitic intrusions (Southwick *et al.*, 1988). Here, the Milles Lacs Group rests with apparent unconformity over the Archean basement (Morey and Southwick, 1993). In the Moose Lake-Glen Township terrane quartz arenite,

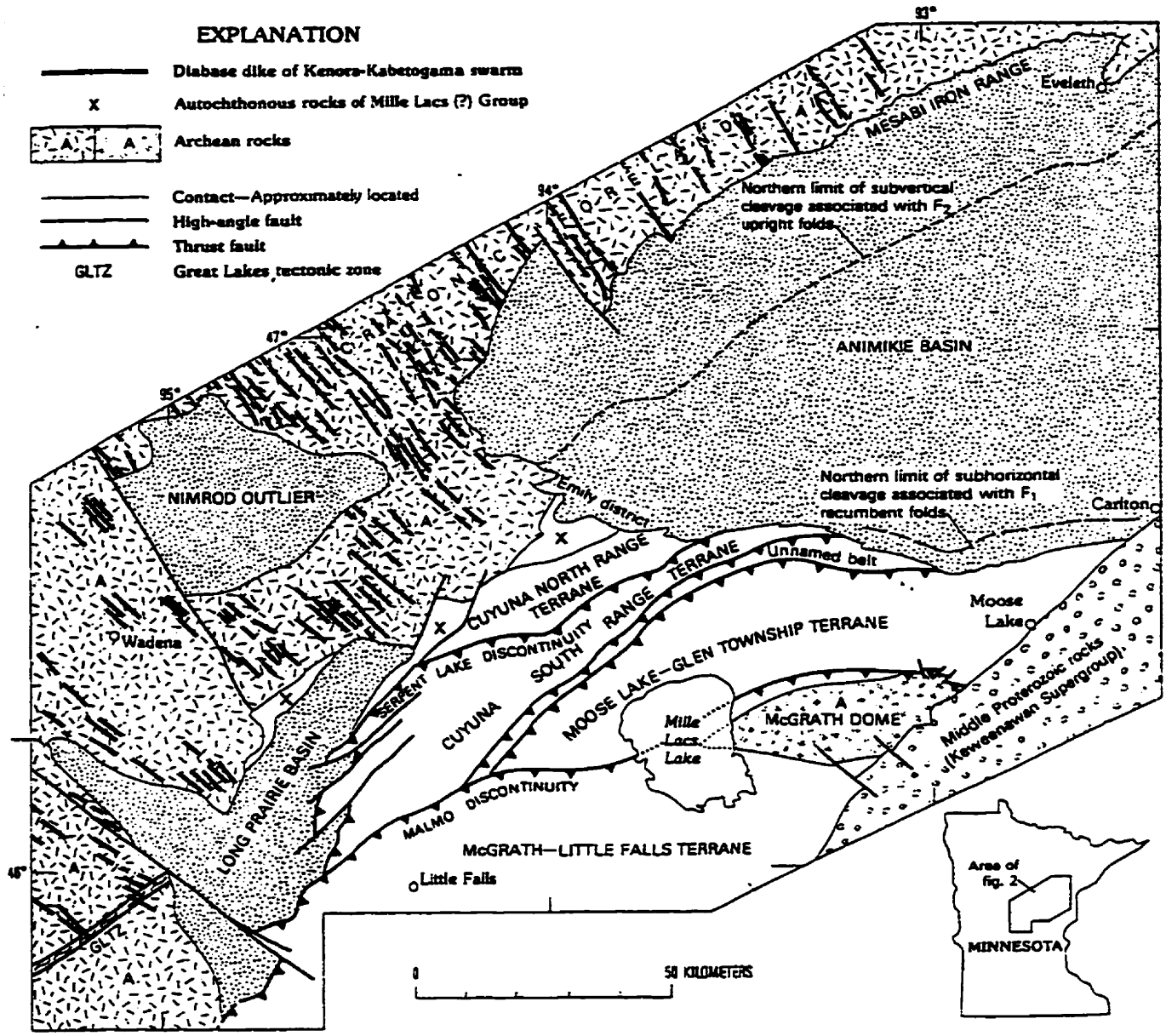

Fig. 6. Generalized tectonic map of Penokean orogeny in east-central Minnesota showing major tectonic subdivisions. Southern, more complexly deformed part of orogen consists of four named structural terranes, coupled with a fifth unnamed belt between the Cuyuna south range and Moose Lake-Glen Township terranes. From Southwick and Morey (1991).

resembling the Denham Formation of the Milles Lacs Group, is overlain by carbonaceous shales, iron formation and mafic volcanic rocks of the Glen Township Formation. Rocks of the Cuyuna South Range terrane (Cuyuna south range) are composed mainly of shale and iron formation of the Milles Lacs Group. The Cuyuna North Range terrane (Cuyuna north range) consists of the Milles Lacs Group unconformably overlain by rocks of the North Range Group (Morey and Southwick, 1993). Here, the Milles Lacs Group also rests unconformably over the Archean basement and is comprised of quartz-rich sedimentary rocks with iron formation and volcanic rocks in the lower part and quartz sandstones and minor dolomite and volcanic rocks in the upper part (Morey, 1978). The North Range Group consists, in ascending order, of the Mahnomen Formation, a lower fine-grained sandstone, siltstone sequence, the Trommald Formation, a middle manganese-rich slaty iron formation, and the Rabbit Lake Formation, an overlying succession of shale and siltstone.

Midcontinental rift system

Rocks of the Midcontinental rift system (1.1 Ga) form the youngest major terrane in the Lake Superior region (Sims, 1991). It is an assemblage of Mesoproterozoic, igneous and sedimentary rocks that formed in a rift that aborted before significant crustal separation was achieved (Wold and Hinze, 1982; Van Schmus and Hinze, 1985) (Sims, 1991). The rocks are dominantly bimodal basalt and rhyolite, which occupy a central uplifted graben bounded by high-angle reverse

faults; gabbro and anorthosite complexes, which are intruded along the unconformity along the margins of the rift between Archean and Early Proterozoic rocks and the younger Keweenawan lava flows; and red-bed, but locally carbon-rich sedimentary rocks (Sims, 1991).

1.4 Previous work

Gunflint Range

The Gunflint iron formation was discovered in 1850. The earliest recorded geological investigation of the Gunflint was conducted by E. D. Ingall in 1887 (Ingall, 1888), who briefly described the iron-bearing strata near Silver Mountain and Whitefish Lake. Other early accounts were made by Smith (1905) and Silver (1906). Van Hise and Leith in 1911 presented a general overview of the iron bearing rocks in the Thunder Bay district. In 1924 J. E. Gill was the first to describe the Gunflint in detail, and in 1926, its stratigraphy northeast of Silver Mountain. In 1927 Gill published again, this time on the origin of the chemical sediments. T. L. Tanton described the iron prospects at Mink Mountain in 1923, and in 1931 gave an overview of the general geology in the vicinity of Thunder Bay.

In 1956 the iron formation was divided by Goodwin (1956) into six major

sedimentary facies representing two depositional cycles and four members, a 1) Basal Conglomerate Member, 2) Lower Gunflint Member, 3) Upper Gunflint Member and 4) Upper Limestone Member; which are largely correlative with Broderick's (1920) four-fold division of the Gunflint iron range in northeastern Minnesota and Wolff's (1917) subdivision of the Biwabik iron range in east-central Minnesota. He also drew attention to evidence of widespread volcanism associated with deposition of the chemical sediments and suggested a volcanic source for the iron and silica. In 1960 Goodwin and Moorehouse published the first detailed geological maps of the region (scale 1:31 680) and reported on the economic potential, mineralogy and chemistry of the iron bearing strata, and modified Gunflint stratigraphy into a Lower and Upper Gunflint depositional cycle composed of 10 members; a Basal Conglomerate, Lower Algal Chert, Lower Shale, Lower Taconite, Local Lava Flows, Upper Algal Chert, Upper Jasper, Upper Shale, Upper Taconite and an Upper Limestone member. Fralick and Barrett (1995) have recently redefined Gunflint stratigraphy as simply consisting of 2 members; a lower member comprised of basal algal and oolitic cherts, and cherty grainstones, and an upper member similar in stratigraphy to the lower member. They have interpreted this succession as representing a wave- and tide-dominated inner shelf sequence.

Floran and Papike (1975), Randazzo and Markun (1980), Lougheed (1983) and Simonson (1987) have given detailed petrographic descriptions of mineral assemblages comprising the Gunflint iron formation. The Gunflint volcanics

(Goodwin, 1956,1960) have been petrographically described by Hassler and Simonson (1989). Their REE geochemistry has been determined by Kissin and Fralick (1994). Carbon and sulfur isotopic studies have indicated a hydrothermal exhalative origin as the source for the iron (Cameron, 1983; Carrigan and Cameron, 1991). Other geochemical investigations (Kronberg and Fralick, 1992) have attributed the alteration of the Archean basement to the penetration of Gunflint-derived fluids under diagenetic or low-grade metamorphic conditions. The overlying Rove Formation was described by Morey (1967, 1969). Detailed accounts of microfossils preserved within Gunflint chert are recorded by Tyler and Barghoorn (1954), Barghoorn and Tyler (1965a,b), Edhorn (1973) and Awramik (1976).

The absolute age of the Gunflint Formation is not known but several isotopic investigations have constrained its depositional age between 1.6 and 2.0 Ga. Hurley *et al.* (1962) obtained a minimum age of deposition of about 1.6 Ga by both Rb-Sr and K-Ar methods, to which they applied an empirical correction factor, which allowed them to propose an age of approximately 1.9 Ga (Stille and Clauer, 1986). Faure and Kovach (1969) also obtained a Rb-Sr isochron age of approximately 1.6 Ga. More recently, Stille and Clauer (1986) obtained a Sm-Nd isochron age of about 2.08 Ga for volcanic slates interbedded with iron-bearing strata of the Gunflint Formation.

Mesabi Range

The Biwabik iron formation was first discovered in 1886 (Morey, 1983). Mining commenced shortly thereafter in 1892. Since that time the Mesabi has yielded 3.4 billion tonnes of ore (1992 estimates) (Morey, 1993). In 1992 it was estimated Biwabik iron ores comprised 7 % (41.5 million tonnes) of the estimated world production of iron (Morey, 1993). The name "Biwabik", a Chippewa word for a piece of iron, was given to the iron bearing-strata in northern Minnesota by Van Hise and Leith (1901).

The historic papers on this important iron district are those of Spurr (1894), Van Hise and Leith (1911), Wolff (1915, 1917), Broderick (1919), Grout and Broderick (1919), Gruner (1922a,b, 1924, 1946) and White (1954). Van Hise and Leith (1911) published the first comprehensive geological reports on northern Minnesota. Wolff (1915, 1917) conducted the earliest detailed stratigraphic and structural investigations of the Mesabi iron range. He subdivided the Biwabik iron formation into a lower cherty, lower slaty, upper cherty and upper slaty horizons; the four-fold division still in use today. Broderick (1919) added considerable knowledge to Mesabi stratigraphy by describing each of Wolff's horizons in detail. Grout and Broderick (1919) made the first detailed account of the Mesabi stromatolites. Gruner discussed the origin of the chemical sediments (1922b, 1930, 1937a) and conducted some of the earliest petrographic/stratigraphic studies of the Biwabik iron ores (Gruner, 1922a,b, 1924, 1937a, 1946). He also

made significant contributions to unravelling the structure and composition of greenalite (Gruner, 1936), stilpnomelane (Gruner, 1937b) and minnesotaite (Gruner, 1944). White (1954) reexamined the stratigraphy, structure and petrography of the Biwabik iron ores, further elaborating on Wolff's (1915, 1917) stratigraphic breakdown. He was the first to stress the importance of physical sedimentary processes and changes in relative sea level as primary controls on iron formation genesis.

More recently French (1968) conducted a detailed investigation of the metamorphic mineral assemblages comprising the Biwabik ores and recognized four distinct metamorphic zones; an unaltered taconite, transitional taconite, moderately metamorphosed taconite and highly metamorphosed taconite zone. Morey (1992) comprehensively described the chemical composition of iron-bearing strata in the Main Mesabi. Ojakangas (1983) interpreted the Pokegama Quartzite, a basal sandstone succession which conformably underlies the Biwabik iron formation, as being deposited in tide dominated settings. Lucente and Morey (1983) have conducted a detailed stratigraphic and sedimentological study of the Virginia Formation, a shale-siltstone sequence conformably overlying the Biwabik iron formation, and interpreted it as representing turbidite deposition on the middle portion of a submarine fan complex.

Isotopic studies have constrained the depositional age of the Animikie Group

in northern Minnesota between 1.6 and 2.1 Ga. The Pokegama Quartzite is constrained to be younger than 2 120±67 Ma (Beck and Murthy, 1982), based on its unconformable relationship with the Kenora-Kabetogama dike swarm (Southwick and Day, 1983), and older than 1930±25 Ma (Hemming *et al.*, 1990) based on the Pb-Pb age of a quartz vein cutting the sandstone (Hemming, 1994). The upper age constraints on the deposition of chemical and clastic sediments in northern Minnesota are based on its deformation from the Penokean orogeny and by Rb-Sr whole rock age of 1.6 Ga for the Virginia Formation by Peterman (1966) (Hemming, 1994).

Cuyuna Range

Iron formation was first discovered in the Cuyuna iron range in 1893. Mining began eleven years later in east-central Minnesota in 1904 (Morey, 1983). The North range was the principal site of mining activity, which had largely ceased by about 1975 (Morey *et al.*, 1991). The last mine closed in 1984. Mining never commenced in the Emily district and only a few mines operated in the South range during the early part of this century (Morey *et al.*, 1991).

The original papers on the Cuyuna range are those of Van Hise and Leith (1911), Harder and Johnston (1918), Zapffe (1925), Woyski (1949), Grout and Wolff (1955) and Schmidt (1963). Van Hise and Leith (1911), Harder and Johnston (1918) and Zapffe (1933) recognized the existence of a single major iron

formation in the Cuyuna district, which they named the "Deerwood" (Marsden, 1972). Grout and Wolff (1955) emphasized the correlation of the iron-bearing strata in the Cuyuna north range with the Biwabik iron formation. Schmidt (1963) described the ores of the north range in detail and proposed the name "Trommald Formation" for these iron-bearing strata.

In 1978 Morey (1978) correlated the Emily district, the north range and the south range to the Animikie Group in northern Minnesota. The tectonic framework of east-central Minnesota as mapped by Morey *et al.* (1981) was guided by gravity (Krenz and Ervin, 1977; McGinnis *et al.*, 1977, 1978) and magnetic (Bath *et al.*, 1964, 1965) data available in the 1970's (Morey *et al.*, 1991). In the early 1990's the acquisition of high-resolution aeromagnetic data (Chandler, 1991) and shallow test drilling of selected anomaly patterns in east-central Minnesota by the Minnesota Geological Survey have aided in further refining stratigraphic and structural relations in the Cuyuna iron range. Recently research has focused on evaluating the resource potential and genesis of the manganese-rich ores of the Cuyuna north range and the Emily district (Beltrame *et al.*, 1981; Morey, 1991; Morey *et al.*, 1991; Morey and Southwick, 1993).

A depositional age for the Mahnomen, Trommald and Rabbit Lake Formations of the North Range terrane has not been established. However, Peterman (1966) obtained a metamorphic, Rb-Sr whole rock isochron age of about 1.87 Ga. The

volcanic rocks interbedded with iron formation and slate of the Glen Township Formation from the Glen Township-Moose Lake terrane have yielded a Sm-Nd isochron age of approximately 2.2 Ga (Beck, 1988).

The Animikie Basin

The earliest sedimentological models for the Animikie Basin relied on the work of James (1954) who concluded that iron formation successions evolved from a "miogeosynclinal" sequence to a "eugeosynclinal" assemblage during Paleoproterozoic time. James' original ideas were then discarded in the mid 1970's in favour of deposition of Animikie sediments in a rift-like basin (Cambray, 1978). In this model rifting was followed by the ultimate closure of the basin with the Penokean orogeny. In the early 1980's Young (1983), by analogy with other Phanerozoic and Proterozoic depositional basins, interpreted the tectonic and sedimentary history of Proterozoic rocks in the northern Great Lakes region in terms of an aulacogen model. Unfortunately, there was no general consensus on the driving force which caused the basin to form and the characteristic sediments analogous to rift/aulacogen depositional systems are absent. In the mid 1980's continued research lead to significant advancements in understanding the tectonics associated with basin development. These strides lead Hoffman (1987) to suggest deposition of chemical-sediments occurred in a migrating peripheral foreland basin which formed in response to crustal loading during the Penokean orogeny. Southwick *et al.* (1988) and Southwick and Morey (1991) then reinterpreted the

segment of the Penokean orogeny (Goldich, *et al.*, 1960) in Minnesota. Like Hoffman, (1987) they also concluded that the Animikie Group accumulated in a peripheral foreland basin and that iron formation deposition occurred in three distinct tectonic settings as the orogeny evolved. Recently, Pufahl (1995) and Hemming (1994, 1995) have demonstrated that this tectonic model is no longer valid. Hemming (1994, 1995) contends that Nedodimium and Lead isotopic evidence for the provenance of the Animikie Group is consistent with the tectonic evolution of the Animikie Basin beginning as a passive margin within a back arc basin, and ending as a telescoped back arc basin that closed as a result of a change in relative plate convergence direction. Nevertheless, in recent years the foreland model has reached widespread acceptance based on high resolution aeromagnetic data, exploratory drilling through structurally complex regions, and sedimentological investigations of clastic units above and below iron-bearing strata (Hoffman, 1987; Southwick *et al.*, 1988; Southwick and Morey, 1991; Ojakangas, 1995).

1.5 Methodology

Basin analysis was carried out using a "depositional systems approach" to stratigraphy. This technique diverges considerably from the formal stratigraphic methods used in the past for defining lithologic units in the Animikie Group.

Instead of focusing on the description of formations and members, erection of stratotypes, etc., the basis of this method is the application of Walther's Law and the facies model concept to large scale depositional tracts, up to and including the entire basin (Miall, 1984). The approach is essentially genetic stratigraphy, in which the focus of the analysis is on the interpretation of the interrelations of large sediment bodies, based on an understanding of the depositional environments and syndepositional tectonics which controlled their formation (Miall, 1984). Sedimentological techniques, including facies analysis and basin mapping techniques are of paramount importance, as is the application of refined stratigraphic correlation (Miall, 1984).

At the heart of any basin analysis project is the careful compilation of vertical stratigraphic sections (Miall, 1984). In this study sections were constructed using data collected from eighteen cored drill holes through the Gunflint, Mesabi and Cuyuna iron ranges in Ontario and Minnesota. Drill holes in Ontario are from O'Connor and Blake Townships in the Thunder Bay District and those in Minnesota are from northern Cook, St. Louis, Itasca, and Crow Wing Counties (Fig. 2).

Drill core was logged in the same way clastic rocks are logged for purposes of basin analysis; great care was exercised in recording changes in grainsize, bed thickness, and type. This procedure provides critical insight as to whether the

organization of iron formation facies was governed by an autocyclic (process controlled) or allocyclic mechanism (fluctuating sea level), or both. Changes in mineralogy were also noted but not focused on as mineral assemblages comprising iron-bearing strata are largely the result of diagenesis and metamorphism (Simonson, 1985). Polished sections were made from selected samples representative of iron-bearing, clastic and volcaniclastic lithologies. Each polished section was examined in detail using a Lietz Laborlux 12 POL, binocular, transmitted light microscope and a Wild M8 reflected light microscope. Photomicrographs were taken with a Wild Photoautomat MPS45 metering system and camera.

Once petrographic descriptions of iron formations were complete a facies (Walker, 1979; Reading, 1986) nomenclature for iron formation in Minnesota and Ontario was developed. The purpose of this nomenclature was to generalize, categorize and simplify what was seen in drill core (Miall, 1984). This need arose from the lack of consistency used in the past in defining iron formation facies between individual iron ranges. Without a standardized nomenclature meaningful lithofacies associations are never recognized, accurate intrabasinal correlations are impossible and correct paleogeographic interpretations necessary for basin analysis are hindered. Commonly associated facies were then grouped into informal members for purposes of stratigraphic correlation.

Correlation of stratigraphic units began with those comprising the Gunflint in O'Connor Township. Here, correlation on a network of closely spaced holes 50 m apart afforded excellent vertical and lateral control of facies trends, and enabled detailed facies analysis of iron-bearing units not otherwise possible in a regional stratigraphic synthesis. This provided valuable information on the depositional controls which governed the organization of iron formation facies, and permitted detailed facies modelling of iron-bearing members. Once localized controls on iron formation accumulation were understood regional stratigraphic correlations between the Gunflint, Mesabi and Cuyuna iron ranges were made. This provided critical insight into the stratigraphic architecture of the Animikie Basin in Ontario and Minnesota, and allowed paleogeographic interpretation of systems tracts responsible for the deposition of iron formation from the Gunflint, Mesabi, and Cuyuna ranges.

1.6 Correlation problems, east-central Minnesota

Recently, the long-standing premise that the strata comprising the Cuyuna north and south ranges are correlative with the Animikie Group (Morey, 1978; Morey and Van Schmus, 1988) has been challenged (Southwick *et al.*, 1988; Southwick and Morey, 1991; Hemming, 1994). Based on map view geophysical discordances and shallow test drilling Southwick *et al.* (1988) and Southwick and

Morey (1991) contend that iron formation in east-central Minnesota was deposited in three distinct depositional settings as the Penokean orogeny evolved through time. The first phase occurred in close association with mafic volcanism, following initial rifting of the continental margin. Iron-bearing strata deposited in this episode comprise unnamed units within the Milles Lacs Group. The second phase began with deposition of the Trommald iron formation and associated iron formation units of the Cuyuna North Range terrane in a small restricted basin that was incorporated into the Penokean fold-and-thrust belt. The third episode occurred on the cratonic rim at a later time in the history of the orogeny, in a migrating, peripheral foreland basin. Iron formation units of this type include the Biwabik and Gunflint iron formations of the Animikie Group and the thin units of iron-bearing strata of the Emily district of the Cuyuna iron range (Morey and Southwick, 1993).

This interpretation is largely based on the assumption that the relatively undeformed strata of the Animikie Group occurs above a major, deformed unconformity that cuts across the folded strata of the Cuyuna north range; an assumption difficult to prove in a region where the rocks are very poorly exposed and deep drilling through stratigraphically complete sections of clastic and chemical sedimentary rocks has never been undertaken. Even Southwick *et al.* (1988) concede that a totally objective rendering of the stratigraphy and structure of the Cuyuna iron range will not be attained unless and until drilling has been completed on an unrealistically close-spaced grid. Nevertheless Southwick *et al.* (1988) and

Southwick and Morey (1991) contend that geophysical discordances present in shaded-relief aeromagnetic maps and Poisson analysis of gravity and magnetic data (Chandler, 1983a,b,c, 1985; Chandler and Malek, 1991) support this unconformable relationship. Other equally valid interpretations are however possible. This geophysical break may represent a major thrust fault along which the clastic and chemical sedimentary rocks of the Emily district were structurally juxtaposed against rocks of the Cuyuna north range during the Penokean orogeny. It may also mark the presence of a "triangle zone", similar to the one developed in the Canadian Rocky Mountain foothills. There, west dipping, tectonically delaminated rocks of Paleozoic to Tertiary age are juxtaposed against tilted, east-dipping Upper Cretaceous and Tertiary strata (Lawton *et al.*, 1994). This deformation front represents emplacement of a tapered wedge of rock inserted into undeformed foreland basin strata during late stages of the eastward progradation of deformation associated with the Laramide orogeny (Lawton *et al.*, 1994). The important feature of either of these scenarios is that iron-bearing strata in the Emily district would be correlative with the Trommald iron formation of the North Range Group in the Cuyuna north range; only one episode of iron formation deposition may have occurred.

Recently Hemming (1994, 1995) has used geochemical and Samarium (Sm)-Neodymium (Nd) isotopic evidence for the provenance of the Animikie Group and the metasedimentary rocks comprising the structural terranes assembled during the

Penokean orogeny in east-central Minnesota. The results of this investigation indicate that each terrane has distinctive crust formation ages; metasedimentary rocks of the Milles Lacs Group have Late Archean to Paleoproterozoic crust formation ages (2.1 to 3.1 Ga), metasedimentary and metavolcanic rocks of the Moose Lake-Glen Township terrane yield Paleoproterozoic Nd model ages (2.2 Ga), and metasedimentary rocks of the Cuyuna North Range terrane have dominantly Late Archean crust formation ages (2.5 to 3.0 Ga). The Animikie Group in northern Minnesota records a progression from Archean sources in the Pokegama Quartzite (2.8 to 3.1 Ga) at its base, to Paleoproterozoic sources in the Virginia Formation (2.1 to 2.4 Ga).

At first glance these Nd model ages appear to further complicate stratigraphic and structural relations within the Penokean fold-and-thrust belt. However, before meaningful interpretation of crust formation ages can be achieved two criteria must first be satisfied; (1) the geochemical system must remain "closed" to migration of radiogenic nuclides and daughters, and (2) the stratigraphic relations of lithologic units from which samples are taken must be precisely known. The first of these conditions is easily fulfilled. Under normal circumstances Sm/Nd ratios of sediments are extremely resistant to geologic changes which effectively "reset" other isotopic systems (i.e. chemical weathering, transport, deposition and diagenesis) (Faure, 1986). Nd model ages of sedimentary rocks are therefore good proxies for their sources (Hemming *et al.*,

1995) and are a valuable tool in deciphering chronostratigraphic relations in structurally complex terranes. The reader is referred to Faure (1986) for a comprehensive review of the systematics of the Sm-Nd isotopic system.

The second criteria is not convincingly met. Clastic samples for provenance studies of the North Range Group were taken from four stratigraphically incomplete drill cores; the Arko, Hillcrest, Northland, and Merritt holes first described in detail by Grout and Wolff (1955) (Fig. 7). The Arko core is comprised entirely of finely-laminated slates. Core recovered from the Hillcrest hole is primarily composed of an upper unit of slate and a lower unit of interbedded fine-grained sandstones and slates. Iron formation was not intersected in either hole. The Merritt core consists of an upper unit of cherty iron formation, a middle unit of slate and a lower unit of slate and fine-grained sandstones. Core recovered from the Northland hole is comprised of an upper unit of brown oxidized cuttings, and a lower unit of interbedded fine-grained sandstones and slates. Grout and Wolff (1955) attempted to correlate units within these drill holes, but contend that this effort was not totally satisfactory. Their correlations were hampered by folding and faulting associated with the Penokean orogeny and the lack of deep drill holes through complete sections of the North Range Group. They tentatively correlated the slates and fine-grained sandstones at the base of the Merrit and Northland (Mahnomen Formation) cores. The North Hillcrest core was placed at a stratigraphically higher position (Rabbit Lake Formation) based on the presence of some quartz-sandstone

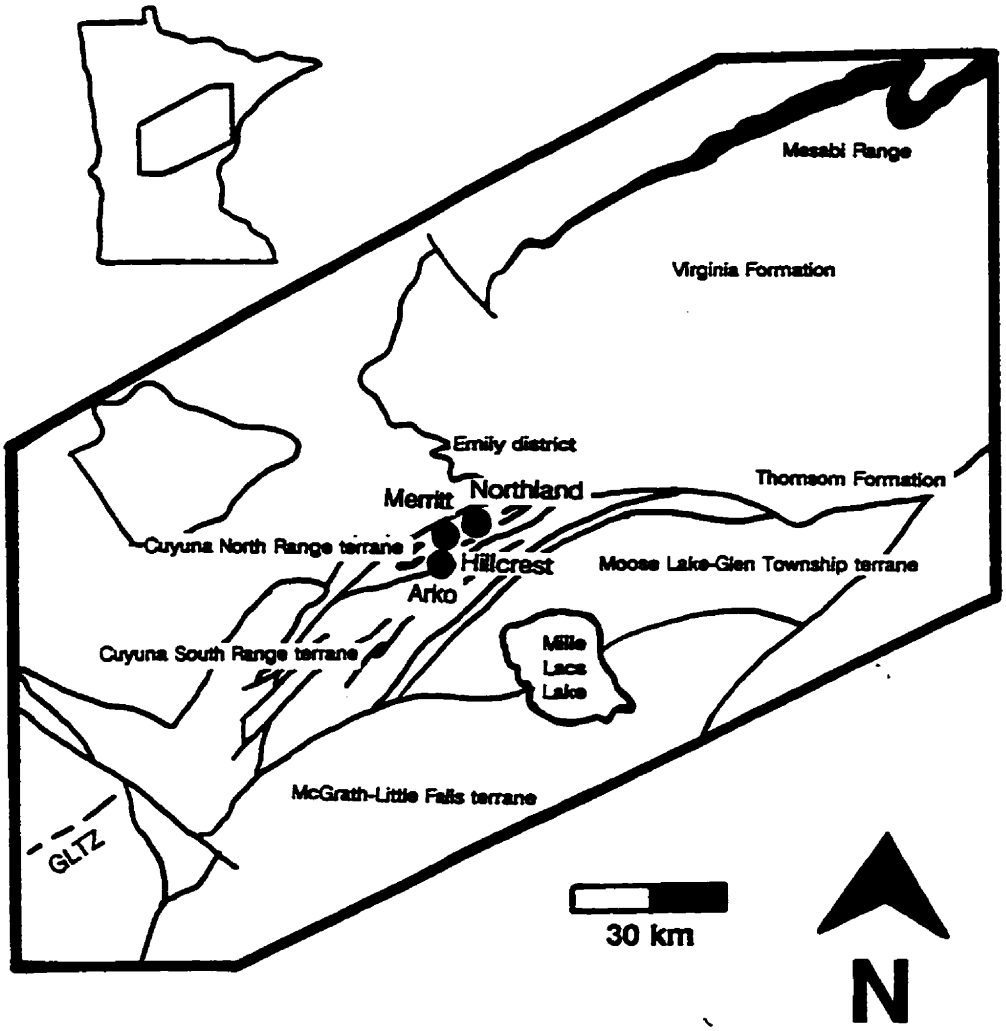

Fig. 7. Map of the Penokean orogeny of east-central Minnesota showing location of Arko, Hillcrest, Merritt and Northland drill holes. Modified from Hemming (1994).

beds not observed in the Merritt and Northland cores. The Arko core was also placed at a higher stratigraphic position after Wolff thought he had recognized some features similar to those in the North Hillcrest core. Similar correlation problems were also discussed by Schmidt (1963).

As can be seen stratigraphic relations between units comprising these sections are equivocal at best. At the very most Hemming's (1994) Late Archean Nd model ages of these lithologically similar, clastic units within the Arko, Hillcrest, Merritt and Northland cores indicate that Grout and Wolff's (1955) correlations are wrong. Nd isotopic evidence suggests that these units are correlative, belonging to the Mahnomen Formation, and occupy the same stratigraphic position as the Pokegama Quartzite at the base of the Animikie Group in northern Minnesota, which also has a Late Archean provenance. Without knowing the precise stratigraphic relations of units from which samples were taken nothing more can be said.

Only until deep drilling of stratigraphically complete sections through each of the structural panels comprising the Penokean fold-and-thrust belt in east-central Minnesota is undertaken, and seismic profiling across this tectonic front is accomplished, will stratigraphic and structural relations in east-central Minnesota be known unequivocally. It is because of these uncertainties that the author will use the stratigraphic correlations summarized in Morey and Van Schmus (1988). In

this synthesis the Mahnomen, Trommald and Rabbit Lake Formations of the Cuyuna iron range are correlative with the Pokegama Quartzite, Biwabik iron formation and the Virginia Formation of the Mesabi iron range.

CHAPTER 2: FACIES NOMENCLATURE FOR SUPERIOR TYPE IRON FORMATION

2.1 Introduction

The following facies categorization is an attempt to standardize how iron formation facies are defined in the Lake Superior region. This need arose from the lack of consistency used in defining iron formation facies between individual iron ranges. Without a standardized nomenclature meaningful lithofacies associations are never recognized, accurate intrabasinal correlations are impossible and correct paleogeographic interpretations necessary for basin analysis are never made.

Unlike James' (1954) division of iron formation into an oxide, carbonate, silicate and sulfide facies the nomenclature set forth in this chapter is not based solely on the mineralogical attributes of the iron-bearing strata. Instead it focuses on the sedimentological characteristics (bed thickness, grainsize, type of primary sedimentary structures present, etc.) of iron formation in the same way clastic rocks are described for purposes of basin analysis. This is a powerful technique which enables hydrodynamic interpretation of systems tracts responsible for iron formation genesis. It does not restrict the study of iron formation to simply an exercise in mineralogy but allows regional synthesis of paleoenvironments. Terms used in section 2.2 to describe the composition of framework grains and textures displayed by interstitial quartz in the chemical sedimentary facies are those of

Simonson (1987) (Table 1).

2.2 Lithofacies descriptions

Clastic lithofacies

*Matrix and/or clast supported, pebble conglomerate (**Cp**)*

Beds composing the **Cp** facies are poorly sorted, range between 2 and 6 cm in thickness and are slightly graded in some instances. Beds are cross-cut by mega-quartz veinlets 0.2 to 0.4 mm wide and have undergone pervasive iron carbonate alteration. Five types of clasts compose beds; 1) subrounded clasts of a variety of older rocks, 2) subrounded mosaic chert grains, 3) ripped-up aggregates of subrounded mosaic chert grains, 4) finely laminated subangular stromatolitic rip-ups, and 5) oncolitic fragments. Subrounded to rounded rock fragments range in diameter from 1 to 3 cm and reflect the composition of the underlying basement. Subrounded, polycrystalline quartz grains 0.3 to 5 mm in diameter (average 3 to 4 mm) are the most common type of detrital fragment. Subrounded mosaic chert grains typically range between 2 and 3 mm in diameter. Some oblate spheroidal grains have their long axis parallel to bedding. Ripped-up aggregates of mosaic chert grains average 6 mm X 4 mm (Figs. 8 and 9). Finely laminated subangular stromatolitic rip ups are commonly 2 mm X 4 mm. Cryptalgal intraclasts occasionally have bases composed of ripped-up aggregates of mosaic chert.

Table 1. Commonest textures displayed by interstitial chert and mega-quartz in iron formation grainstones. From Simonson (1987).

Name	Crystal Size	Texture
Spherulitic chert	≤10 μm across	Aggregates of fibrous to equant crystals displaying both length-fast (the majority) and length-slow spherulitic figures.
Fibrous rims	≤10 μm across	Chert encrusting sand grains and displaying either domain texture or length-fast orientation of crystals normal to clast edge; commonly isopachous.
Domain chert	≤25 μm across	Equant crystals grouped into domains with diffuse boundaries, and up to around 0.3 mm across, displaying sweeping extinction internally.
Mosaic chert	≤25 μm across	Homogeneous mosaic of equant, randomly oriented crystals.
Blocky mega-quartz	≥50 μm but ≤0.2 mm across	Homogeneous mosaic of equant, randomly oriented crystals.
Drusy mega-quartz	≤0.4 mm long	Crystals coarsening inward from clast edges to pore centers.

Fig. 8. Cp facies. Mosaic chert intraclasts and oncolites. Oncolites coat polycrystalline quartz grains (lower left) and smaller ripped-up fragments of mosaic chert (upper middle). Field of view 4 mm, trans. XN.

Fig. 9. Cp facies. Large rounded mosaic chert intraclast (middle), polycrystalline quartz grains and a well developed oncolite in clast support. Field of view 4 mm, trans. XN.

Oncolitic fragments vary from 1 to 1.5 mm in diameter. These organosedimentary structures commonly coat polycrystalline quartz grains 0.5 to 1mm in diameter, and have inundated grain boundaries which conform sympathetically around opposing grains (Figs. 8 and 9). Amorphous, microcrystalline iron carbonate is the dominant pore filler. In O'Connor Township where **Cp** facies grainstones overly granitic basement sericite is an important secondary matrix constituent.

*Fine- and medium-grained, quartz sandstone (**Cs**)*

A detailed sedimentological investigation of this siliclastic-facies was not within the scope of this study. Consequently information regarding the **Cs** facies sandstones is limited. Some generalities can however be made. In the Mesabi iron range sandstone beds at the transition into the iron bearing strata of the Biwabik iron formation are 10 to 50 cm thick, massive, fine- and medium-grained, and highly altered. Beds are formed almost exclusively of moderately well sorted, grain supported, subrounded to subangular monocrystalline quartz grains 0.2 to 1.0 mm in diameter. In some instances subrounded, iron carbonate replaced, mafic grains, 0.2 to 1.0 mm in diameter also comprise beds. Grains are enveloped in a matrix of intimately intergrown, prismatic crystals of chlorite 0.05 mm in length. In the Cuyuna iron range **Cs** facies sandstones are typically finer-grained and have undergone a higher degree of alteration than their Mesabi counterparts. As a consequence, primary features within beds have been obliterated by metamorphism and ensuing alteration. Information regarding the type of sedimentary structures

present within beds (if any) is therefore equivocal at best. Clusters of prismatic needles of iron silicates, 0.04 mm in diameter, are the dominant matrix phase. For a detailed treatment of this clastic facies in the Mesabi iron range the reader is referred to Ojakangas (1983). The following paragraph summarizes Ojakangas' (1983) lithofacies and their related descriptions.

In the Mesabi iron range 3 lithofacies comprise this basal unit; a shale, shale-siltstone-sandstone and sandstone facies. The shale facies consists dominantly of thinly bedded shale with some interbedded siltstone laminae and sandstone beds. Minor channelling is a common feature at the base of the thicker beds. Small-scale cross bedding and soft sediment deformation structures are also not uncommon. The shale-siltstone-sandstone facies is dominated by thin-bedded siltstone with minor shale and sandstone. Layers are either parallel or wavy bedded. Small scale cross-bedding, flaser bedding, small flute casts and runzel marks are common. Troughs as large as 7 cm deep by 20 cm wide are also present. The sandstone facies is characterized by medium- to coarse- grained sandstone beds 1.5 m thick separated by thin beds of shale or siltstone. Beds appear massive but may be cross stratified in some instances. Ripple marks and possible syneresis cracks are also observed.

Volcaniclastic lithofacies

Slate (Vs)

Near Thunder Bay non-graded, parallel laminated layers (0.3 to 4.0 mm thick) with sharp upper and lower contacts comprise this facies. Subhedral sanidine crystals 0.02 to 0.06 mm exhibiting carlsbad twinning are commonly observed disseminated throughout slaty laminations. Feldspar composes only 1 to 2% of the mineralogical composition of slaty layers and in many cases are absent. In these instances angular, monocrystalline, matrix supported, silt-sized, quartz crystals 0.1 to 0.2 mm in diameter form the coarsest grains. In all cases the matrix is composed completely of interlocking, crystals of prismatic chlorite 0.01 mm length.

In Minnesota many slaty laminations are sometimes graded, coarsening from a silty bottom to a clay-rich top. Rare, well rounded, polycrystalline quartz grains 0.5 mm in diameter are sometimes observed within layers. Laminations are monomineralic, composed entirely of interlocking prismatic crystals of chlorite 0.01 mm in length. Layers are commonly cross-cut by iron carbonate veinlets 0.5 mm wide. These veinlets frequently contain small clusters of prismatic crystals of minnesotaite and greenalite 0.1 to 0.2 mm in diameter.

Lapillli tuff (Vt)

Highly altered, deformed lapilli 0.04 to 1 mm in diameter form this facies.

The matrix is composed almost entirely of silt-sized, interlocking, prismatic crystals of chlorite with minor amounts of silt-sized grains of plagioclase and quartz disseminated throughout. Angular anhedral sanidine crystals 0.07 to 0.1 mm and intraclasts of cherty grainstone 0.2 mm X 0.07 mm exhibiting undulose extinction are also common matrix components.

Chemical-sedimentary lithofacies

Massive and/ or cross stratified, medium- and coarse-grained chert-carbonate grainstone (Gc)

Gc facies grainstones are composed of moderately well sorted grains 0.5 to 1.2 mm in diameter. Subrounded mosaic chert grains with thin (0.15 mm thick) isopachous rims of fibrous chert, subrounded and rounded carbonate grains, and rare, subrounded, hematite grains compose beds. Chert grains are commonly shrinkage cracked, and in some instances posses a thin 0.15 mm thick coating of skeletal magnetite or hematite (Fig. 10). When hematite grains are present they too are fractured and infilled with mosaic chert. In many instances dolomite rhombs 0.3 mm in diameter have epitaxially overgrown hematite grains. Carbonate grains are formed of euhedral, recrystallized iron carbonate crystals 0.2 mm in diameter. All grains possess inundated grain boundaries which sympathetically conform around one another. Matrix phases include mosaic chert, and blocky and drusy mega-quartz. Regions which have undergone carbonate alteration are composed of euhedral carbonate crystals.

Fig. 10. Gc facies. Mosaic chert grains coated with hematite and fibrous chert rims in a matrix of blocky and drusy mega-quartz. Grains also contain abundant silt-sized subhedral hematite crystals disseminated throughout. Field of view 2 mm, trans. XN.

Beds range in thickness from 10 to 50 cm (average 20 cm) and are non-graded. Rare, wavy laminated, magnetite-rich slaty iron formation layers 1 to 2 mm thick, forming packages 1 to 2 cm thick, sometimes occur between grainstone beds. However parallel and wavy bedded, very fine-grained, non-graded chert grainstone beds 8 mm to 1.5 cm thick are more prevalent between thicker, coarser-grained grainstone beds. Veins which crosscut beds are infilled with iron carbonate, blocky mega-quartz and mosaic chert. All grains posses inundated grain boundaries which sympathetically conform around opposing grains.

*Massive and/or cross stratified, medium-grained, hematite-rich chert-carbonate grainstone (**Gm**)*

Gm facies grainstones are comprised of massive and cross stratified hematite-rich, chert-carbonate grainstone beds 10 to 40 cm thick. Beds are dominantly medium-grained and in some cases slightly graded. The coarsest beds (coarse-grained) commonly contain abundant hematite- and magnetite-rich slaty iron formation rip-ups at their bases. Packages of parallel and wavy laminated hematite- and magnetite-rich slaty iron formation 1 to 6 cm thick are frequently interbedded between grainstone beds. In some instances very-fine grained and fine-grained, graded chert beds 1 to 2 cm thick separate coarser layers.

Subrounded and rounded clasts comprising beds range in diameter from 0.3 to 0.9 mm and are composed of mosaic chert, iron carbonate and hematite. Carbonate grains appear as amorphous microcrystalline masses and are commonly

coated with a thin, fibrous, carbonate alteration rind 0.05 mm thick. In some instances a thin veneer of hematite 0.05 mm thick also coats carbonate grains. Hematite grains are frequently shrinkage cracked and infilled with blocky mega-quartz (Fig. 11). Chert grains are frequently coated with hematite (Fig. 12). The dominant pore fillers are mosaic chert and drusy and blocky mega-quartz. Clusters of prismatic crystals of minnesotaite and greenalite 0.2 mm in diameter commonly occur disseminated throughout these cherty matrix phases. In regions which have undergone pervasive carbonate alteration ankerite and siderite are the primary pore fillers. In these areas mosaic chert grains are wholly or partially replaced by carbonate creating a complex melange of ankerite, siderite and chert.

The wavy and parallel laminated hematite- and magnetite-rich slaty iron formation packages between grainstone beds are formed of alternating chert-rich and magnetite/hematite-rich layers. In all instances bounding surfaces between laminations are sharp. Chert-rich layers are non-graded, range between 2 and 8 mm in thickness and are composed of rounded, silt-sized and very fine-grained sand-sized mosaic chert, hematite and magnetite grains in grain to grain contact, and small, angular rip ups 2 to 5 mm in length made of aggregates of silt-sized mosaic chert grains. Slaty iron formation laminations vary in thickness from 1 to 2 mm and are dominantly composed of subhedral, magnetite and hematite crystals 0.2 to 0.5 mm in width with lesser amounts of rounded, silt-sized grains of mosaic chert and subhedral grains of graphite 0.03 to 0.05 mm in diameter. Rare,

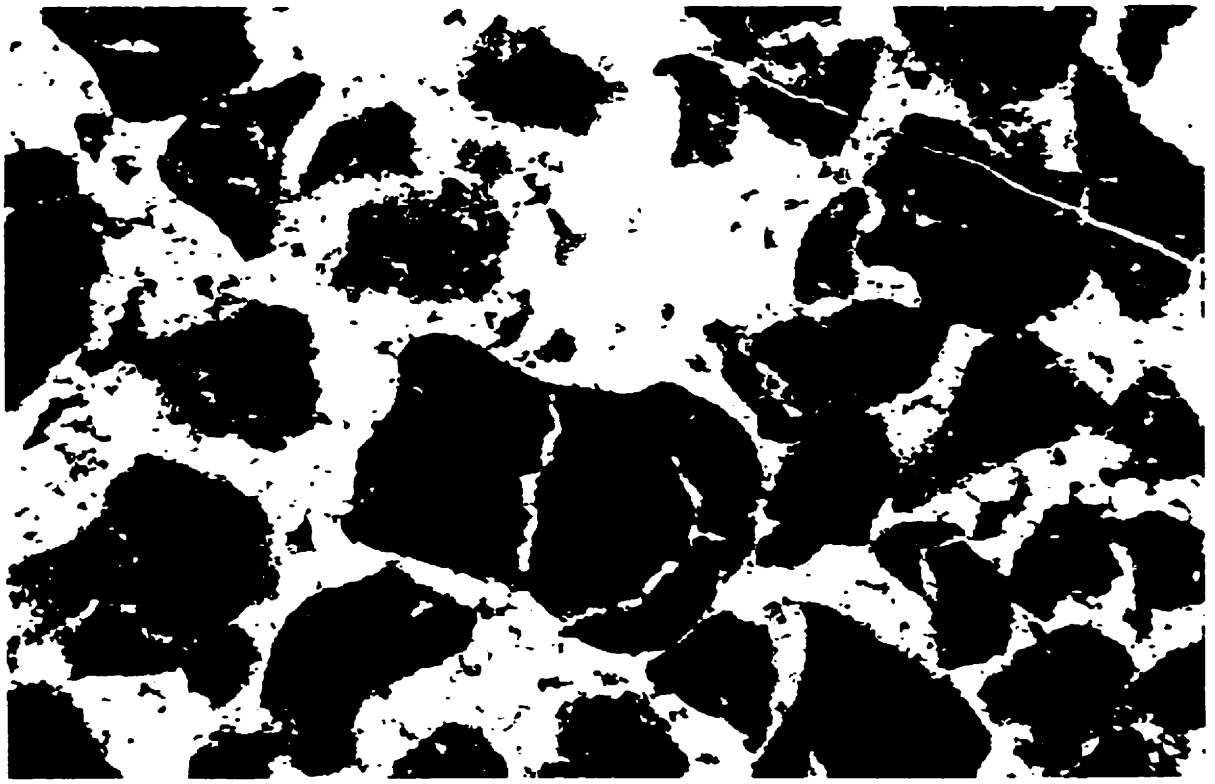

Fig. 11. **Gm** facies. Rounded mosaic chert grains coated with hematite in matrix of blocky mega-quartz. Grains have inundated boundaries and appear "squeezed" into one another. Field of view 2 mm, trans. XN.

Fig. 12. **Gm** facies. Subrounded, shrinkage cracked hematite grains coated with isopachous rims of fibrous chert, in a matrix of blocky and drusy mega-quartz. Field of view 2 mm, trans. XN.

carbonate altered mosaic chert and hematite grains 2 mm in diameter are sometimes observed disseminated throughout cherty and slaty layers.

Gm facies grainstones are characteristically finer-grained, more hematite-rich and regularly contain thicker slaty iron formation packages between grainstone beds than their **Gc** facies counterparts. Like **Gc** facies grainstones however, grains which comprise this facies also possess inundated grain boundaries which sympathetically conform around opposing grains.

Massive, medium- and/or coarse-grained, chert-carbonate grainstone with rip ups (Gi)

Beds composing the **Gi** facies are between 5 and 20 cm thick (average 8 to 12 cm thick), fine-grained, moderately well-sorted, and generally massive. Some thicker beds may be cross stratified, however, this interpretation is somewhat equivocal because accurate assessment of these larger-scale bed forms in the drill core was not always possible. Magnetite- and hematite-rich slaty iron formation rip-ups at the base of beds vary from 7 X 3 mm to 15 X 4 mm. Chert, iron carbonate, hematite grains comprising beds are rounded and range in diameter from 0.3 to 1.5 mm, averaging 0.75 to 0.9 mm. The largest grains observed where 2.0 mm in diameter. Siliceous grains are formed of mosaic chert and posses inundated grain boundaries which sympathetically conform around opposing grains (Fig. 13). Many grains are coated with a thin isopachous rim of fibrous chert (Fig. 13). Carbonate grains are in grain to grain contact and also appear squeezed into one

Fig. 13. **Gi** facies. Mosaic chert grains with inundated grain boundaries and fibrous chert rims. Matrix phases include drusy and blocky mega-quartz. Also disseminated throughout grains are silt-sized subhedral hematite crystals. Field of view 2 mm, trans. XN.

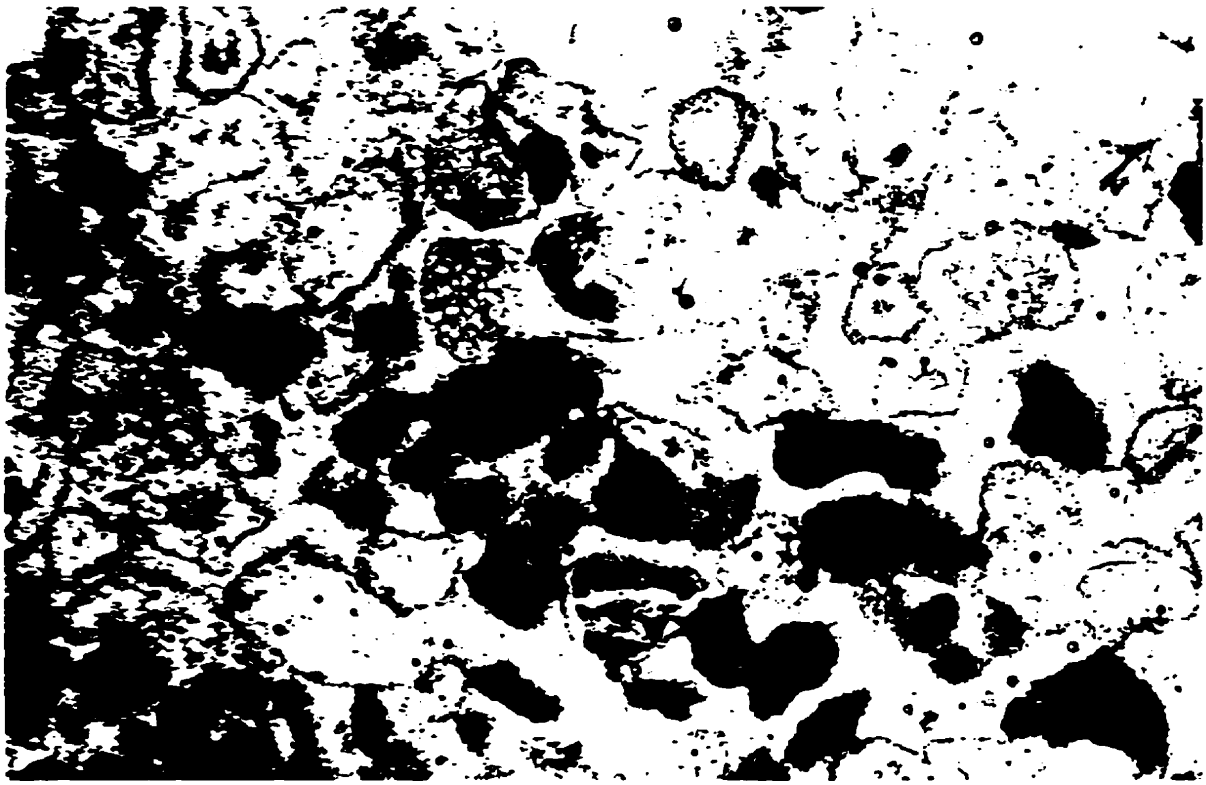

Fig. 14. **GI** facies. Subrounded iron carbonate and hematite grains (dark) with inundated grain boundaries. Field of view 4 mm, trans. PPL.

another as if they have been plastically deformed (Fig. 14). They are slightly finer-grained than their chert counterparts (average between 0.60 to 1.0 mm in diameter) and are coated with a thin, amorphous carbonate alteration rind 0.1 mm thick. Drusy and blocky mega-quartz are the dominant matrix phases. Unlike beds which comprise the **Gc** and **Gm** facies grainstones, **Gi** facies beds are stacked one directly upon the other; the interbedded magnetite-rich slaty iron formation packages and/or fine grained chert beds are absent within this facies.

Flaser bedded, medium-grained, chert-carbonate grainstone (Gf)

Two bed types comprise the **Gf** facies; 1) greenish, fine-grained beds composed of subangular to subrounded magnetite, mosaic chert and carbonate grains 0.3 to 0.7 mm in diameter and 2) greyish, slightly coarser beds formed of intensely altered, subangular, iron carbonate grains 0.5 to 1.0 mm in diameter. Both are massive, flaser bedded and loaded. Beds range in thickness from 10 to 20 cm (average 10 to 15 cm). Beds are identical to fine-grained chert beds composing the **Gw** facies, however, the magnetite rich slaty packages present within the **Gw** facies are absent in the **Gf** facies. Instead, magnetite laminae 1 to 4 mm thick are present as isolated concave upward simple and bifurcated flasers between grainstone layers.

Chert grains composing finer-grained beds are commonly coated with a thin (0.01 mm thick) isopachous rim of fibrous chert. Grains are typically in grain to

grain contact but show no evidence of deformation. The matrix is composed of a complex melange of mosaic chert, blocky mega-quartz and spherulitic chalcedony. Rare, carbonate oncolitic fragments within the matrix are pervasively replaced by chert forming atoll textures.

Slightly coarser beds composed of subrounded altered iron carbonate grains are moderately well sorted. Grains are in matrix and clast support, have inundated grain boundaries, and are commonly coated with a thin carbonate alteration rind 0.01 to 0.02 mm thick formed of small clusters of prismatic iron carbonate crystals (Fig. 15). Drusy mega-quartz is the dominant pore filler in these beds.

Often pervasively altered, very fine-grained grainstone laminations, 2 to 3 mm thick, are interbedded between coarser beds. Angular clasts comprising these finer laminations are formed of moderately well sorted, iron carbonate grains which average 0.25 mm in diameter (the largest is 0.5 mm). The dominant matrix phases are chalcedony with subordinate amounts of mosaic chert. Stylolites and carbonate veins which cut across bedding planes are not uncommon within the Gf facies.

*Wavy bedded, medium-grained, chert-carbonate grainstone (**Gw**)*

Greenish grainstone beds forming this facies are well-sorted, fine-grained, range in thickness between 3 and 20 cm (average 5 to 10 cm) and are probably

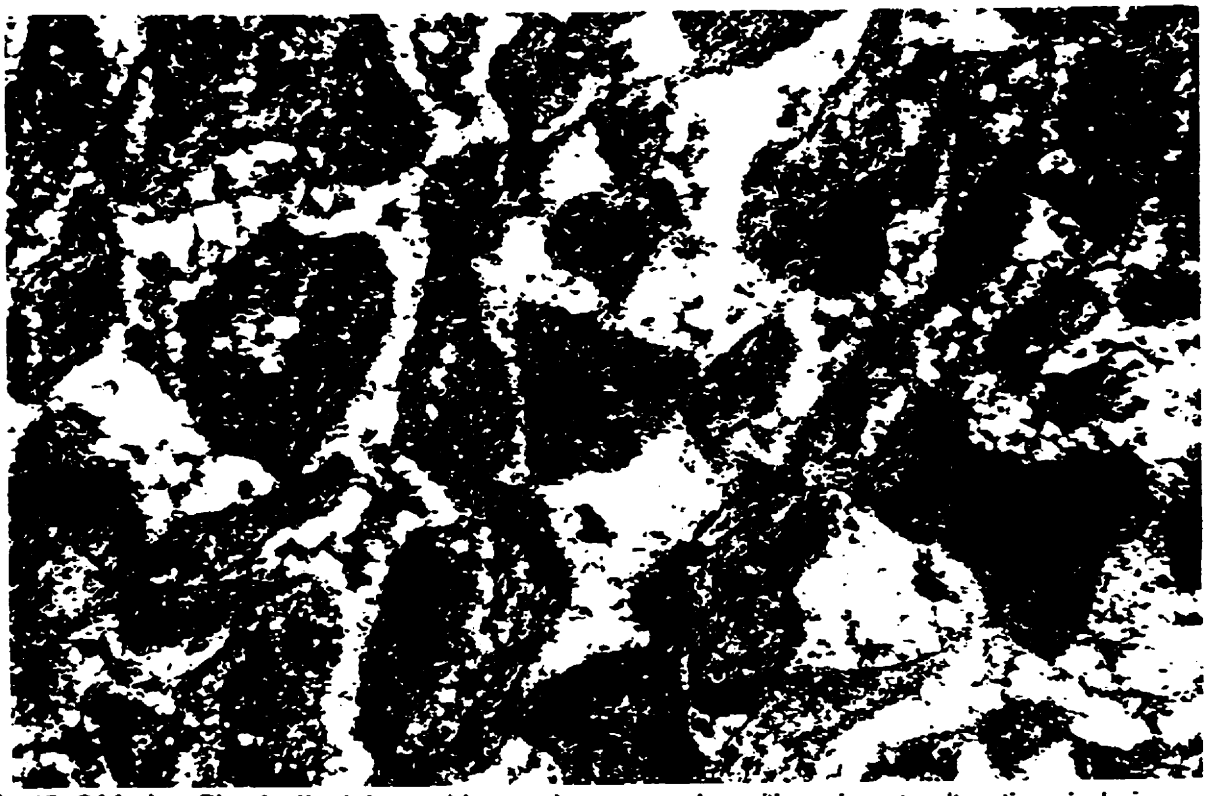

Fig. 15. **Gf** facies. Plastically deformed iron carbonate grains with carbonate alteration rinds in a matrix of drusy mega-quartz. Field of view 2 mm, trans. XN.

Fig. 16. **Gw** facies. Subrounded mosaic chert and shrinkage cracked magnetite grains (dark) with isopachous rims of fibrous chert. Fractures are infilled with blocky mega-quartz. The matrix is composed of blocky mega-quartz. Field of view 2 mm, trans. XN.

cross stratified; thinner beds may be ripple laminated. Interbedded between grainstone beds are black, magnetite-rich, slaty packages, 2 to 4 cm thick composed of slightly graded wavy and parallel laminated layers 2 to 3.5 mm in thickness. Grainstone beds are comprised of equal proportions of subrounded magnetite and mosaic chert grains 0.3 to 0.6 mm in diameter. Rounded carbonate grains form only a minor constituent (1 to 2 %) of **Gw** facies beds. Magnetite grains are commonly fractured and infilled with mosaic chert and blocky mega-quartz (Fig. 16). Clasts are in grain-to-grain contact and conform sympathetically around each. All grains are coated with a thin (0.15 mm thick) isopachous rim of fibrous chert (Fig. 16). The matrix is composed of blocky mega-quartz and mosaic chert with small zones of recrystallized, subhedral carbonate crystals.

Parallel bedded, fine- and/or medium-grained, chert-carbonate grainstone (Gp)

Two intimately interbedded bed types compose this facies; 1) slightly graded, clast supported, parallel bedded, fine- to medium-grained chert/carbonate beds 0.5 to 20 cm thick (average 1 to 6 cm) and, 2) hematite-rich slaty iron formation laminations 1.5 to 2 mm thick forming 1 to 3 cm thick packages interbedded between grainstone beds (Fig. 17). Bounding surfaces between beds are sharp.

Grainstone beds are comprised of subrounded, poorly to moderately well sorted, carbonate, mosaic chert, and hematite grains 0.2 to 0.5 mm in diameter

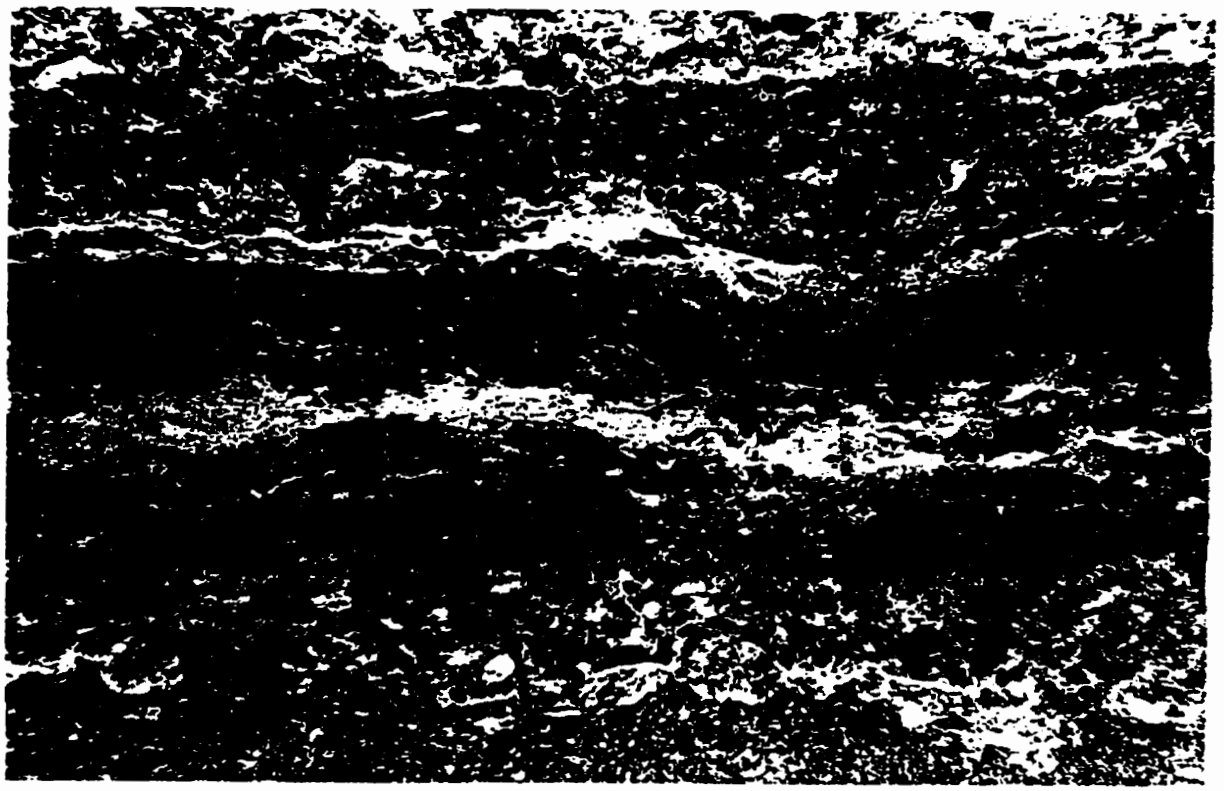

Fig. 17. Gp facies. Interlayered parallel bedded, hematite-rich grainstones and disrupted, hematite-rich slaty laminations. Slaty layers are frequently loaded. Field of view 6 mm, ref. PPL.

(average 1 mm). Chert and hematite grains are shrinkage cracked and are infilled with secondary mosaic chert and iron carbonate crystals. Carbonate grains are commonly squeezed into opposing grains. Some are enveloped in a thin isopachous rim of calcite 0.3 mm thick and contain isolated prismatic clusters of minnesotaite and greenalite 0.1 to 0.2 mm in diameter. The dominant matrix phase is mosaic chert. The thickest and coarsest beds contain hematite-rich slaty iron formation rip-ups, up to 8 mm in length, at their bases.

Hematite-rich slaty laminations composing packages have undergone pervasive, post-depositional carbonate alteration; epitaxial dolomite laths (0.25 to 0.5 mm in diameter) commonly cut across slaty layers. Small wisps of grainstone 1 mm X 5 mm frequently highlight bounding surfaces between laminations. In some instances very fine-grained, slightly graded, hematite-rich grainstone laminations are interbedded between slaty layers. Grainstone laminations are composed of subangular hematite, mosaic chert and carbonate grains 0.1 to 0.2 mm in diameter and silt-sized, angular, monocrystalline, quartz grains and graphite flecks. Slaty layers in close proximity to thicker grainstone beds are frequently disrupted and loaded (Fig. 17).

*Hummocky-cross-stratified, fine-grained, hematite-rich, chert grainstone (**GHCS**)*

This facies is closely associated with the **Gp** facies and is comprised of reddish-brown very fine-grained and fine-grained, gently curving grainstone layers

0.5 to 1.5 cm thick which terminate at low angles. Similar fine-grained sandstone layers within drill core from the Cardium and Nikanassin Formations in southern and central Alberta have been interpreted by Walker (1984) as representing hummocky-cross-stratification. Like the chemical sedimentary layers those in the Cardium and Nikanassin Formations are also gently curving and terminate at low angles.

Grains comprising layers within this facies range in diameter from 0.2 to 1.0 mm (the largest grain was 2.0 mm), are composed of moderately well-sorted, fine-grained, subrounded mosaic chert and hematite grains, and are commonly fractured and shrinkage cracked. Fractures are filled with blocky mega-quartz. Some chert grains are coated with a thin veneer of hematite dust 0.3 mm thick. Large, subhedral, optically continuous carbonate crystals which form the matrix (blocky carbonate cement) envelop individual chert grains and cut across bedding planes forming a poikiolitic texture. Sometimes, rare, rounded, detrital quartz grains are scattered throughout beds. Bedding parallel stylolites are also abundant throughout the **GHCS** facies.

*Interbedded, parallel and wavy laminated, magnetite-rich slaty iron formation and fine/very fine-grained chert grainstone (**Sc**)*

Two highly altered, intimately associated bed types compose this facies, 1) parallel and wavy laminated magnetite-rich slaty iron formation, and 2) fine/very fine-grained chert layers. Each possesses sharp upper and lower bounding surfaces and show no evidence of grading. Wavy and parallel laminated magnetite-

rich layers range in thickness from 1 to 4 mm (Fig. 18). Laminations are comprised of subhedral and euhedral magnetite crystals 0.05 to 0.2 mm in diameter (average 0.08 to 0.1 mm), in a matrix of intricately intergrown prismatic iron silicate crystals, 0.02 mm in length (minnesotaite and/or greenalite) and mosaic chert. Blocky and drusy mega-quartz are common pore fillers between larger magnetite grains.

Pervasively altered chert layers vary in thickness from 0.2 to 3 cm and are comprised of a complex melange of subrounded and rounded, magnetite, iron carbonate and mosaic chert grains 0.05 to 0.2 mm in diameter. Grains are moderately well-sorted, in grain-to-grain contact and are enveloped in a matrix of microcrystalline ankerite and siderite. Carbonate grains are frequently coated with a thin veneer of magnetite 0.05 mm thick. In many instances chert grains have been completely or partially replaced by iron carbonate. Unlike chert beds comprising **Gp** and **GHCS** facies grainstone beds, those comprising this facies are finer-grained and enriched in magnetite.

Parallel, and wavy laminated, magnetite-rich, slaty iron formation (Sl)

This facies is composed of monotonous, black, parallel and wavy laminated, magnetite-rich layers ranging in thickness from 1 to 4 mm. Laminations possess sharp upper and lower bounding surfaces and in most circumstances do not exhibit grading. Layers are generally monomineralic, composed almost entirely of

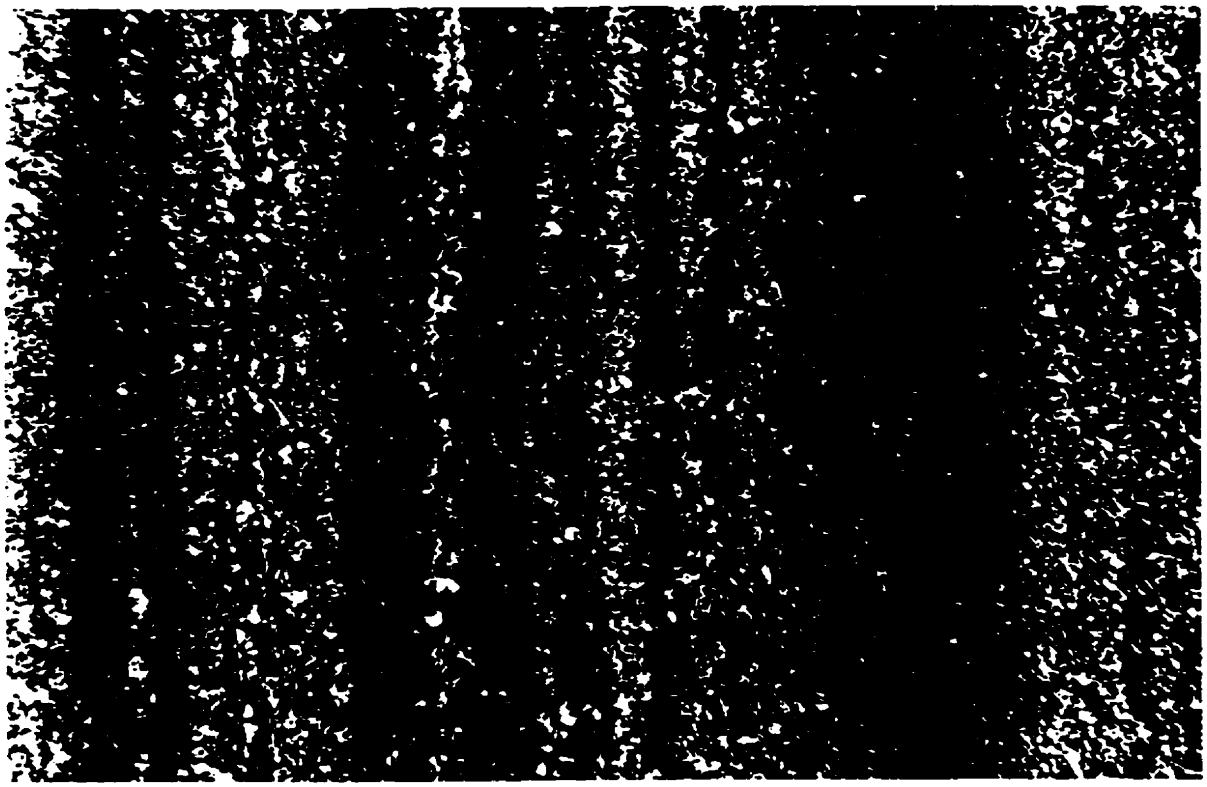

Fig. 18. Sc facies. Slaty laminations with sharp upper and lower bounding surfaces. Dark areas are magnetite-rich and lighter regions are chert-rich. The younging direction is to the left. Field of view 4 mm, trans. PPL.

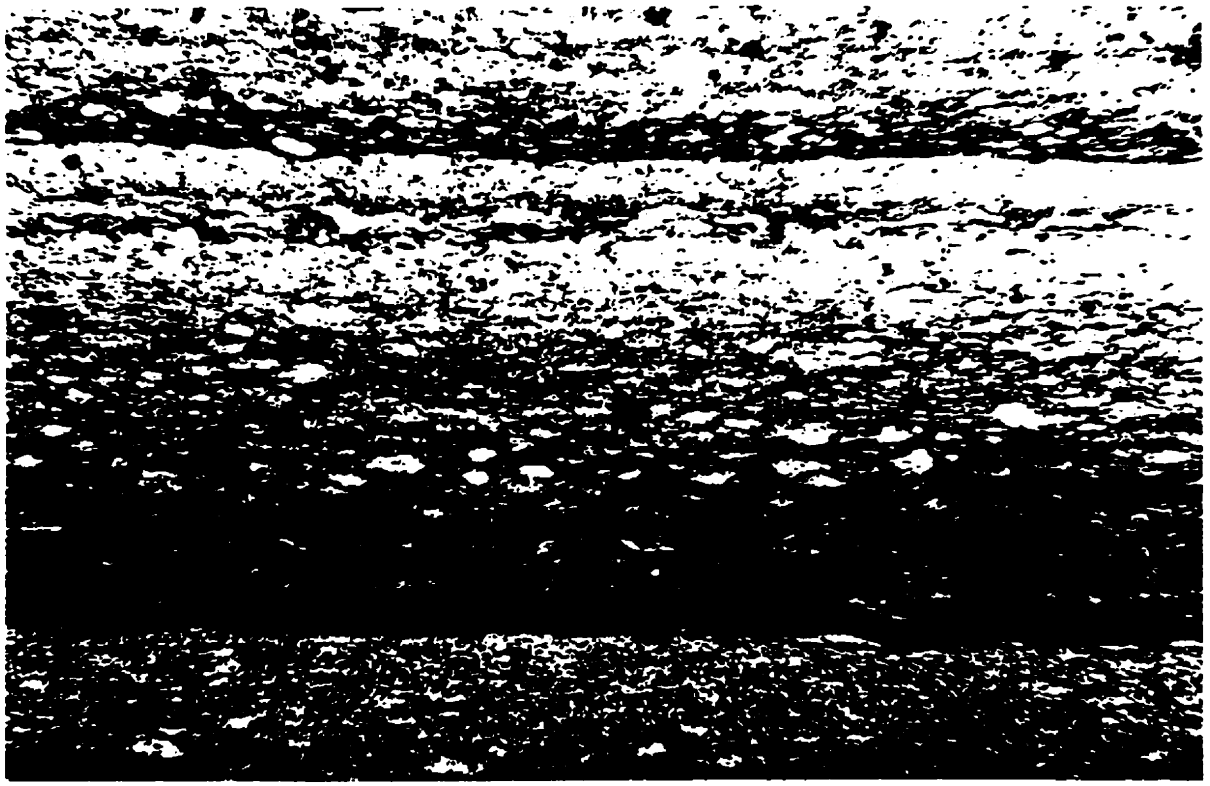

Fig. 19. Sl facies. Graded slaty lamination with magnetite-rich bottom (dark) and chert-rich top (light). Field of view 2 mm, trans. PPL.

subhedral and euhedral magnetite crystals 0.2 to 0.4 mm in diameter with silt-sized carbon flecks disseminated throughout. In the manganese-enriched chemical slates from the Cuyuna north range in east-central Minnesota (Fig. 2) manganese oxide forms an important matrix constituent between magnetite grains. More siliceous laminations contain rounded grains of mosaic chert, varying in diameter from 0.1 to 0.15 mm, in clast support in a magnetite matrix. In rare instances these chert-rich layers are very slightly graded, changing from a magnetite-rich bottom to a chert-rich top (Fig. 19). Sometimes, subrounded, detrital, silt-sized monocrystalline quartz grains exhibiting undulose extinction are also present within layers.

Cryptalgal lithofacies

Stromatolities (Ad)

Stromatolitic horizons average between 2 and 6 cm in thickness and are stacked one upon another. Field investigations (this study) demonstrate that most algal bioherms are LLH structured (Logan, 1964). In O'Connor township stromatolites are hematite-rich and have been wholly replaced by chert. Internally, they are composed of discontinuous, wispy laminations of mosaic chert 0.5 to 2.0 mm thick, which are sometimes interbedded with rare 1 to 3 mm thick laminations of fine- to medium-grained chert grainstone. A thin veneer of hematite commonly coats bounding surfaces between laminations. Rare, small, detrital polycrystalline quartz grains, 0.5 mm in diameter, are sometimes present within this coating. Prismatic ankerite laths, 0.2 to 1.0 mm long, and euhedral dolomite rhombs, 0.3

mm in diameter, frequently appear as epitaxial overgrowths between cryptalgal laminations. Bedding parallel stylolites commonly cut across iron carbonate-rich, cryptalgal laminations. Also found within layers are abundant, disseminated, subhedral hematite grains 0.1 to 0.2 mm in width.

Oncolites (Ao)

Oncolitic beds composing this facies vary in thickness from 3 to 8 cm. Cryptalgal structures are both in clast and matrix support, and moderately well-sorted and average 1 to 5 mm in diameter. The largest oncolites (5 X 15 mm) have grown on hematite- and magnetite-rich slaty iron formation rip ups. These rounded, ovoid and oblate SS structured (Logan, 1964) organosedimentary structures occur in two modes; randomly stacked hemispheroids (R-type), and concentrically stacked spheroids (C-type) (Fig. 20) (Logan, 1964). Discontinuous laminations composing cryptalgal structures range between 0.05 and 0.1 mm. Oncolites grew around fine- and medium grained polycrystalline quartz and mosaic chert grains (Fig. 20). In some instances their core has been pervasively replaced by blocky mega-quartz. Oncolites are commonly coated with a thin isopachous rim of fibrous chert, 0.05 to 0.1 mm thick. This rim is overlain by a spherulitic chalcedony rind 0.2 to 0.3 mm thick. Blocky and drusy mega-quartz are the dominant pore fillers. Spherulitic chalcedony is the primary matrix phase between larger oncolites. Smaller organosedimentary structures, 1 to 2.5 mm wide, are pervasively replaced by iron carbonate and in some instances replaced only slightly

Fig. 20. Ao facies. R-type (randomly stacked) and S-type (concentrically stacked) oncolites with cores of monocrystalline quartz (lower left) and mosaic chert (right). Elongate oncolite is R-type and others are S-type. The discontinuous laminations comprising oncolites (best seen in elongate oncolite) distinguishes them from concentrically zoned, ooids. Field of view 4 mm, trans. XN.

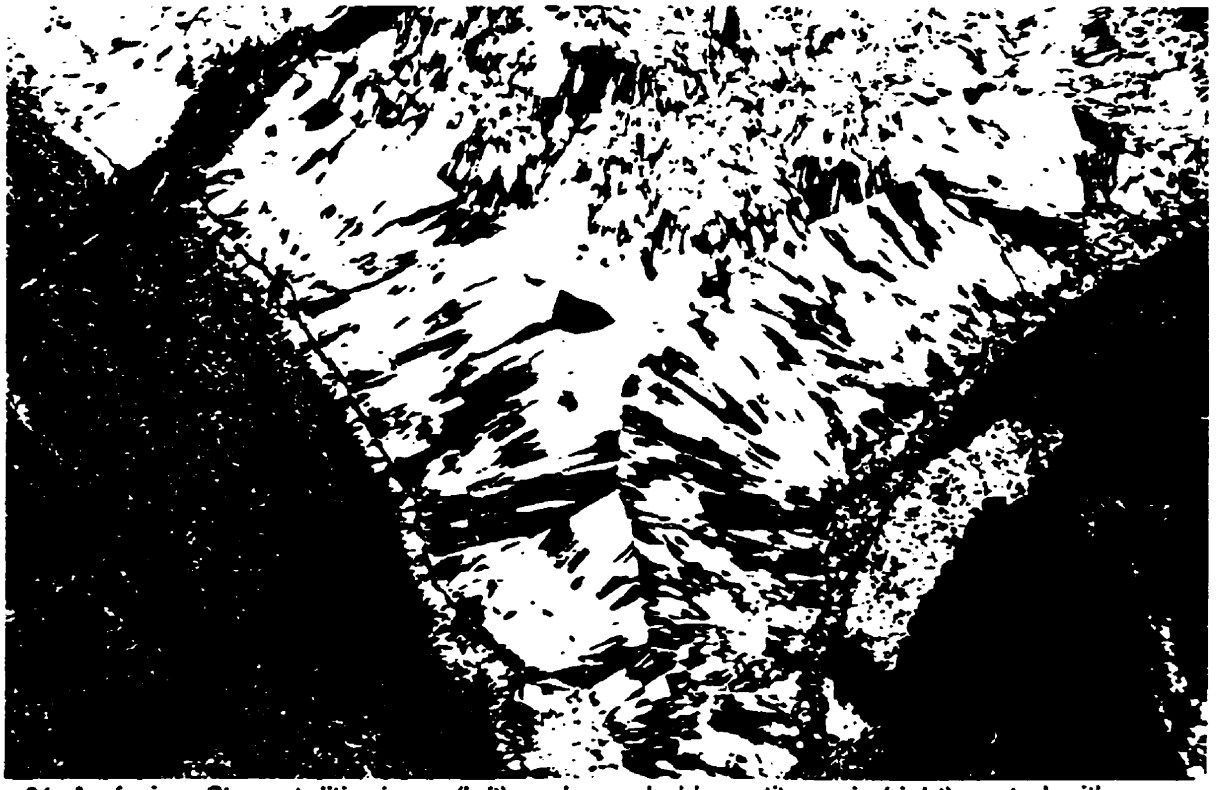

Fig. 21. Ao facies. Stromatolitic rip up (left) and rounded hematite grain (right) coated with an isopachous rim of chert in a matrix of spherulitic chalcedony. Field of view 2 mm, trans. XN.

by mosaic chert.

Stromatolitic rip-ups 1 to 4 mm in length are the only other framework grains present (Fig. 21). Like the larger oncolites they too are coated with a thin isopachous rim of fibrous chert 0.1 mm thick and are enveloped in a matrix of shperultic chalcedony.

CHAPTER 3: GUNFLINT IRON FORMATION- DETAILED CORRELATIONS

3.1 Introduction

The approximately 1.9 Ga, flat lying Gunflint and Rove Formations comprise the Animikie Group in the Thunder Bay district in northwestern Ontario (Figs. 1, 2 and 3). The Gunflint is approximately 175 m thick and is essentially a sequence of grainstones comprised of eleven lithofacies (Fig. 22). The Kakabeka conglomerate (Tanton, 1931) conformably underlies the Gunflint and forms the base of the sequence. This thin, discontinuous, pebble conglomerate reaches a maximum thickness of 1.5 m (Goodwin, 1956, 1960) and rests directly on the Archean basement. The Rove formation, a 700 m thick succession of volcanic slates and turbiditic siltstones (Morey, 1967, 1969; Guel, 1970, 1973), conformably overlies the Gunflint in Ontario and north-eastern Minnesota.

Detailed stratigraphic investigations (this study, Shegelski, 1982) have demonstrated that Goodwin's (1956, 1960) division of Gunflint strata has become less useful as more units have been discovered. Goodwin (1956, 1960) also recognized iron formation facies largely based on diagenetic or low grade metamorphic mineral assemblages; a technique not regarded as being a sensitive indicator of paleoenvironment (Chapter 2). Consequently, the need arose to redefine Gunflint stratigraphy to ensure an accurate paleoenvironmental

FACIES


Cp


Gc


Gf


Gw


Gp


Gi


Vs


Vt


Ad, Ao


Superior province

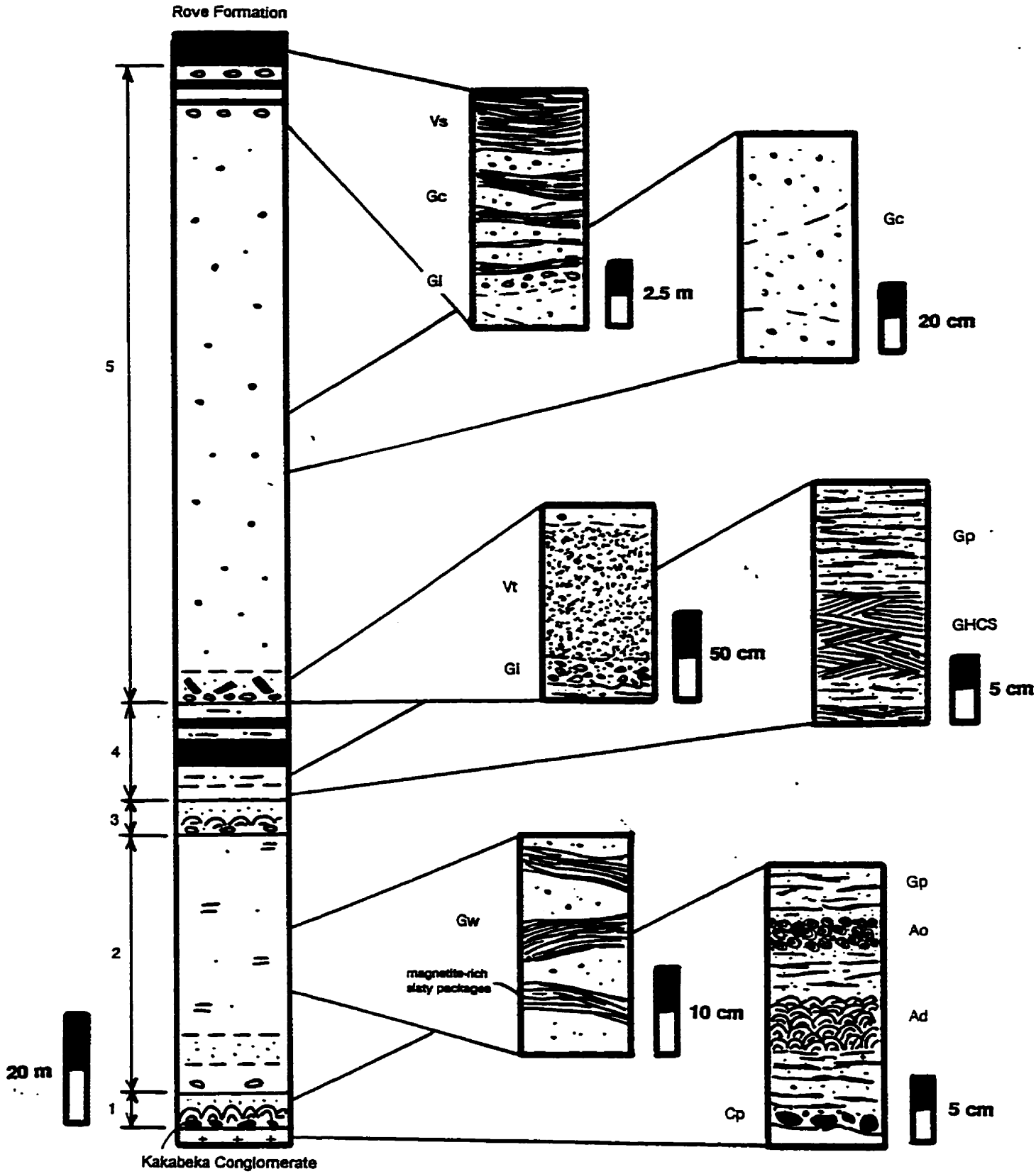

Fig. 22. Generalized stratigraphic section of the Gunflint Formation in the vicinity of O'Connor and Blake Townships. Numbers along the left side of the section correspond to members 1, 2, 3, 4, and 5. Details of facies associations comprising members are shown on the right.

interpretation of iron-bearing strata.

3.2 Vertical facies changes

The Gunflint Formation reaches a maximum thickness of 175 m in Blake Township and is formed of 5 members comprised of 11 lithofacies (Fig. 22). The Kakabeka Conglomerate (**Cp** facies) forms the base of the Animikie Group in the Thunder Bay region. It is thin (0.22 m) and discontinuous, and rests unconformably on the greenstone-granite terranes of the Superior province; a medium- to coarse-grained hornblende granite in the vicinity of O'Connor Township. The Kakabeka Conglomerate is conformable into the base of the member 1. In O'Connor Township grainstones at this transition are hematite-rich. The members which comprise the Gunflint in O'Connor and Blake Townships, in ascending, order are;

Member 1

Member 1 is an 8 m thick unit comprised of **Gp**, **Ad** and sometimes **Ao** facies (Fig. 22). Member 1 is conformable with the underlying **Cp** facies conglomerate. Chert-carbonate grainstone facies at this transition are hematite-rich. When the Kakabeka conglomerate is absent member 1 forms the lowermost unit and rests unconformably over the Archean basement. Its basal contact contains abundant rip ups. Cryptalgal facies form two discrete horizons

interbedded within **Gp** facies grainstones. The first occurs 6 to 10 cm from the base of member 1 and is composed entirely of **Ad** facies. The second rests 3 to 6 cm above the first and is comprised of **Ao** facies organosedimentary beds 3 to 8 cm thick. **Ao** cryptalgal horizons always occur at slightly higher stratigraphic positions than those formed of **Ad** facies (Fig. 22). Bottom and upper contacts of stromatolitic and oncolitic beds are sharp with **Gp** facies grainstones.

Member 2

Member 2 is approximately 50 m thick and rests conformably over member 1 (Fig. 22). The base is characterized by a 7 m thick package of **Gi** facies grainstone overlain by a 6 m thick package of **Gf** facies grainstone. The remaining 37 m is composed of **Gw** facies grainstone, which is sometimes interbedded with 5 m thick packages of **Gf** facies grainstone. In Blake Township **Gw** facies grainstones of member 2 rest in gradational contact with **Gp** facies grainstone of member 1.

Member 3

Member 3 is an 8 m thick unit composed of **Gf, Ad** and **Ao** facies lying conformably over member 2 (Fig. 22). Cryptalgal facies of member 3 form two discrete horizons interbedded with **Gf** facies grainstones. The first is a 3 to 4 cm thick stromatolitic (**Ad** facies) layer underlain by a 6 cm thick bed of **Gi** facies grainstone. The second, when present, occurs 6 to 8 cm above the first as either a 2 to 3 cm thick LLH stromatolitic (**Ad** facies) horizon or a 2 to 3 cm thick SSR

interbedded within **Gp** facies grainstones. The first occurs 6 to 10 cm from the base of member 1 and is composed entirely of **Ad** facies. The second rests 3 to 6 cm above the first and is comprised of **Ao** facies organosedimentary beds 3 to 8 cm thick. **Ao** cryptalgal horizons always occur at slightly higher stratigraphic positions than those formed of **Ad** facies (Fig. 22). Bottom and upper contacts of stromatolitic and oncolitic beds are sharp with **Gp** facies grainstones.

Member 2

Member 2 is approximately 50 m thick and rests conformably over member 1 (Fig. 22). The base is characterized by a 7 m thick package of **Gi** facies grainstone overlain by a 6 m thick package of **Gf** facies grainstone. The remaining 37 m is composed of **Gw** facies grainstone, which is sometimes interbedded with 5 m thick packages of **Gf** facies grainstone. In Blake Township **Gw** facies grainstones of member 2 rest in gradational contact with **Gp** facies grainstone of member 1.

Member 3

Member 3 is an 8 m thick unit composed of **Gf, Ad** and **Ao** facies lying conformably over member 2 (Fig. 22). Cryptalgal facies of member 3 form two discrete horizons interbedded with **Gf** facies grainstones. The first is a 3 to 4 cm thick stromatolitic (**Ad** facies) layer underlain by a 6 cm thick bed of **Gi** facies grainstone. The second, when present, occurs 6 to 8 cm above the first as either a 2 to 3 cm thick LLH stromatolitic (**Ad** facies) horizon or a 2 to 3 cm thick SSR

and SSC oncolitic (**Ao** facies) cryptalgal bed. Cryptalgal horizons in member 3 are not as well developed, or extensive as those forming the organosedimentary beds in member 1. The transition into member 4 is gradational.

Member 4

Member 4 varies in thickness from 23 to 27 m and is formed of **Gp**, **GHCS** and **Vs** facies (Fig. 22). **Gp** facies grainstones of member 4 differ significantly from **Gp** facies comprising member 2; they are slightly finer-grained, more hematite-rich and possesses more hematite-slaty interlaminations between parallel bedded very-fine-grained and fine-grained chert grainstones. Rare coarse-grained hematite-rich chert beds 0.5 to 1.0 cm thick are sometimes interbedded within finer parallel laminated beds. When **GHCS** facies grainstones occur they appear at the base and top of member 4 intimately interbedded with **Gp** facies as 0.5 m thick packages (Fig 22). A pulse of volcanism is preserved as a 6 m thick volcaniclastic horizon (**Vs** facies) 7 m from the base of member 4 in O'Connor Township. Its bottom contact is sharp while its upper bounding surface is gradational into the parallel bedded chert- and hematite-rich beds (**Gp** facies) of member 4.

Member 5

Member 5 is composed entirely of **Gc** facies grainstones (Fig. 22). It extends vertically 80 m and is gradational into the overlying Rove Formation (Morey, 1967, 1969). In O'Connor Township the transition into the Rove has been

erosively removed, preserving only 23 m of member 5. The base of this uppermost member rests sharply on member 4 and is composed of a 20 cm thick bed of **Gi** facies grainstone which is abruptly overlain by a 1 m thick lapilli tiff bed (**Vt** facies) (Fig. 22). The tuff's upper contact is sharp and marks a sudden transition into the massive and cross stratified chert-carbonate grainstones. Here, grainstones are very coarse-grained and completely void of carbonate grains. In some instances small hematite-rich rip-ups are present. In Blake township the transition into the Rove Formation is marked by the intimate interbedding of individual chert-carbonate grainstone beds with wavy and parallel laminated packages of Rove slates (**Vs** facies) 2 to 6 cm in thickness. Also characterizing this transition are interbedded, sharp based, 6 to 10 cm thick **Gi** facies grainstone beds.

The Rove Formation is a sequence of slate, siltstone, very-fine-grained sandstones and rare, intraformational conglomerate, quartzite and carbonate rocks (Morey, 1967, 1969). Two members comprise this formation, a lower slaty (**Vs** facies) member 120 to 130 m thick, and an upper member composed of interbedded slates, siltstones, and very-fine-grained sandstones 600 m thick (Lucente and Morey, 1983). The uppermost 240 m also contains medium and thickly bedded beds of quartz-rich sandstones (Lucente and Morey, 1983).

3.3 Lateral facies changes

Members which comprise the Gunflint formation are generally laterally continuous over the well constrained, 300 m span of drill holes in O'Connor Township and over a distance of 15 km between townships (Figs. 23 and 24). The sequence thickens and coarsens slightly to the southeast.

The Kakabeka Conglomerate and member 1 were only intersected in holes TB0642 and TB0633, a span of 50 m. Their presence in hole TB0641 is uncertain as pervasive barite veining has destroyed the contact between the Gunflint and the basement. The Kakabeka conglomerate, is absent in Blake township (TB0218). Here a 6 cm thick bed of **Gi** facies grainstone forms the base of member 1 and unconformably overlies the Archean basement. Member 1 is laterally persistent between townships and does not exhibit any appreciable thickening or thinning over this 15 km interval. The thin cryptalgal beds (**Ao** and **Ad** facies) of member 1 intersected in drill holes TB0642 and TB0633 from O'Connor township are absent in drill hole TB0218 Blake Township. Stromatolitic and oncolitic beds are correlative only over these short, well constrained, 50 m intervals. Data which suggests otherwise is currently lacking as surrounding drill holes in O'Connor Township do not intersect these lowest-most units.

Member 2 is laterally continuous as a 50 m thick unit between townships

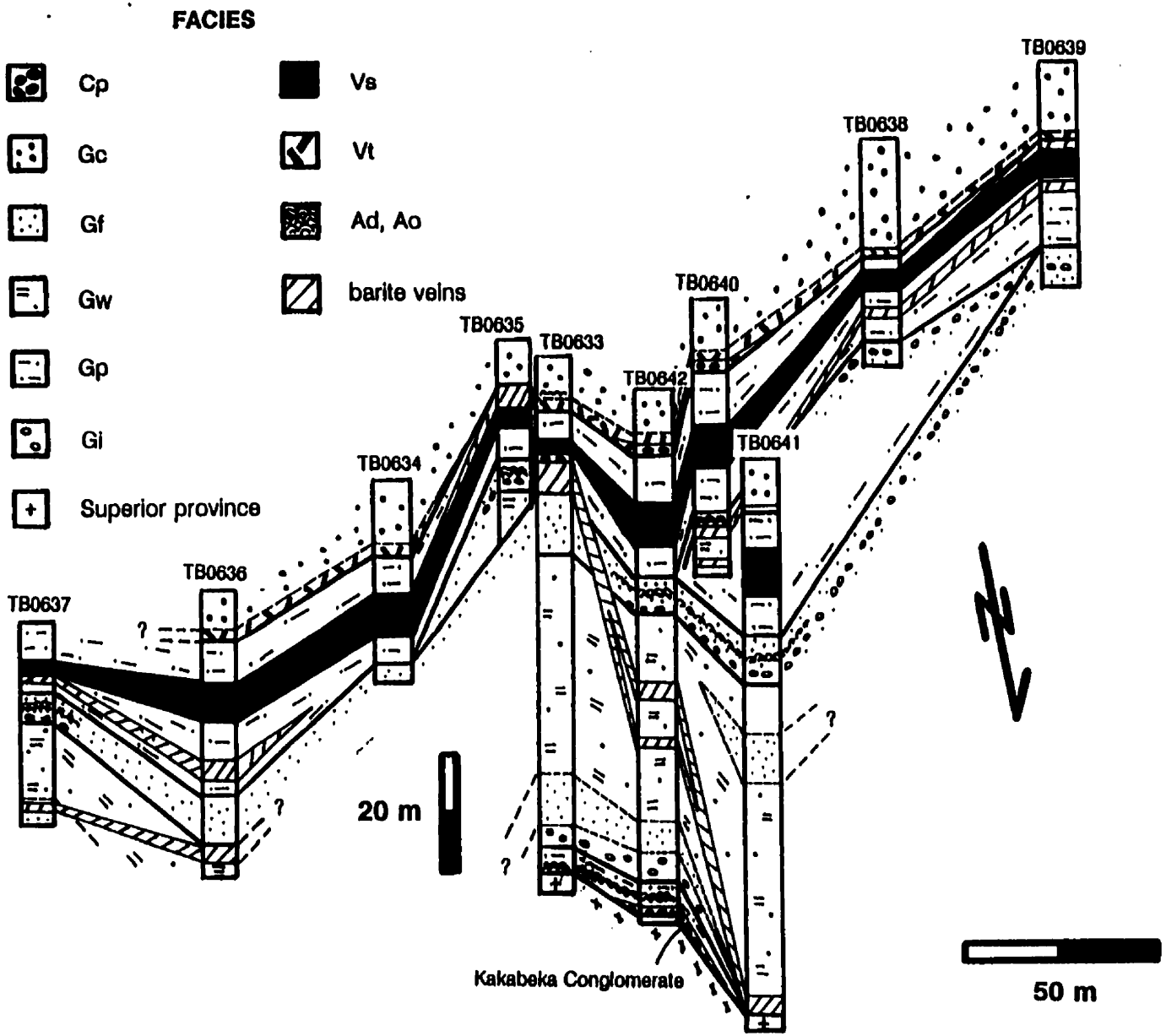

Fig. 23. Fence diagram showing detailed stratigraphic correlations of iron-bearing members between closely spaced drill holes in O'Connor Township.

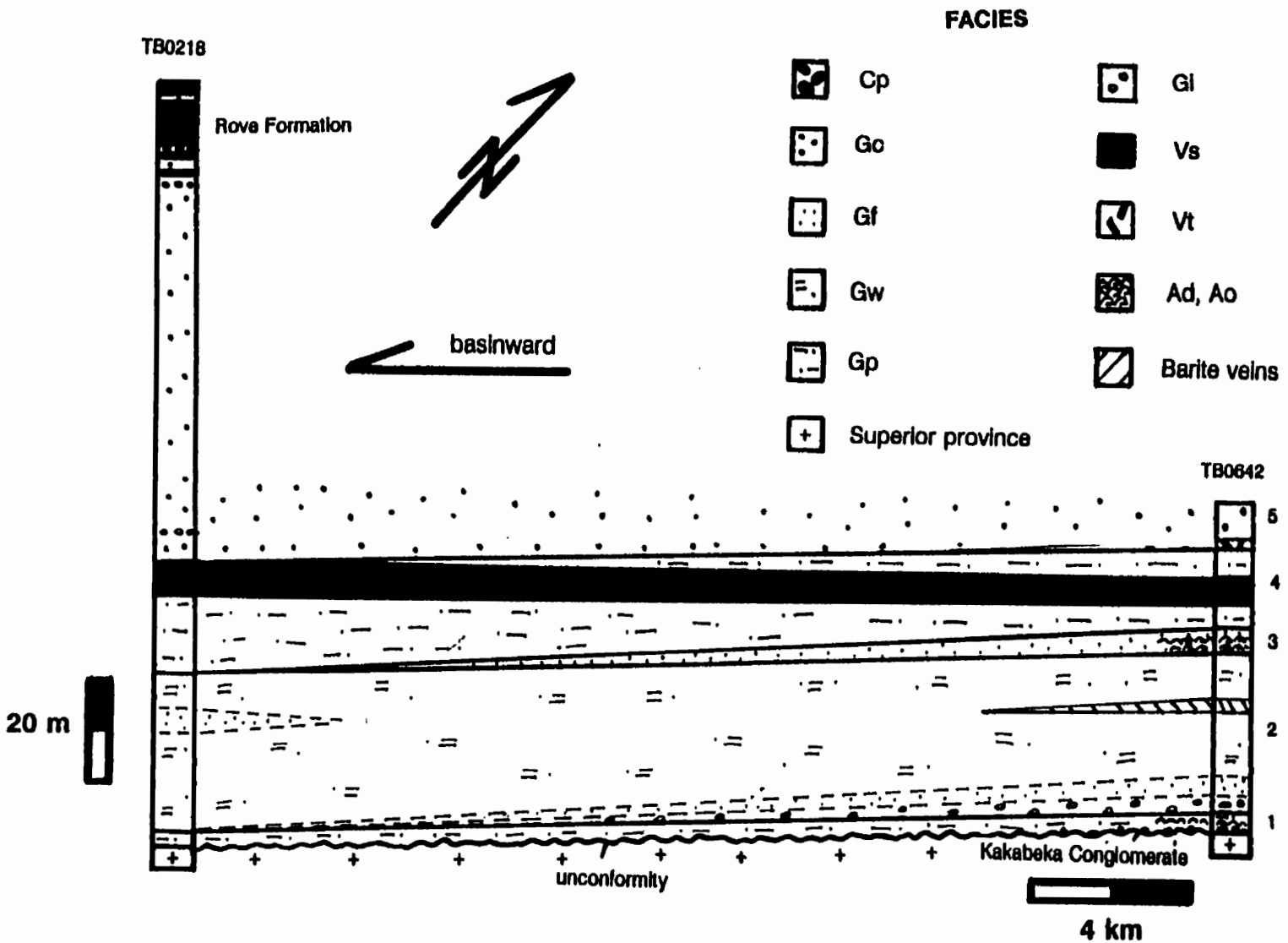

Fig. 24. Fence diagram showing stratigraphic correlations of iron-bearing members between O'Connor and Blake Townships.

and shows no considerable change in thickness. In O'Connor Township the basal package of **Gi** and **Gf** facies grainstone is correlatable only between drill holes TB0642 and TB0633, a distance of 50 m. It pinches laterally to the northwest towards drill hole TB0641. Their lateral continuity to the south is uncertain as surrounding drill holes do not intersect the base of this member. 8 to 10 m thick packages of **Gf** facies grainstones near the top of this unit are present within drill holes from O'Connor and Blake Townships (TB0641 and TB0218 respectively). These units are laterally continuous over at least a 50 to 100 m interval. Drill hole data which suggests otherwise is lacking.

Member 3 is correlatable only in O'Connor Township. It forms a laterally continuous unit showing little or no change in thickness. Stromatolitic and oncolitic horizons (**Ad** and **Ao** facies) present within member 3 (TB0641, TB0642 and TB0637) pinch laterally over a span of 50 to 75 m. The **Gi** facies bases of stromatolitic beds are laterally persistent over a larger interval than the cryptalgal beds which overlie them. These beds correlate over a distance of 100 to 125 m (TB0640, TB0641, TB0642, TB0637, TB0638, TB0639). Oncolitic horizons (**Ao** facies) are less laterally persistent than their stromatolitic counterparts (**Ad** facies). Member 3 pinches laterally to the south towards Blake Township.

Member 4 is present in O'Connor Township as a laterally continuous unit which exhibits a marked variation in thickness. It ranges from 4 m in drill hole

TB0637, to 27 m in drill hole TB0641 and TB0642. The **GHCS** grainstones at the base of this member (TB0640, TB0641, TB0642, TB0637 and TB0639) are correlatable over a distance of 100 to 125 m. The presence of **GHCS** facies grainstone in drill hole TB0633 is uncertain as pervasive barite veining has destroyed the lowermost part of member 4 in this drill hole. In Blake Township the **GHCS** facies grainstone is absent, however, its presence may be obscured by the lack of lateral control of drill holes. Member 4 thickens slightly towards Blake Township reaching a maximum thickness of approximately 30 m. The 6 m thick volcaniclastic horizon (**Vs** facies) present within this member is also laterally persistent between drill holes in O'Connor and Blake Townships.

Member 5 is correlatable between townships. The **Vp** facies volcaniclastic bed comprised which marks the base of this member is present only in the closely spaced drill holes of O'Connor township; it pinches laterally towards the southeast. In Blake Township a 10 m thick package of **Gc** facies grainstone enriched with fine volcaniclastic sediment forms the base of this member.

3.4 Depositional cyclicity

Examination of vertical grainsize trends of facies comprising the Gunflint formation shows that three changes in relative sea level punctuated, and controlled

Gunflint sedimentation (Fig. 25); a basal, 20 m thick, fining upward transgressive succession extending from the base of the sequence to the middle of member 2, a middle, 20m thick, coarsening upwards regressive succession, and a 125 m thick upper transgressive phase, the lower portion (member 5) of which consists of numerous, stacked, coarsening upwards, chert-carbonate grainstone sequences. These previously unrecognized trends span a vertical distance of 5 to 10 m and coarsen gradually from medium-grained chert-carbonate **Gi** facies grainstones to coarse-grained, chert-carbonate **Gi** facies grainstones. Their top contact is gradational over a distance of 1 m into the base of the overlying cycle. The average grainsize of each cycle becomes progressively finer upward, toward the Rove Formation. The presence of similar allocyclic trends has been recorded by Morey (1983). However, their relative stratigraphic positions differs significantly from those observed in this study.

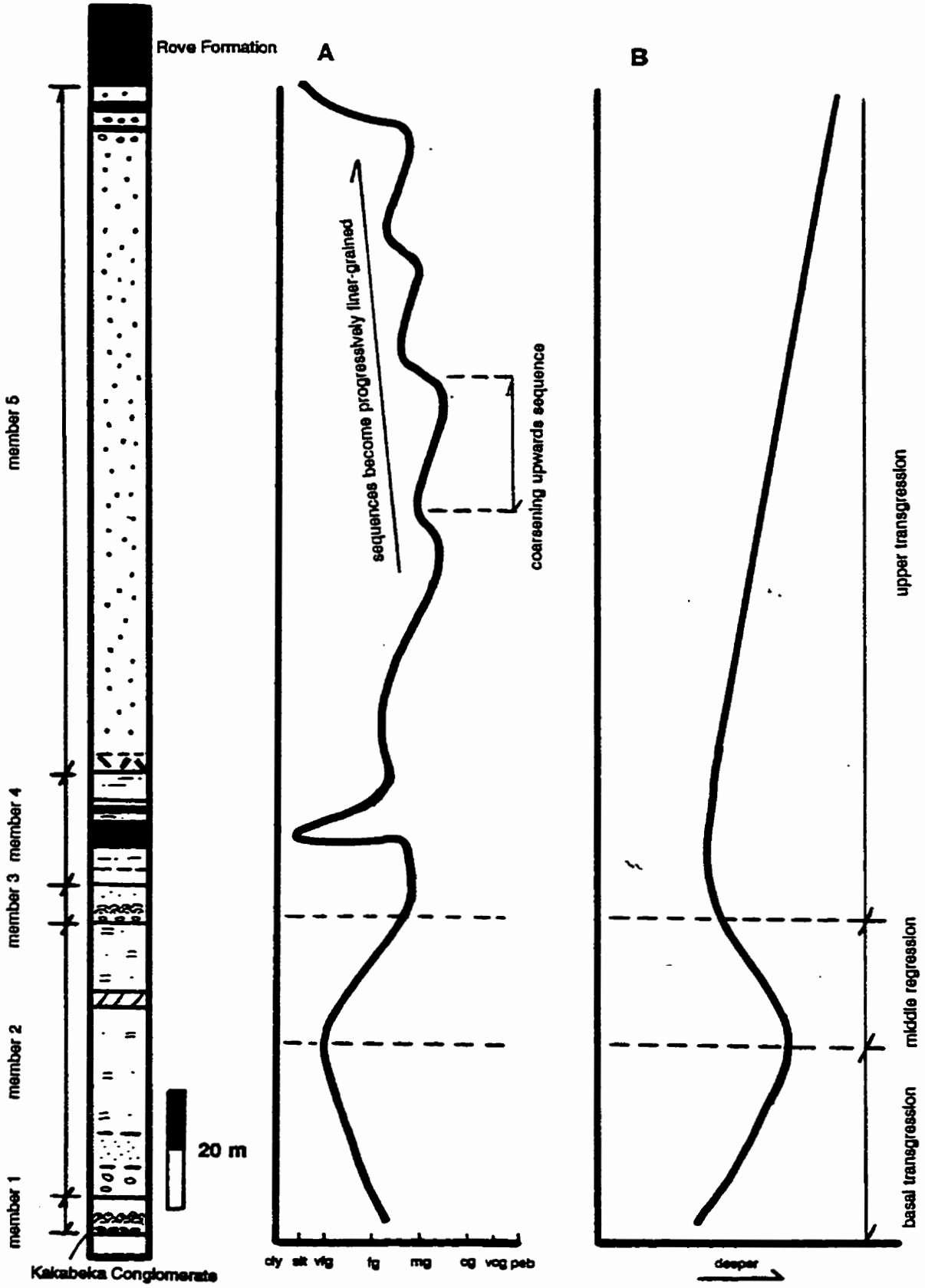

Fig. 25. Generalized stratigraphic section of the Gunflint Formation and moving average plot of grain-size (A) with corresponding sea level curve (B). Grain-size plot reveals that iron formation deposition in O'Connor and Blake Townships was controlled by three changes in relative sea level, and that member 5 is comprised of smaller coarsening upwards grainstone successions which become progressively finer grained stratigraphically upward.

CHAPTER 4: GUNFLINT IRON FORMATION-PALEOGEOGRAPHIC RECONSTRUCTION

4.1 Introduction

Lateral and vertical facies changes within the Gunflint Formation indicate deposition occurred on a shallow, non-barred, microtidal, storm-enhanced shelf with little clastic influx. Bedforms and internal sedimentary structures composing Gunflint strata are directly comparable to those found in modern nearshore-to-shallow marine clastic and carbonate depositional systems. These facies trends record energy transformations from deep water, offshore waves to nearshore, shoaling waves under fairweather and storm conditions. Minor mafic flows (Goodwin, 1960) and extensive tuffaceous horizons (Hassler and Simonson, 1989) within the Gunflint indicate that the region was volcanically active at the time of basin formation and subsidence (Fralick and Barrett, 1995). The main morphological elements, bedforms and internal sedimentary structures along a typical beach-shoreface-offshore profile are shown in Fig. 26. The following summary of these features is taken from Walker and Plint (1992), Einsele (1992) and Clifton *et. al.* (1971).

The *foreshore*, also synonymous with beach, consists of the portion above the low tide line and is dominated by the swash and backwash of breaking waves. In the foreshore zone the most characteristic feature is parallel to low-angle cross-

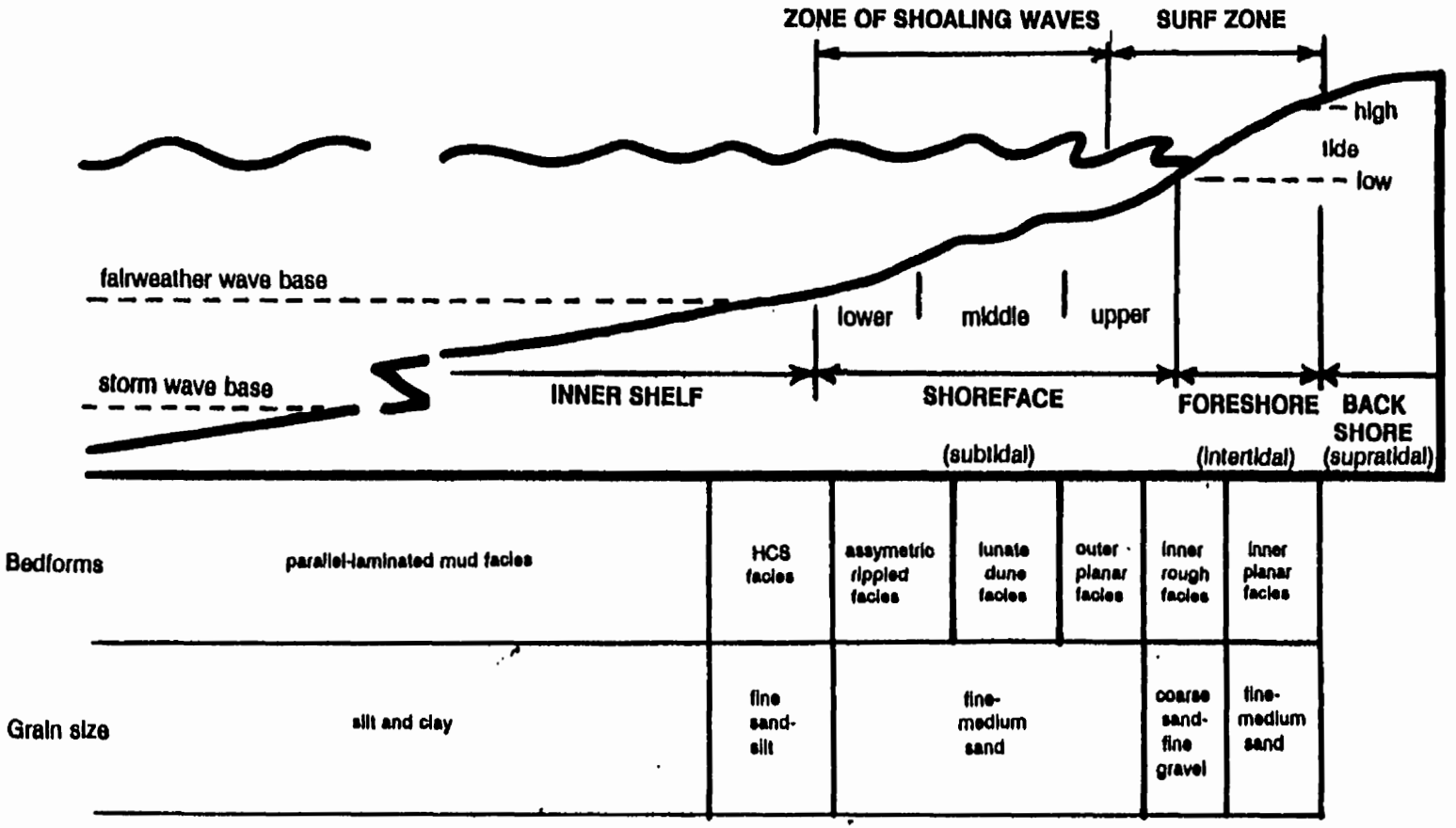

Fig. 26. Shoreline to shallow marine profile locating foreshore, shoreface and offshore, as well as the approximate locations of lithofacies across this profile. Fairweather wave base lies at depths of about 10 to 20 m. Modified from Walker and Plint (1992), and Einsele (1992).

bedding dipping seaward. On non-barred high energy shorelines, two planar laminated zones occur, an inner (upper foreshore), planar zone and an outer (lower foreshore) planar zone within the zone of breaking waves. In between these two zones the bedding surface becomes rough due to dotted and irregular erosional and depositional features. In tidally dominated systems the foreshore and upper shoreface is comprised of flaser, wavy, and lenticular bedded sands and muds typical of sedimentation on inter- and subtidal, mixed sand-mud flats. The *shoreface* lies below low tide level and is characterized by day-to-day sand transport above fairweather wave base. The shoreface normally has a concave-upward profile, which is in equilibrium with the waves that shape it. On the lower shoreface, at depths near or below fairweather wave base (10 to 20 m), are long crested symmetrical wave ripples, produced by storm waves (Fig. 26). Landward, on the middle shoreface, these inactive ripples pass into active ripples which become increasingly asymmetric, irregular, and short-crested. Larger, trough cross stratified, lunate dunes are frequently observed on the upper shoreface in the breaker zone. All these bedforms are associated with small-scale or larger-scale cross bedding which is predominantly oriented toward the land. Because the sediments of this zone are under continuous agitation, the deposition of mud is prevented. The mud-dominated *shelf* is typically below fairweather wave base and has a lower depositional slope than the foreshore and shoreface. Muds are typically parallel laminated and highly bioturbated in modern shallow-marine depositional systems.

In storm enhanced shallow marine non-barred, environments the shoreface processes described thus far, as well as processes in deeper regions of the inner and outer shelves are strongly affected and modified by storm events (Davis, 1992; Einsele, 1992). Storms can deposit sandy material in the supratidal zone, as well as generate special non-channelized flow conditions in deeper water. These high energy events frequently produce characteristic sheet-like sand and mud beds, called *tempestites*, of considerable lateral extent (Johnson and Baldwin, 1986; Morton, 1988; Nummedal, 1991; Einsele, 1992). Storm-generated bed forms show a distinct trend from the beach into deeper water (Fig. 27). The upper shoreface (surf zone) displays dunes oriented parallel to the shoreline. When flow becomes channelized longshore and rip currents erosively scour fairweather sediments, depositing medium- and coarse-grained, trough and planar, cross stratified sands. The middle shoreface is dominated by both flat and swaley bedforms with nearly horizontal or low-angle swaley cross stratification. Because of the continual agitation of sediments through wave action on the upper and middle shoreface the record of heavy storms is usually destroyed. On the lower shoreface (5 to 20 m water depth), the stress of storm surge ebb currents reaches about the same magnitude as the oppositely directed storm-wave induced oscillatory flow (Fig. 28) (Einsele, 1992). Thus, for a short time, both currents may stir up sand and mud, which are redeposited as parallel and hummocky cross-stratified fine-grained, graded beds at the same location or nearby (Einsele, 1992; Dott and Bourgeois, 1982). On the inner shelf and parts of the outer shelf,

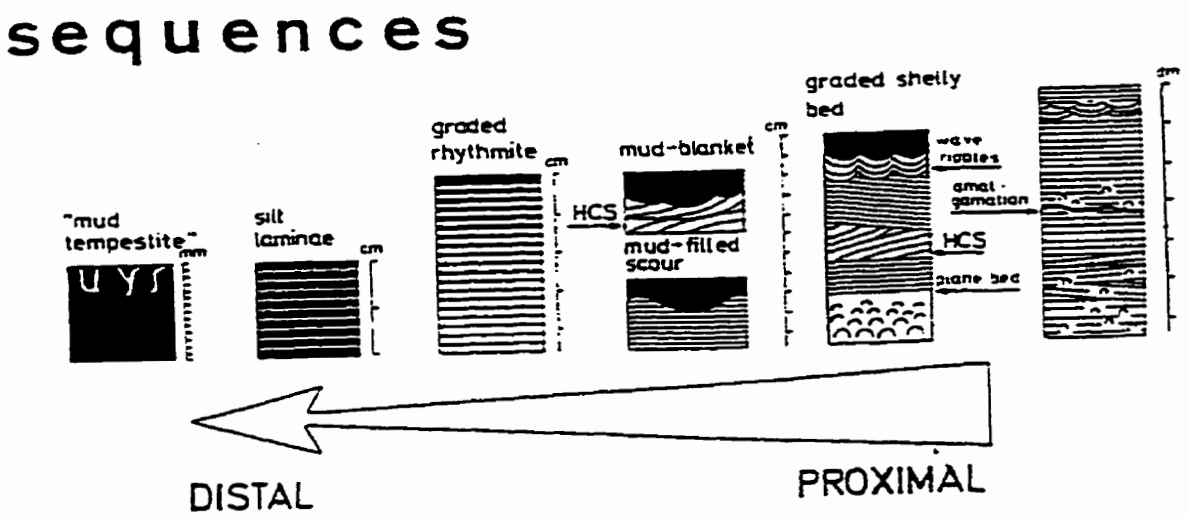

Fig. 27. Schematic diagram showing proximal and distal facies of typical storm sand sequences. Thin very coarse, irregular and fan shaped spillover lobes characterize supratidal storm sedimentation. In the foreshore storm deposits consist of a sharp erosional base, followed by reworked coarse sands, parallel laminated sands and a wave- rippled top. Storm deposition on the shoreface consists of erosive bases, followed by laminated sand which may be overlain by wave-ripple lamination. The transition into the inner shelf is characterized by "proximal" storm sands (proximal tempestites) due to their spatial association to the shoreface source area. The basal surfaces of proximal storm sands are erosional and often irregularly scoured. Internally, proximal tempestites consist of parallel laminated sands which are weakly graded. Laminations are often hummocky cross stratified (low-angle laminations with minor internal discordances). Thinner and mostly finer-grained sand/silt layers (distal tempestites) predominate the inner and outer shelf. They are the lateral, deep water equivalent to proximal tempestites further away from coastal sand sources. Internally they are parallel laminated, sometimes forming graded rhythmites. Ripple cross lamination is rare. Mud tempestites represent the distal end member of storm sedimentation. From Ainger (1985).

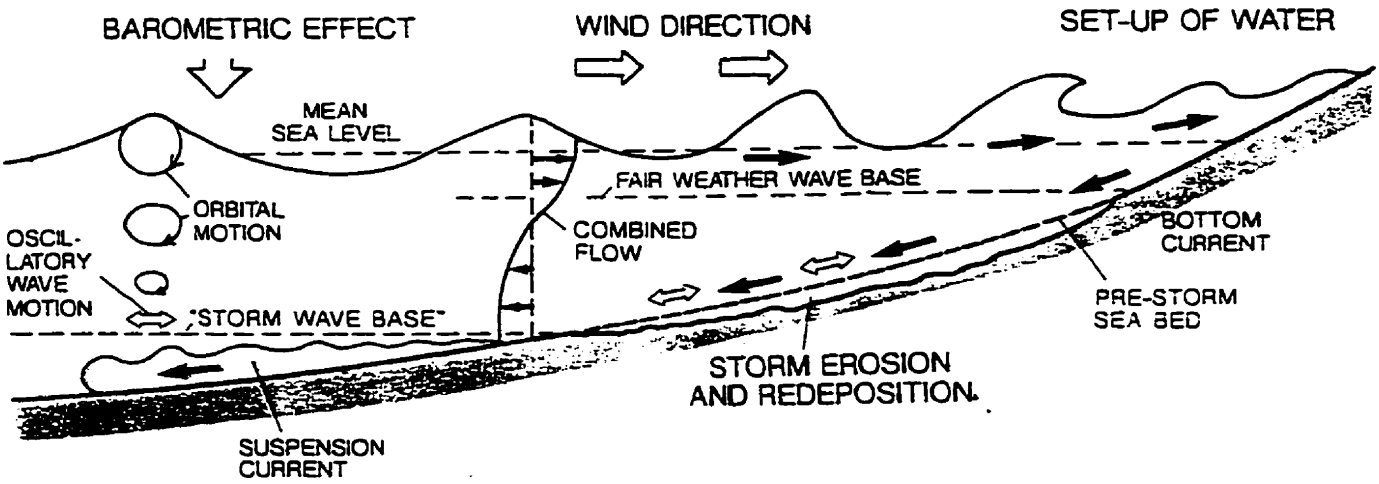

Fig. 28. Hydraulic regime during storm in a section across the shoreface and inner shelf. Coastal set-up of water and basinward bottom return current superimposed with oscillatory storm wave motion (combined flow). Combined flow typically occurs on the lower shoreface and results in the deposition of hummocky cross stratified storm sands.

particularly in high-energy environments, storm-induced combined flow may still generate HCS or thin, graded, sandy beds resulting from laterally flowing suspension currents. If the suspension originates from storms and the sandy layers alternate with shelf muds, the storm induced beds represent distal tempestites (Aigner, 1985; Einsele, 1992). At greater water depths on the shelf, the current component of the combined storm flow becomes dominant, leading to current rippled, offshore, fine sand and silt beds and graded rhythmites (Fig. 27) (Aigner, 1985; Einsele, 1992). Since only the largest storms can affect the sea floor in this zone, storm events are followed by long periods of quiescence and mud deposition.

4.2 Paleogeographic interpretation

The following discussion has been divided into three sections. Each deals with interpreting the vertical and lateral facies trends comprising the basal transgressive, middle regressive and upper transgressive depositional cycles of the Gunflint Formation in detail.

Basal transgression

This 20 m thick, upward fining cycle extends from the base of the Animikie Group to the middle of member 2 (Fig. 25). The base of the cycle is characterized by the Kakabeka Conglomerate, a backshore, pebbly beach deposit preserved as a

transgressive pebble lag. This intraformational conglomerate was formed by the localized weathering of the peneplain. Then, through subsequent storm-generated wave action (swash/backwash) these intraclasts were reworked into crudely stratified, matrix supported, pebbly, supratidal, beach deposits (Figs. 22 and 29). Ojakangas (1983) has made a similar interpretation of the conglomeratic unit forming the base of the Pokegama quartzite in the Mesabi iron range in east-central Minnesota.

As the basal transgression progressed these coarse beachface sediments were on-lapped by the fine- and medium-grained **Gp** facies grainstones of member 1 (Figs. 22 and 29). The hematite-enriched transition from member 1 may indicate a change in the redox state of the depositional system accompanying a rise in sea level or, more simply, it may represent oxidation of iron-bearing sediments by late phase oxygen-rich meteoric waters percolating along this lithologic boundary. Deposition of this thin, parallel bedded grainstone unit marks the onset of intertidal sedimentation on the foreshore. Member 1's relative thinness (5 m) and apparent lack of desiccation features suggests that the intertidal zone was not well developed on the Animikie shoreline, a situation typical of modern, microtidal environments (tidal range <2 m) (Reineck and Singh, 1975). LLH stromatolitic bioherms (**Ad** facies) at the base of member 1 may have developed in much the same way modern, columnar stromatolites and cryptalgal knolls form in the low energy intertidal flats of Shark Bay, Australia (Hoffman, 1976; Schreiber, 1986).

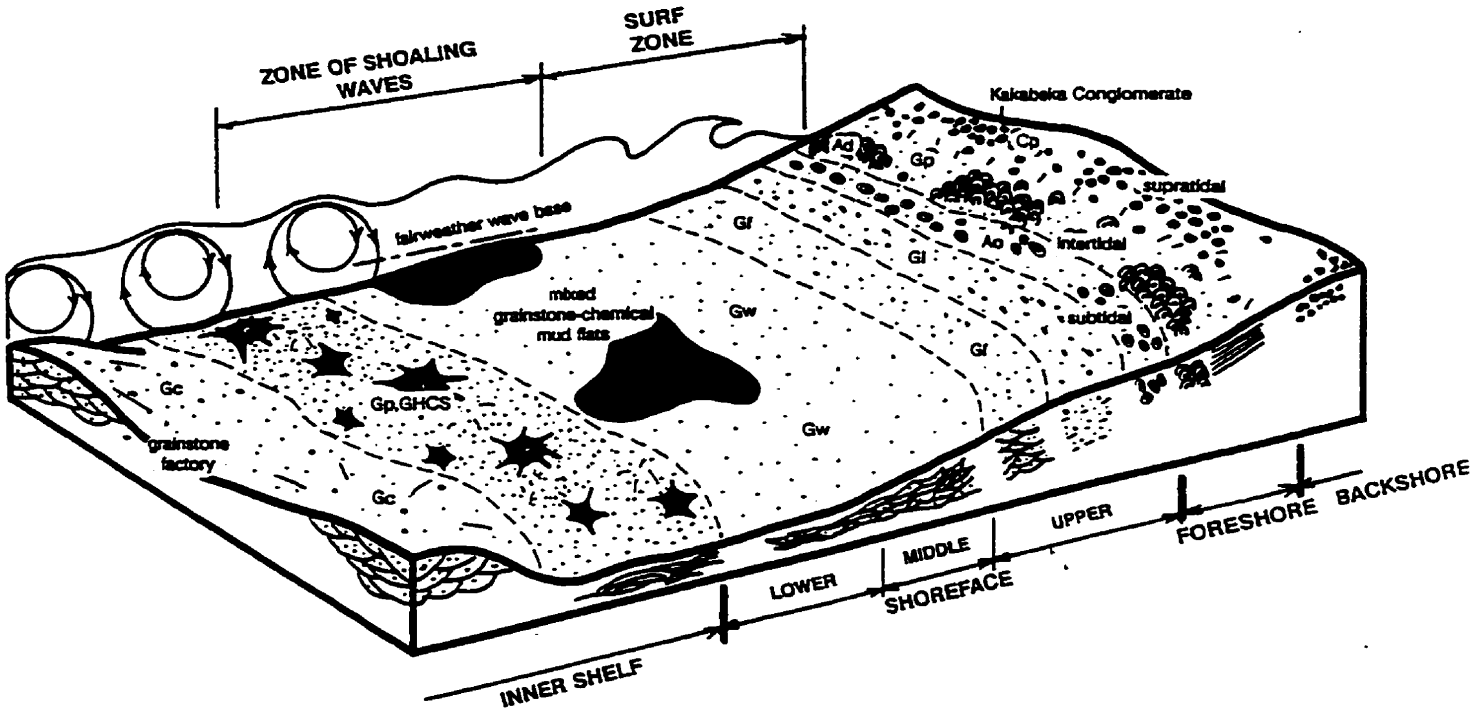

Fig. 29. Paleogeographic reconstruction of the Gunflint Formation. Lateral and vertical facies changes within the Gunflint Formation indicate that deposition of iron formation occurred on a shallow, non-barred, microtidal, storm-enhanced shelf with little clastic influx. Facies transitions record transformations from deep water, offshore waves to nearshore, shoaling waves under fairweather and storm conditions. Cp facies conglomerates were deposited as crudely stratified, storm-reworked supratidal beach deposits. Gp facies grainstones and Ad facies cryptalgal structures represent intertidal sedimentation on the foreshore. Ao facies organosedimentary structures mark the transition into subtidal depositional settings. Gl, Gf and Gw facies grainstones record the transition from the high energy surf and breaker zones of the upper and middle shoreface to the lower energy, storm-influenced, mixed grainstone-chemical mud flats of the lower shoreface. Gl facies grainstones characterize this change and represents deposition in the surf and breaker zones. GHCS and Gp facies grainstones were deposited on the lower shoreface below fairweather wave base and mark the transition into the inner shelf. Gc facies grainstones represent the development of "grainstone factories" on the inner shelf which frequently underwent storm reworking (large wave orbitals).

Here columnar stromatolites develop in the lower intertidal zone in response to strong wave action. The oncolitic horizon (**Ao** facies) above these intertidal, algal mats mark the transition into the subtidal (Figs. 22 and 29) (Logan *et al.*, 1964; Ginsburg, 1960, Sellwood, 1986). Ginsburg (1960) compared modern oncolites from the Florida and Bahama Banks to Devonian, Permian and Precambrian examples and found they formed 1 to 8 feet below mean water level at or near the subtidal transition. Oncolites from the Paris Basin, a non-barred, shallow epeiric sea covering much of northwestern Europe during the Middle Jurassic, were also determined to characterize this transition (Sellwood, 1986).

The overlying flaser and wavy bedded chert-carbonate grainstones (**Gf**, **Gw** facies) of member 2 (Figs. 22 and 29) represents subtidal deposition on a shallow, storm enhanced, non-barred shoreline. Similar Middle and Upper Cambrian, cyclic, peritidal, carbonate, tempestites compose the Elbrook and Conococheague Formations in the Virginia Appalachians (Demicco, 1985, Koerschner and Read, 1989). This 1.6 km thick carbonate sequence formed on the Cambro-Ordivician continental shelf; an aggraded, rimmed, mature, passive continental margin (Koerschner and Read, 1989). Cycles typically range between 1 and 7 m in thickness, possess a sharp basal transgressive surface, are overlain by a subtidal unit passing into a tidal flat cap, and record regional changes in sea level over very short intervals of time (Koerschner and Read, 1989). Three types of cycles are recognized, thin-based cycles, thrombolitic-based cycles, and thick based cycles

(Fig. 30). The latter has been divided into three subcycles, those which are digitate-algal-bioherm-based, grainstone-based and ribbon-carbonate-based. Ribbon-carbonate-based cycles most closely resemble member 3 and therefore will be the only cycle fully reviewed in the following discussion. For a full treatment of these cyclic, peritidal carbonates the reader is referred to Koerschner and Read (1989).

Ribbon-carbonate-based cycles are composed of 1 to 5 m thick fining and coarsening upwards sequences of flaser bedded coarse-grained carbonate grainstones/packstones which are comprised of wavy and lenticular bedded finer-grained pelletal carbonates and rare lime conglomerates intimately interbedded with parallel laminated dolomitic mudstones. The term comes from the field appearance of the alternating thin-beds (ribbons) of differentially weathered limestone and dolostone (Demicco, 1983). The coarse-grained ribbon carbonates and pellet packstones are most similar to the **Gf** facies chert-carbonate grainstones of member 3 in the Gunflint chemical sedimentary succession. Coarse-grained ribbon carbonates are unlayered or have low-angle cross bedding with weakly graded foreset laminae. Pellet packstones have horizontal laminations, climbing wave-ripple lamination and wave ripple cross-lamination. Mud-poor pellet-rich ribbon carbonates and mud-and-pellet rich ribbon sequences most closely resemble **Gw** facies chert-carbonate grainstones. Mud-poor, pellet-rich ribbon carbonates are planar laminated; mud-and-pellet-rich ribbon sequences are comprised of wavy and

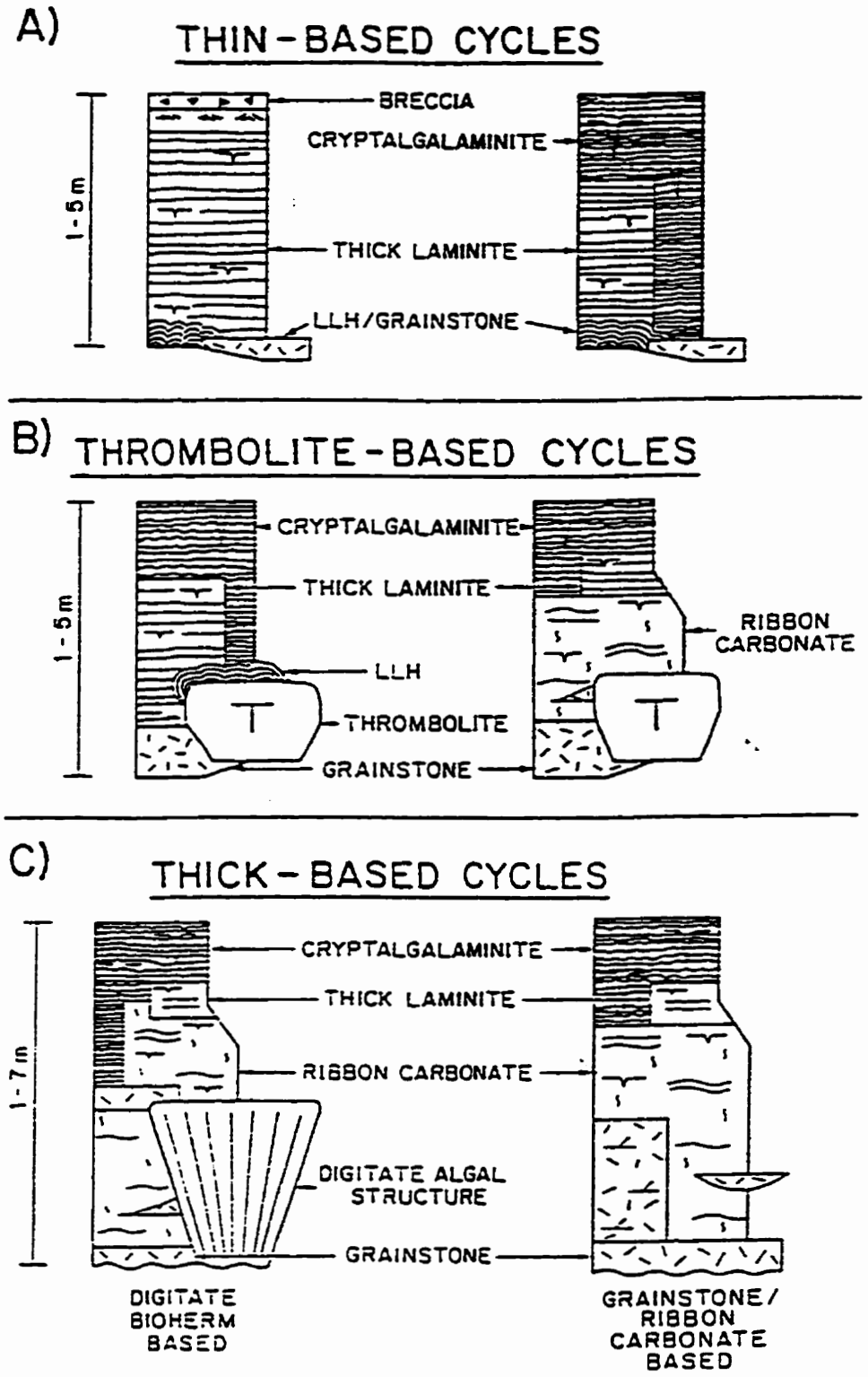

Fig. 30. Cycle types from the Elbrook and Conococheague Formations. A. Idealized thin-bedded cycles. B. thrombolite-based cycles. C. Idealized thick-based cycles. These include digitate-bioherm based cycles (left) and grainstone- and ribbon-carbonate-based cycles (right). From Koerschner and Read (1989).

lenticular bedded pellet layers interbedded with form-discordant wave ripples, starved ripples and parallel laminated dolomite mudstones (Koerschner and Read, 1989).

Demicco (1983) and Koerschner and Read (1989) interpret these ribbon sequences as recording shallowing by aggradation from storm-influenced subtidal settings floored by interlayered lime muds and sands, to subtidal sand flats on a rimmed shelf on a mature. Coarsening-upward sequences record low energy, subtidal conditions, followed by upward-shallowing into high energy shallow water settings (ie. surf zone and breaker zone). Koerschner and Read (1989) contend these coarse-grained ribbon carbonates formed on sand flats, where coarse layers were reworked during storms and less common fine layers settled out as storm/tidal energy waned. The rare lime conglomerate interbeds were deposited during storms which swept semi-lithified peloidal sands from shallow subtidal and intertidal settings. Fining upwards ribbon sequences record transgressive high-energy conditions that gave way to low energy conditions as the platform shallowed. Fine-grained peletal, ribbon carbonates formed on lower energy, subtidal, mixed sand flats in response to wave action and grade landward into mixed sand-mud flats (Koerschner and Read, 1989). Fairweather reworking of wave rippled beds alternated with deposition of thick storm layers of pelletal sediment with amalgamated hummocky cross stratification, and wave and current ripples (Koerschner and Read, 1989). Similar clastic, shallow, tidal marine

sequences occur in the modern North Sea (Demicco, 1983).

Like the peritidal, ribbon successions of the Elbrook-Conococheague Formations the **Gi, Gf** and **Gw** facies grainstones of member 2 also characterize storm influenced, subtidal deposition on a non-barred shoreline. These nearshore facies record the transition from the high energy surf and breaker zones of the upper and middle shoreface through to the lower energy, storm-influenced lower shoreface (Figs. 22 and 29). The package of **Gi** facies grainstone at the base of member 2 in O'Connor Township marks this transition and is characteristic of deposition in the surf and breaker zones of the middle and upper shoreface (Fig. 26). These massive, and cross stratified, rip-up-rich, chert-carbonate beds represent lunate dune and plane bed development typical of this agitated, high energy environment (Fig. 26) (Einsele, 1992; Clifton *et. al.*, 1971). With a continued rise in sea level depositional energies waned and this basal package was onlapped by **Gf** facies chert-carbonate grainstones of the middle shoreface. This rip up-free, flaser bedded grainstone package marks the formation of lunate megaripples in the zone of shoaling waves (Fig. 26).

The overlying **Gw** facies grainstones marks the progressive onlap of storm enhanced, fairweather-wave dominated deposition over the middle and parts of the upper shoreface. Like the ribbon carbonates of the Elbrook and Conococheague formations these wavy bedded chemical sediments also formed largely in response

to fairweather oscillatory wave and tidal currents acting on the mid to lower shoreface; forming a subtidal, mixed grainstone-chemical mud flat (Fig. 29). Fairweather reworking of these interbedded chert/carbonate grainstones and magnetite-rich slaty iron formation packages was punctuated by deposition of coarser, more massive, chert-carbonate storm beds.

Unlike the Cambrian ribbon carbonates of the Virginia Appalachians these flaser and wavy bedded chemical sediments did not form by aggradation of upward shoaling grainstone sequences. Instead, vertical changes in iron formation facies reflect a rate of relative sea level rise which consistently outpaced that of sedimentation.

Middle regression

This minor, 20 m thick, regressive phase begins in the middle of member 2 and extends to the top of member 3. It records the gradual onset of shallowing from the middle shoreface to the lower foreshore. The subtidal mixed grainstone-chemical mud flats of member 2 coarsen upwards to 3 m thick packages (TB0641) of flaser bedded chert-carbonate grainstones (Fig. 22). These coarse packages formed during regressive offlap of lower-middle shoreface facies and, like the flaser bedded package at the base of this member, represent dune development in the surf zone of the upper shoreface.

As sea level continued to fall these flaser and wavy bedded chert-carbonate grainstones were transgressed by the coarser, higher energy, stromatolitic and oncolitic, chert-carbonate, grainstones of member 3 (Fig. 22). These storm enhanced, cryptalgal, lower foreshore deposits mark the regressive peak of this middle cycle (Fig. 25). Like the **Gf** facies chert-carbonate grainstones of member 2 those comprising member 3 also record lunate dune development on a subtidal/lower intertidal chert-carbonate grainstone flat.

The 6 cm thick, **Gi** facies grainstone bed at the base of member 3 in O'Connor township is interpreted as being a proximal tempestite deposited in this shallow, high energy environment. This coarse, storm generated lag is thin, possesses a base which appears to erosively scour the flaser bedded chert-carbonate grainstones of member 2, contains abundant magnetite- and hematite-rich rip ups and pinches laterally towards Blake township; all are characteristics of nearshore sheet storm deposits (Einsele, 1992). With a return to fairweather conditions this storm bed provided an ideal substrate for stromatolites to colonize. It was firm and not easily reworked by normal shelf currents (Fralick, 1988). Development of cryptalgal knolls on this intraformational lag was however not widespread as they colonized only the most stable regions sheltered from fairweather reworking. The thin, discontinuous, stromatolitic and oncolitic horizons which developed above this basal, cryptalgal layer suggests subtidal, stromatolitic growth occurred on a substrate that underwent periodic, fairweather reworking.

The development of these poorly formed, discontinuous LLH and SS stromatolitic bioherms is typical of cryptalgal development on shallow, high energy, subtidal sand sheets of the upper shoreface and lower foreshore (Pratt *et al.*, 1992).

Upper transgression

The upper transgressive cycle extends from the top of member 3, through member 5, possibly to the top of the Rove Formation; a vertical distance of almost 700 m. Its onset is rapid and records the progressive onlap of offshore facies over those of the lower shoreface. The thin package of hummocky cross stratified chert- and hematite-rich grainstones (**GHCS** facies) at the base of member 4 in O'Connor township marks this transition. Modern hummocky-cross-stratified sands occur below fairweather wave base on the lower shoreface of storm dominated, shallow marine depositional systems at or near the transition to the inner shelf (Hamblin and Walker, 1979; Dott and Bourgeois, 1982; Aigner, 1985; Walker and Plint, 1992; Einsele, 1992; Davis, 1992). The parallel bedded, hematite-rich, slaty and cherty iron formation beds (**Gp** facies grainstone) to which this basal hummocky-cross-stratified unit grades (Fig. 22) are also characteristic of storm deposition near this change. They are identical to modern, proximal offshore, storm-sand layers (proximal tempestites) and their more distal equivalents, graded rhythmites (distal tempestites) (Reinick and Singh, 1972; Aigner, 1985). Like the parallel bedded chemical sediments (Fig. 17) these storm beds also posses a sharp base, and in some instances may grade upward into plane laminated mud layers.

In modern tempestites the sand layers are either evenly laminated or are laminated rhythmites, in which the lower laminae are thicker and coarser-grained and grade upwards into thinner and finer-grained laminae (Reinick and Singh, 1972). They are the result of deposition from shallow marine, storm generated turbidity currents (Reinick and Singh, 1972; Walker, 1984; Einsele, 1992; Davis, 1992). The fine- and medium-grained chert- and hematite-rich grainstone beds comprising this member represent episodic development of storm-generated, chemical sedimentary beds. Thicker, graded, coarser beds developed during the most severe storms. The hematite-rich slaty iron formation packages between storm-grainstones represents the return to fairweather sedimentation on the lower shoreface. In Blake township (TB0218) these chemical sedimentary storm layers lay directly on the grainstones of member 2.

The pulse of volcanism preserved in the middle of member 4 as a 6m thick volcaniclastic horizon (**Vs** facies) occurred swiftly, outpacing iron formation deposition (Fig. 22). Its sharp bottom contact indicates rapid influx of volcaniclastic material into the depositional system (Fig. 22). Its gradational upper contact suggests delivery of volcaniclastics to the basin waned gradually over time. The lapilli tuff (**Vt** facies) which characterizes the base of member 5 is interpreted as being reworked and deposited by storms from more proximal, nearshore settings. The **Gi** facies grainstone bed characterizing its base is similar to the the stromatolitic, storm generated lag in member 3; its lower bounding surface is

erosive into the top of member 4 and it also pinches laterally towards Blake Township. Similar volcaniclastic beds within the Gunflint Formation have also been interpreted by Hassler and Simonson (1989) as being reworked and redeposited by turbidity currents.

The coarsening upwards, chert-carbonate, grainstone successions (**Gc** facies) of member 5 (Fig. 25) mark the progressive onlap of inner shelf facies over those of the lower shoreface (**Gp** and **GHCS** facies) (Fig. 29). Similar successions deposited in coastal and open marine environments comprise the Upper Cretaceous, Sussex and Shannon sandstones of the Powder River Basin in northern Wyoming. In Wyoming cycles coarsen from silty offshore mudstones, through thin bedded, storm- and tide-generated sandstones to cross stratified sandstones with abundant clay rip-ups. The depositional model proposed for the Shannon and Sussex sandstones consists of migrating, offshore bar complexes that have their surfaces covered by sand waves (Berg, 1975; Brenner, 1978; Hobson *et al.*, 1982; Davis, 1992). With some modification this model may also be applied to the coarser-grained, shoaling upwards sequences comprising member 5 of the Gunflint Formation.

Like bar development in clastic systems genesis of chemical sedimentary, offshore bar complexes depends on, 1) the availability of coarse sediment to offshore environments and 2) the presence of currents capable of shaping this sand

into well defined, migrating, sand bodies. In clastic, shallow marine depositional systems coarse detritus is supplied to offshore areas by storm (Berg, 1975; Walker, 1984; Tillman and Martinson, 1984) and tide (Spearing, 1976; Brenner, 1978; Seeling, 1978) generated currents. However, unlike their clastic counterparts, bar genesis in chemical sedimentary systems relies on offshore precipitation of iron oxides and silica gel from upwelled enriched bottom waters (Borchert, 1950; Drever, 1974; Morris, 1993), and subsequent current reworking of the substrate into rip-up grains (Simonson and Goode, 1989). Consequently this process does not depend on systems tracts capable of delivering coarse detritus to the shelf. Bar development in a chemical sedimentary, shallow-marine depositional system is therefore governed by the position of areas on the shelf with high; primary chert/carbonate grain production and the presence of currents able to rework these chemical precipitates into bar complexes. The relative stratigraphic position of member 5, over facies characteristic of the lower shoreface (**Gp** and **GHCS** facies) (Fig. 22), suggests that regions of primary grain genesis were below fairweather wave base and that storm-generated, oscillatory flow was responsible for reworking the substrate into rip-up grains (Fig. 29).

Finer-grained, shoaling upwards, chemical sedimentary successions from the Gogebic Iron Range in Wisconsin (Pufahl, 1994) are identical to the coarsening upwards successions comprising the Sussex and Shannon sandstones in Wyoming. They are regarded as being the distal equivalents to the coarse offshore bars of the

Gunflint (Pufahl, 1994). Cycles in Wisconsin coarsen from parallel laminated, magnetite-rich slaty iron formation in much the same way the Cretaceous upwards shoaling cycles coarsen from shelf mudstones.

In a broad sense these offshore regions of primary grain genesis are similar to the "subtidal carbonate factories" responsible for grain production on modern and some ancient carbonate platforms (James and Kendall, 1992). The coarse nature of the Gunflint shoaling upwards cycles in Blake and O'Connor townships suggests bar development occurred at or near a "grainstone factory". As the transgression progressed these factories migrated in step with shoreline retreat resulting in the deposition of slightly finer-grained bar complexes further from regions of primary grain production. The existence of these offshore factories would account for the absence of a mud dominated offshore, which is so characteristic of clastic shallow-marine depositional systems (Walker and Plint, 1992).

Alternatively, these coarsening upwards, **Gc** facies grainstone successions may represent paracycle development (Vail *et al.*, 1977) in regions of high primary grain genesis during relative sea level rise. Paracycles form in response to a punctuated rise in overall sea level. They record a period of rapid, relative sea level rise and still stand, followed by another relative rise with no significant fall intervening (Vail *et al.*, 1977). The sequence that accumulates is coarsening

upwards, suggestive of continued shoaling as sediments accumulate to sea level. In this scenario the medium-grained, chert-carbonate grainstones at the base of coarsening upward cycles would represent grainstone deposition during rapid sea level rise as regions of primary grain genesis migrated shoreward. The coarse-grained tops of cycles would represent accumulation of grainstones near to base level where breaking storm waves were able to winnow the substrate during an interval of relative still. At the present time data is insufficient to choose whether an autocyclic (depositional) or allocyclic (sea level) mechanism governed cycle genesis.

The **Gi** facies chert-carbonate grainstone beds which characterize transitional facies into the overlying Rove in Blake township (Fig. 22) are interpreted as representing deposition from suspension clouds generated by either storms or tectonism during basin subsidence.

CHAPTER 5: GUNFLINT-MESABI-CUYUNA DEPOSITIONAL SYSTEM, REGIONAL CORRELATIONS

5.1 Introduction

The Gunflint-Mesabi-Cuyuna depositional system is comprised of seven iron-bearing members (Fig. 34), five (members 1, 2, 3, 4 and 5) of which have been described and interpreted in detail in the previous sections pertaining to the Gunflint. Only a brief synopsis of facies forming these members will therefore be given in the following section. Attention will instead focus on presenting a comprehensive review of members 6 and 7. The reader is referred to Chapter 3 for detailed descriptions of members 1 through 5. Fig. 31 shows the locations of drill holes used for regional stratigraphic correlation and paleogeographic interpretation of iron-bearing units in Ontario and Minnesota.

5.2 Vertical Facies Changes

The base of the of the Gunflint Formation in Ontario and northeastern Minnesota is characterized by the Kakabeka Conglomerate (Fig. 22). In northern Minnesota the Pokegama Quartzite (**Cs** facies) conformably underlies the Biwabik iron formation of the Mesabi iron range. Like the transition from clastic to chemical sediments in Ontario the change from the Pokegama Quartzite to the iron-bearing strata of the Biwabik iron formation is also hematite-rich. Ojakangas (1983, 1993)

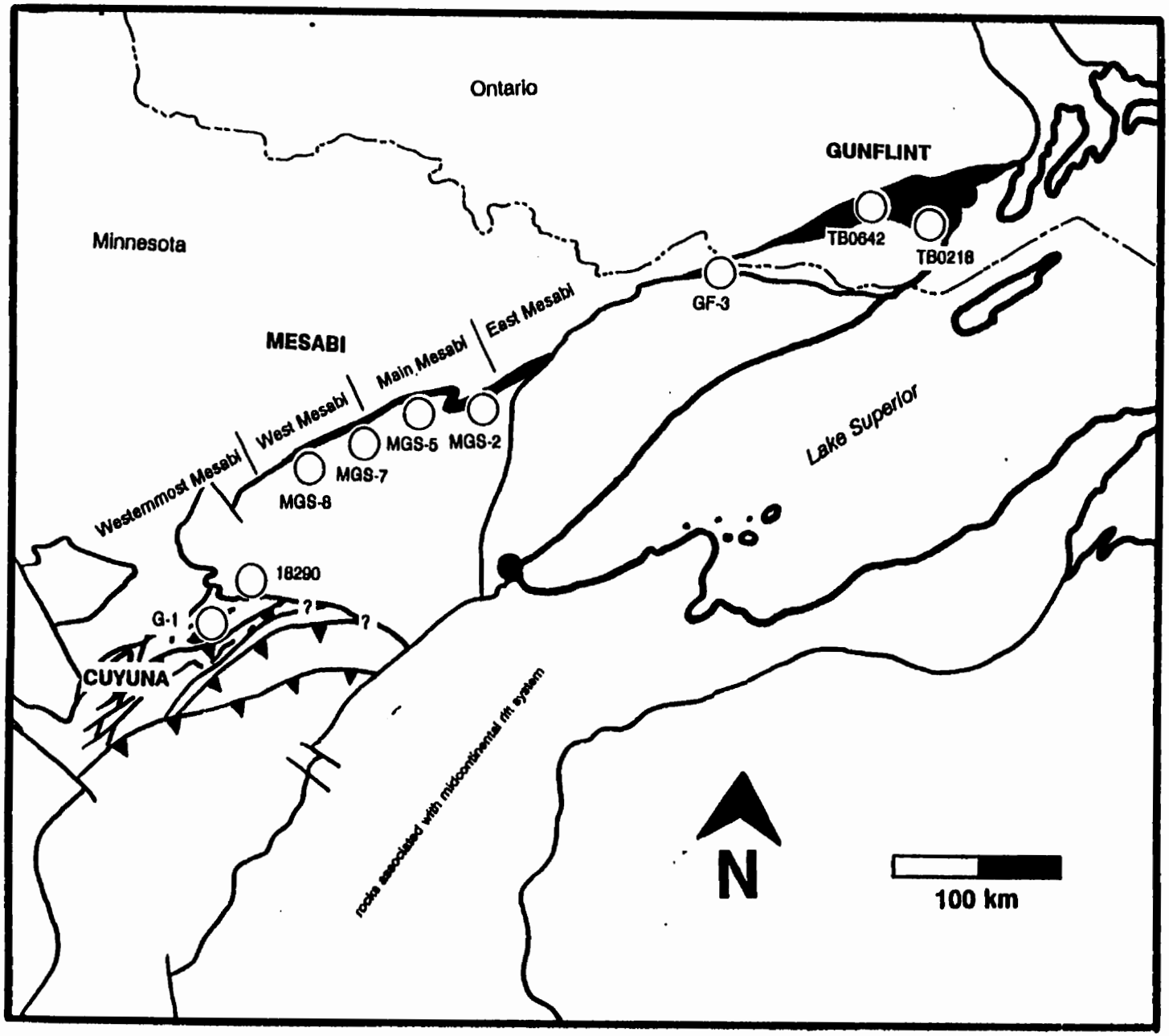

Fig. 31. Location of drill holes used for regional stratigraphic correlation between the Gunflint, Mesabi and Cuyuna iron ranges, and place names mentioned in text.

has subdivided the Pokegama Quartzite into 3 members (Fig. 32) based on lithofacies associations present within **Cs** facies sandstones (Chapter 2). They are 1) a 2 to 10 m thick lower slaty member comprised of shale with minor siltstone and sandstone (slaty facies), 2) a 15 to 25 m thick middle member composed of thin alternating beds of slate, siltstone and sandstone (shale-siltstone-sandstone facies) and 3) a 5 to 15 m thick upper member comprised of fine and medium-grained sandstones with thin siltstone and shale layers (sandstone facies). Limited paleocurrent data (Fig. 33) suggests that dominantly northwest-southeast flowing, bidirectional currents were responsible for deposition of these members (Ojakangas, 1983). Like the Gunflint Formation, the Pokegama Quartzite also rests unconformably directly on the Archean Basement or over a thin, discontinuous basal conglomerate (conglomeratic facies) similar to the Kakabeka Conglomerate.

In east-central Minnesota the Trommald iron formation is conformably underlain by the Mahnomen Formation, a clastic sequence dominated by shales and siltstones. Schmidt (1963) divided The Mahnomen Formation into two informal units; a lower slate-siltstone-rich unit and an upper unit comprised chiefly of quartzite and limestones. Southwick *et al.* (1988) also recognized this two-fold division. Based on aeromagnetic data and sparse drilling they divided the Mahnomen into an upper member containing lean slaty iron formation interlaminated with slates, siltstones and quartz-rich sandstones and a lower member lacking iron-rich beds (Southwick *et al.*, 1988). They have also estimated

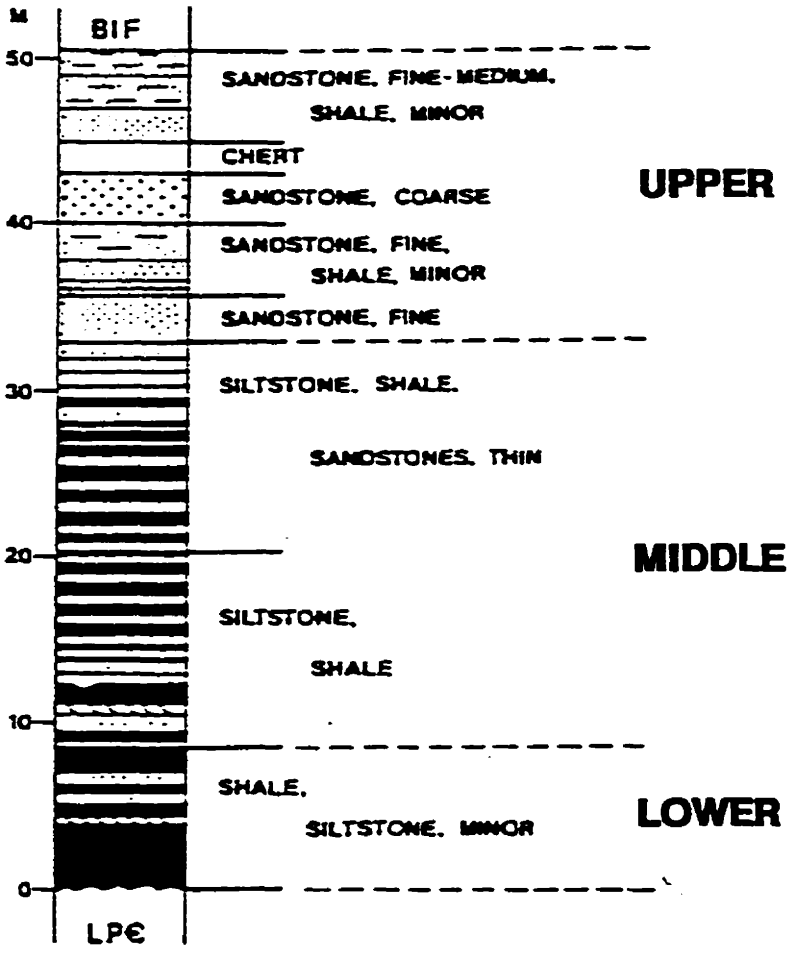

Fig. 32. Idealized stratigraphic section through Pokegama Quartzite. Dark shading represents shale, thin blank units represent siltstone, dotted patterns represent sandstone, BIF is banded iron formation, and LPe is Archean basement. The terms lower, middle and upper refer to members. From Ojakangas (1983, 1993).

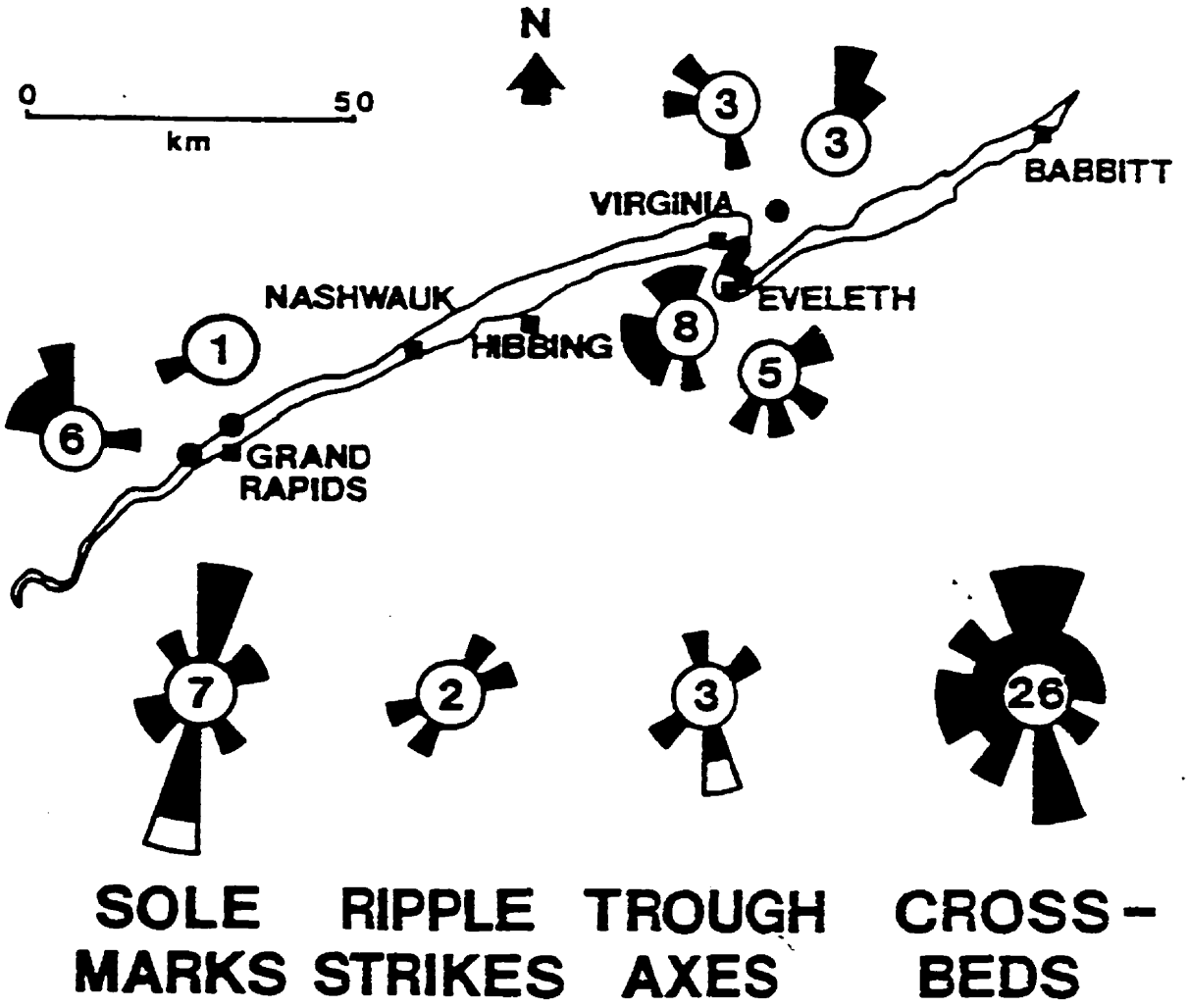

Fig. 33. Map of Mesabi range showing cross-bedding plots of Pokegama Quartzite at 6 localities. Total cross bedding plot is at lower right. Also shown are plots of sole marks, ripples, and troughs; the white measurements represent sense measurements. From Ojakangas (1983).

the thickness of the Mahnomen Formation to be 1.5 km. Its true thickness is not known as its lower contact has never been penetrated by drilling (Southwick *et al.*, 1988).

The basal transition from the clastic sandstones of the Mahnomen Formation and Pokegama Quartzite to the Biwabik iron formation in the Western Mesabi and the Trommald iron formation in the Cuyuna North range is conformable but abrupt over a span of 40 to 50 cm. This lithologic boundary is demarked by the presence of **Cs** facies sandstone beds intimately interbedded with **Sc** facies chemical slates. In the Mesabi this transition is hematite-rich. Data regarding this transition in the Emily district was missing from drill core (18290).

The members comprising the iron formation in east-central, northern and northeastern Minnesota and adjacent areas of Ontario are discussed below and presented in simplified form in Fig. 34. This stratigraphic framework is intended to provide a general understanding of the large-scale vertical and lateral facies trends observed within iron-bearing strata. There is ample room for more detailed sedimentologic and stratigraphic studies of selected units. In ascending order the members are;

Member 1

This 8 m thick unit forms the base of the Gunflint chemical-sedimentary

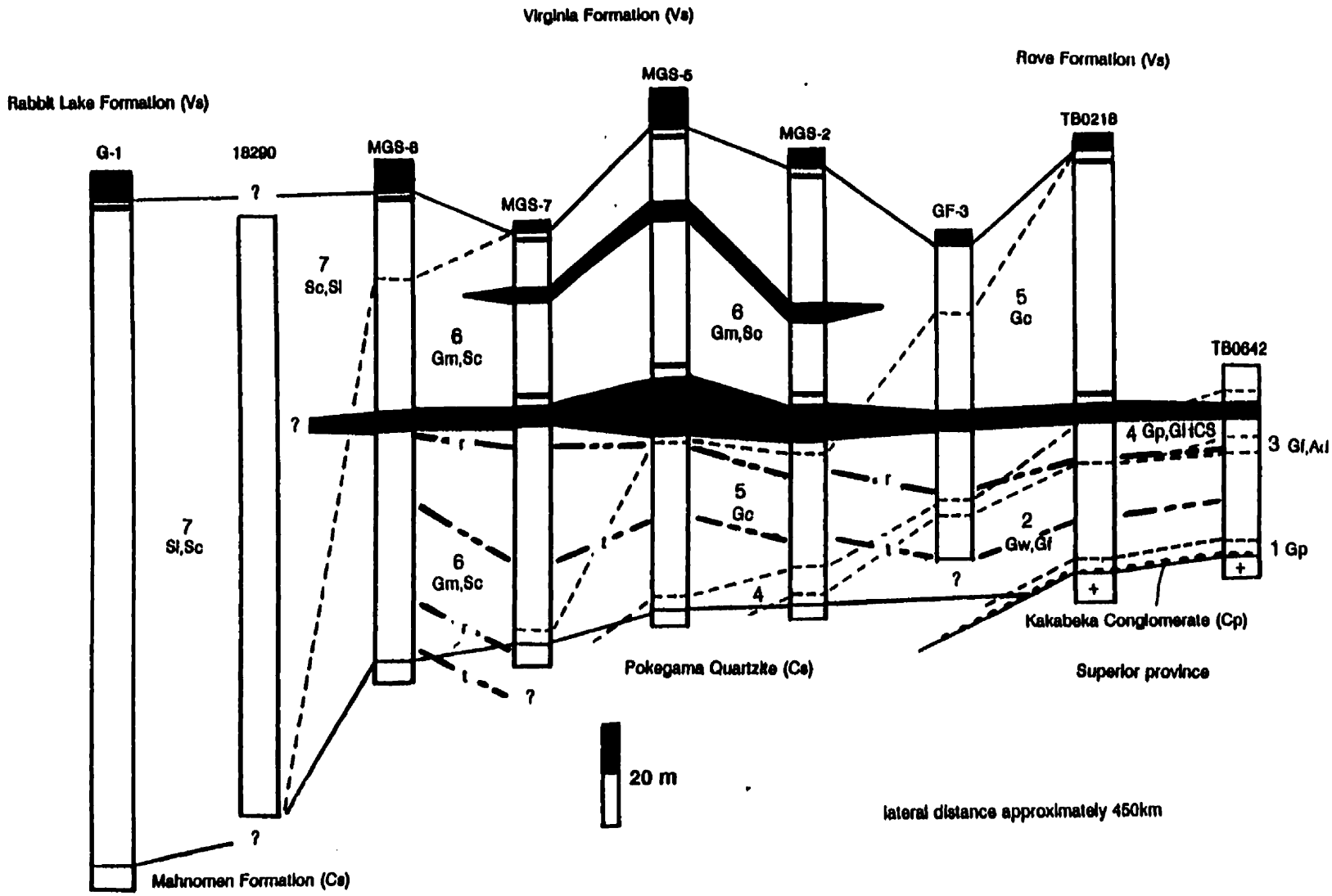

Fig. 34. Idealized cross section showing the stratigraphic architecture across the Gunflint, Mesabi, and Cuyuna iron ranges. Numbers refer to members 1 through 7. Members are diachronous and are cross-cut by three volcaniclastic horizons (black): a lower, middle, and upper. The slaty members of the Rove, Virginia, and Rabbit Lake Formations form the uppermost volcaniclastic layer. Also shown are the relative stratigraphic positions of the "peaks" of the lower transgression and regression, the middle transgression and regression, and the upper transgression (t-transgression, r-regression). Transgressive and regressive peaks were identified in drill holes by plotting average grain size against stratigraphic position.

succession and is composed of **Ad** and sometimes **Ao** cryptalgal facies interbedded with **Gp** facies grainstones. Member 1 rests conformably on the Kakabeka conglomerate in O'Connor township and unconformably over the Archean basement in Blake township.

Member 2

Member 2 is formed of a 50 m thick unit of interbedded **Gf** and **Gw** facies grainstones and is conformable with the organosedimentary grainstones of member 1. Its base in O'Connor township is characterized by a 7 m thick package of **Gi** facies grainstones.

Member 3

Gf, Ad and **Ao** facies comprise member 3. Cryptalgal horizons in this 8 m thick member are not as well developed as those forming organosedimentary beds in member 1. Member 3 is conformable with member 2.

Member 4

In O'Connor and Blake Townships member 4 varies in thickness from 23 to 27 m and is composed primarily of **Gp** facies grainstones. In O'Connor Township its base is formed of a thin package of **GHCS** facies grainstone. In St. Louis County member 4 is 13 m thick and comprised entirely of **Gp** facies grainstones (MGS 2). Like the parallel bedded chert-carbonate grainstones which form this

member in O'Connor and Blake Townships those in St. Louis County (Main Mesabi) are also hematite-rich.

Member 5

Member 5 is composed exclusively of **Gc** facies grainstone. In the Thunder Bay district its base rests sharply, but conformably on member 4 and it extends 80 m into the base of the overlying Rove Formation. In Minnesota member 5 is conformably overlain by member 6, and pinches laterally from 66 m in the Main Mesabi (MGS-2, MGS-5) to 5 m in the West Mesabi (MGS-7). Limited paleocurrent data (Fig. 35) from cherty grainstones from member 6 suggests that it was deposited by bidirectional, northwest-southeast flowing currents (Ojakangas, 1983).

Member 6

Gm facies grainstones intimately interbedded with **Sc** facies slates comprise this member. Member 6 ranges in thickness from 40 m in the eastern Mesabi to 145 m in the western Mesabi. Its transition from member 5 is gradational over a span of 20 m and is characterized by a 15 to 20 m thick **Sc** facies package of chert- and magnetite-rich slates (GF-3, MGS- 2, MGS-5 and MGS-7). The base of this basal package is marked by the frequent interbedding of 8 to 15 cm thick **Gc** facies grainstone beds with **Sc** facies chemical slates. Where **Cs** facies sandstones underlie this member (MGS 8) the contact is also conformable and gradational.

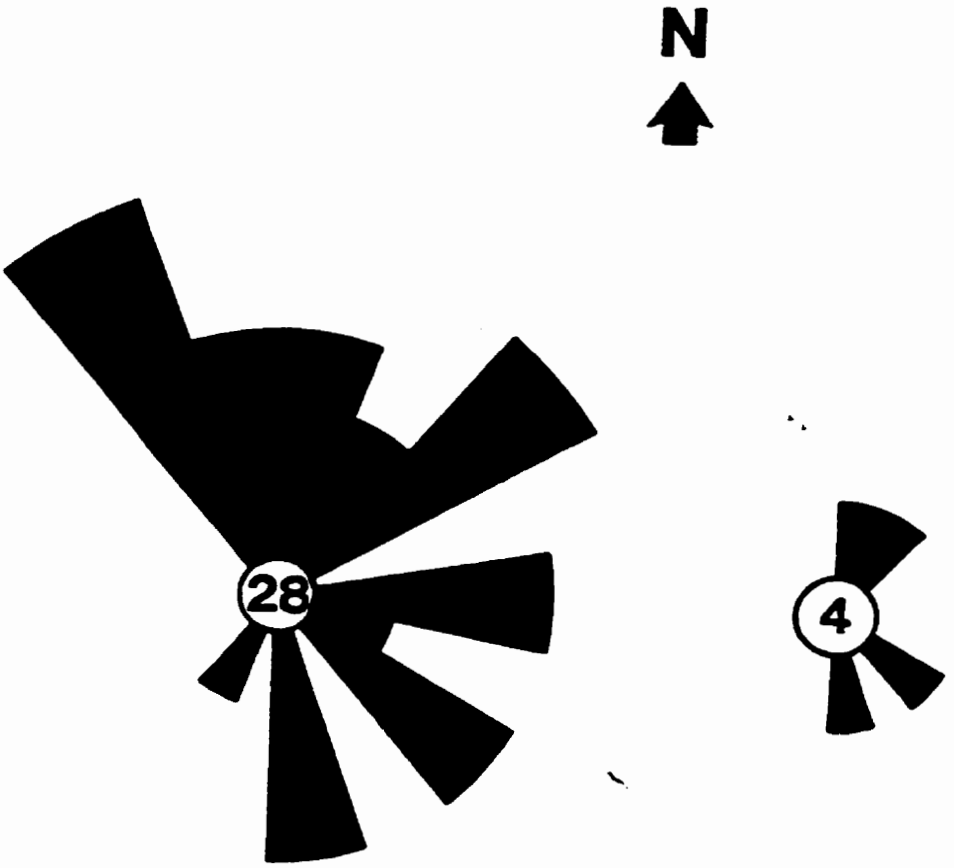

Fig. 35. Rose diagrams summarizing orientation of cross-beds in "cherty" Biwabik iron formation at two localities, Eveleth and northeast of Virginia, Minnesota. Stratigraphic correlations (this study) indicates paleocurrent measurements were taken from chert grainstones in member 6. From Ojakangas (1983).

Member 6's upper bounding surface is a conformable contact with both the Virginia Formation (MGS-2 and MGS-5) and member 7 (MGS-7 and MGS-8). Where the Virginia slates overlie member 6 this transition is characterized by periodic interbedding of 10 to 15 cm thick **Gi** facies grainstone beds with **Vs** facies slates. When overlain by member 7 the transition is gradational over a span of 15 to 20 m and is marked by the appearance of magnetite-rich, **Sl** facies chemical slates.

Member 7

Member 7 is essentially comprised of monotonously interbedded packages of **Sc** and **Sl** facies magnetite-rich chemical slates 13 to 65 m thick (MGS 8, 18290, G-1). It varies in thickness from 55 m in the Western Mesabi to 295 m in the Cuyuna north range where it forms almost the entire Trommald iron formation. In the Emily district and North range graphitic, **Vs** facies, slaty laminations are frequently interlaminated within slaty iron formation packages. Layers typically range from 1 to 3 mm in thickness and commonly form packages 2 to 4 cm thick. Schmidt (1963) has described similar carbonaceous laminations interbedded with Trommald iron formation in several places throughout the Cuyuna north range which he has also interpreted as volcaniclastic layers (**Vs** facies). They are lithologically and chemically identical to the slates comprising the lower portion of the overlying Rabbit Lake Formation (Schmidt, 1963).

In one instance (Merritt hole, Fig. 7) a 60 m thick succession of massive and cross-stratified, hematite-rich chert grainstones (**Gm** facies) was observed interbedded within slaty iron formation packages (Merritt, figure in chapter 1). Unfortunately the relative stratigraphic position this unit is unknown because it was observed in a stratigraphically incomplete drill hole. Schmidt (1963) has recognized similar grainstone beds interbedded with **Sc** and **Sl** facies chemical slates near the top of Trommald iron formation in many places throughout the Cuyuna north range. Beds are generally massive and range in thickness from 2 cm to 2 m. He has also noted the presence of brecciated iron formation intercalated with **Sc** and **Sl** facies chemical slates in several mine sites 4 km south of drill hole G-1, near the southern margin of the Cuyuna north range. Breccias are composed of angular fragments of chert 1 to 2 cm in length suspended in a fine-grained, slaty matrix (Schmidt, 1963). In one case Schmidt (1963) observed iron formation breccia and slabs of **Sl** and **Sc** facies iron formation 30 cm long along the contact of a lenticular body of **Vs** facies slates 12 to 19 m wide and more than 155 m long.

Member 7's upper contact into the overlying Virginia (MGS-7 and MGS-8) and Rabbit Lake Formations (G-1) is gradational over a span of 10 m. This conformable transition is characterized by the frequent interbedding of **Sl** and **Sc** facies iron formation with **Vs** facies slates of the Virginia and Rabbit Lake Formations. Rare, interlayered **Gi** facies grainstone beds 5 cm thick also mark this transition in the Cuyuna north range. Data regarding this lithologic boundary in the

Emily district was not available from drill holes used in this study (18290).

Like the Rove Formation in Ontario and adjacent areas in northeastern Minnesota the Virginia and Rabbit Lake Formations of northern and east-central Minnesota are also essentially composed of interbedded shales, siltstones and fine-grained sandstones. Two members similar to those which form the Rove Formation also comprise the Virginia Formation; a basal slaty member 125 to 140 m thick (**Vs** facies slates) and an upper member of intercalated shale, siltstone and fine-grained sandstone beds approximately 300 m thick (Lucente and Morey, 1983). In the Virginia Formation many of the siltstone and sandstone beds comprising the upper member have sharp basal contacts and upper bounding surfaces that are gradational into overlying packages of shale (Lucente and Morey, 1983). Where they occur as discrete packages, sandstone beds are rarely more than 1 m thick, most are less than 50 cm thick. Beds commonly fine from parallel bedded sands through ripple laminated fine-sands and parallel laminated siltstones to parallel laminated muds (Lucente and Morey, 1983).

The stratigraphy of the Rabbit Lake Formation is somewhat more complicated. It can be subdivided into a 60 m thick, black, lower slaty member similar to the lower members comprising the base of the Virginia and Rove Formations, an intermediate chert-carbonate, iron formation member as much as 300 m thick and upper member of interbedded slate, fine- to very-fine-grained

sandstones and iron formation (Marsden, 1972). On the North range slates comprising the lower member are interbedded with units of chloritized basalt and chlorite-bearing tuffs (Morey, 1978). Paleocurrent data from the Rove (Morey, 1967, 1969) and Thomson Formations (Morey and Ojakangas, 1970) indicate that much of the sediment comprising this siltstone-sandstone sequence was deposited by southward flowing currents (Figs. 36 and 37).

5.3 Lateral Facies Changes

Stratigraphic correlations between iron-bearing members were aided by the presence three volcaniclastic horizons (Figs. 34 and 38). Volcaniclastic horizons are useful stratigraphic markers because they represent synchronous depositional events within a basin, and therefore are not time transgressive. When stratigraphic sections from the Gunflint, Mesabi, and Cuyuna iron ranges are hung from these chronostratigraphic horizons correlations indicate that clastic and chemical sedimentary facies comprising the northwestern segment of the Animikie and North Range Groups exhibit a marked fining and thickening to the southwest over a distance of 450 km (Figs. 34 and 38). The Gunflint Formation, in the vicinity of Blake Township, is approximately 175 m and is primarily comprised of **Gc**, **Gp**, **Gf**, and **Gw** facies grainstones. The Biwabik iron formation is about 185 m thick in the Main Mesabi and nearly 210 m in the West Mesabi. It is essentially composed of

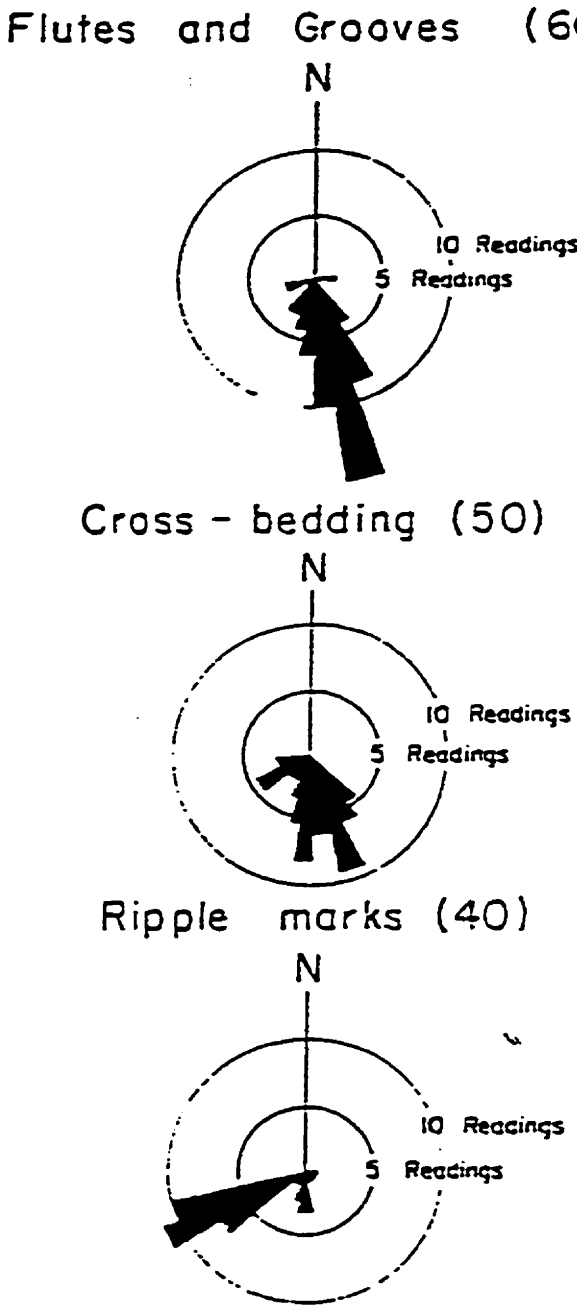

Fig. 36. Rose diagrams summarizing orientation of flutes and grooves, cross-beds, and ripple marks in the Rove Formation. From Morey (1967).

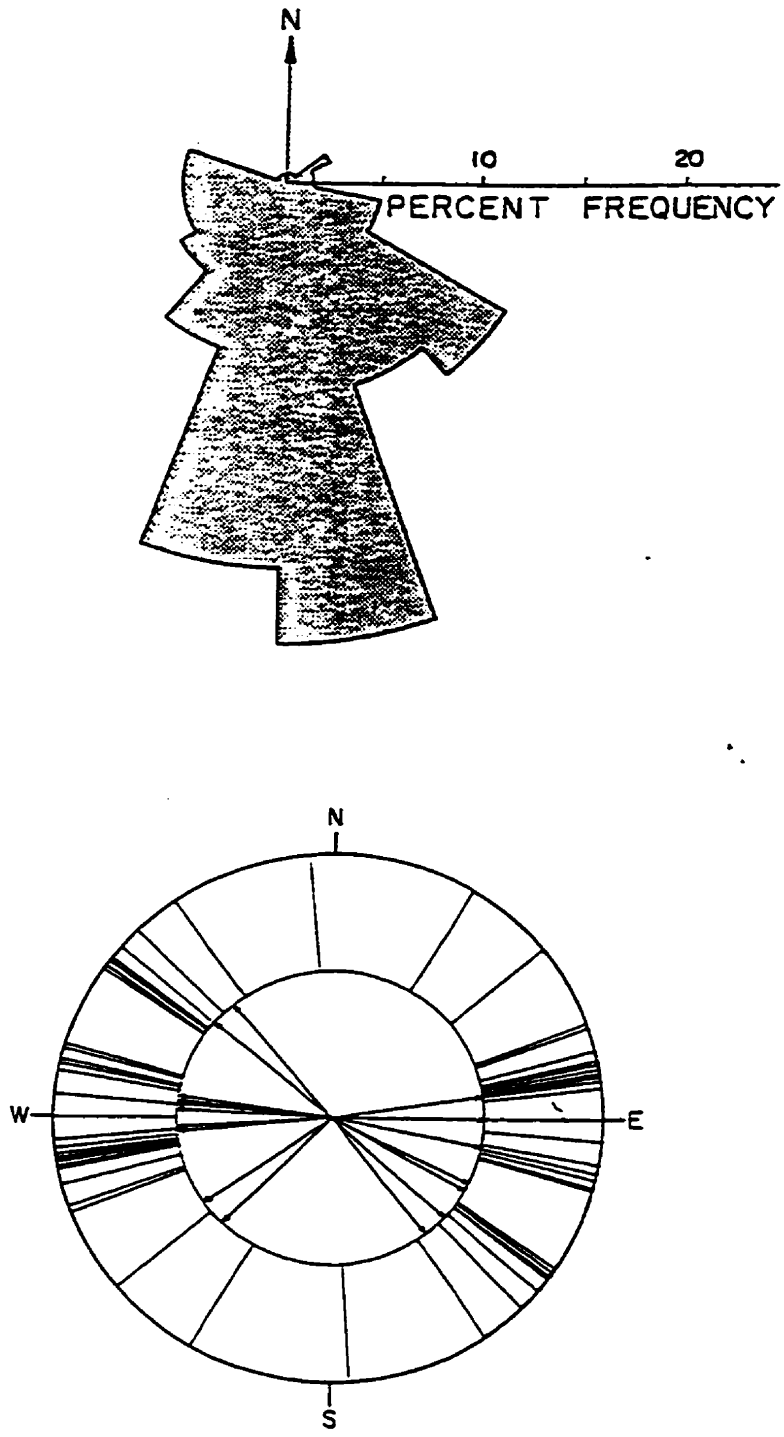

Fig. 37. Rose diagram and histogram summarizing orientation and inclination of 201 cross-bedded units in the Thomson Formation. From Morey and Ojakangas (1970)

Gc and **Gm** facies grainstones interbedded with packages of **Sc** facies chemical slates. In the Emily district the Trommald iron formation is at least 260 m thick and dominated by intimately interbedded **Sc** and **Sl** magnetite-rich, chemical slates. In the Cuyuna north range the Trommald iron formation is about 295 m thick and principally comprised of **Sl** facies chemical slates with subordinate amounts of **Sc** facies iron formation. The limited paleocurrent data (Figs. 33, 35, 36, and 37) from clastic and chemical sedimentary facies comprising the Animikie Group in Minnesota suggests this transect represents an oblique traverse across the basin and that the shoreline generally trended in an east-west direction and deposition occurred on a southward sloping paleoslope.

The base of this chemical sedimentary wedge is characterized by a pebble conglomerate; the Kakabeka conglomerate in Ontario and the unnamed basal conglomerate underlying the Pokegama quartzite in northern Minnesota. This basal unit unconformably blankets rocks of the Superior Province as a thin, discontinuous pebble lag and is thickest in the low relief depressions on the Archean basement. Like the Kakabeka conglomerate the correlative unit in Minnesota is also formed largely from weathered clasts derived from the underlying Archean basement (Ojakangas, 1983). The lateral extent of this basal unit in the Cuyuna North range is unknown as drilling has never penetrated the base of the Mahnomen formation. In northern Minnesota this basal conglomerate is transitional into clastic sandstones of the Pokegama Quartzite.

The Pokegama Quartzite and Mahnomen Formation form a clastic wedge which fines and thickens from the East Mesabi, where it is only a few metres thick, through the West Mesabi where it may be as much as 100 m thick (Ojakangas, 1993), to the Cuyuna north range where it is at least 610 m thick (Schmidt, 1963) and could be as much as 1.5 km thick (Southwick *et al.*, 1988). This clastic sequence has no correlative unit in Ontario. Here, the Kakabeka conglomerate is directly overlain by the iron-bearing strata of the Gunflint Formation.

Iron-bearing members comprising the Gunflint, Biwabik and Trommald iron formations form a chemical sedimentary wedge which fines and thickens from 175 m in Ontario to 295 m in east-central Minnesota (Fig. 38). In Ontario, the base of this wedge is characterized by member 1. This 6 m thick member is only laterally continuous between drill holes in from the Gunflint Formation in O'Connor and Blake Townships (TB0633, TB0642, TB0218) and does not exhibit any appreciable change in thickness. Drill hole data confirming its presence in northeastern Minnesota are lacking (GF-3). Member 2 is laterally persistent over a larger region, encompassing the Gunflint in northern Cook County, Minnesota. It is intersected in drill holes from O'Connor Township (TB0640, TB0641, TB0642, TB0633, TB0636, TB0637), Blake Township (TB0218), and northern Cook County (GF-3) in northern Cook County. Its thickness remains constant over this interval. Member 3 is only correlatable between the closely spaced drill holes in O'Connor Township; it pinches laterally to the south towards Blake Township. Member 4 is laterally

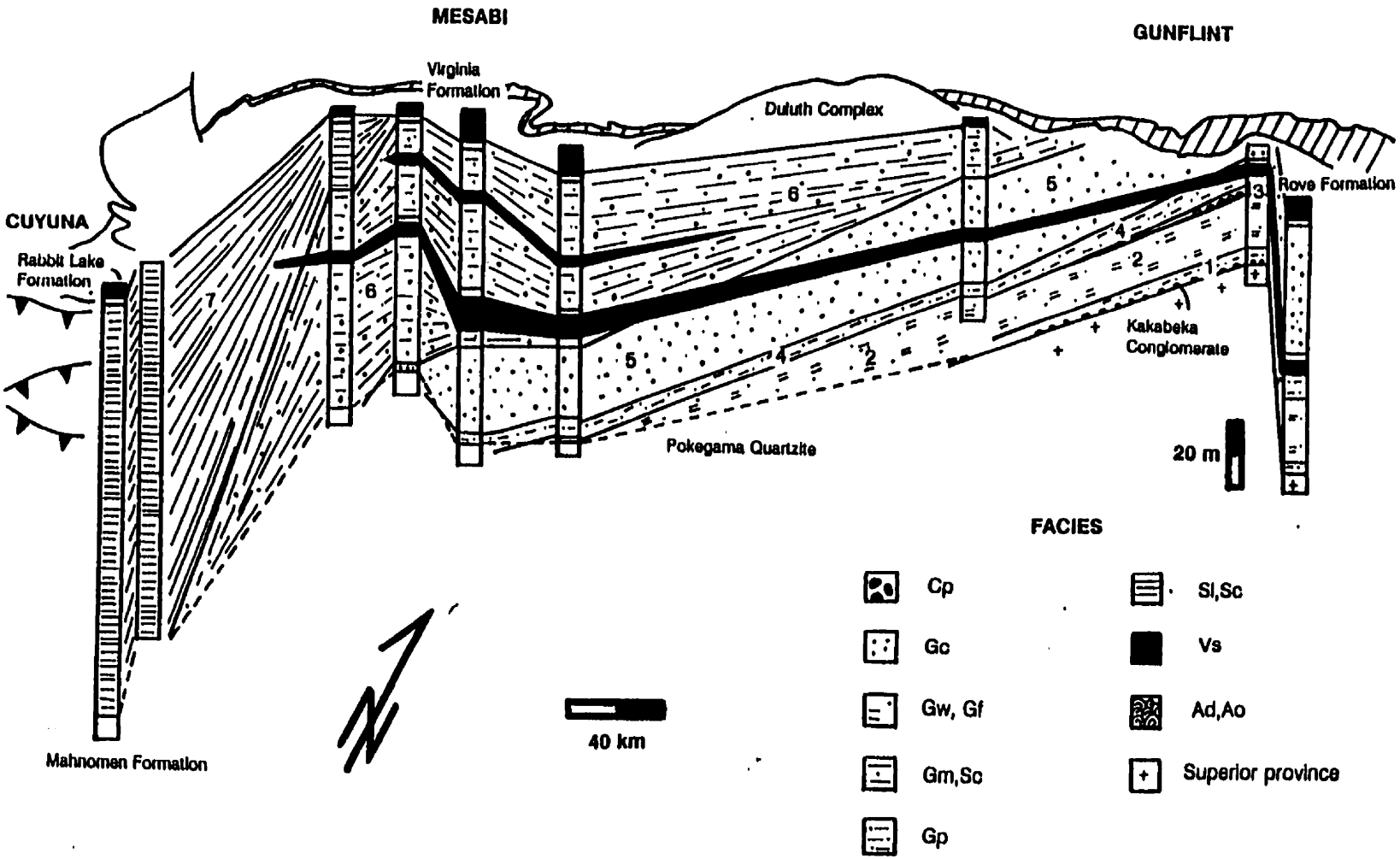

Fig. 38. Fence diagram showing regional stratigraphic correlations between Gunflint, Mesabi, and Cuyuna iron ranges. Stratigraphic data indicates that iron-bearing members form a chemical sedimentary wedge which fines and thickens from the 175 m in the Gunflint to 295 m in the Cuyuna north range over a lateral distance of 450 km. Correlations between iron ranges also show that members are diachronous and are cross cut by three volcaniclastic horizons: a lower, middle, and upper volcaniclastic horizon. The lower slaty members of the Rove, Virginia, and Rabbit Lake Formations form the uppermost volcaniclastic layer. The volcanic episode which produced it overwhelmed the depositional system with volcaniclastics to the point where iron formation could no longer accumulate. It marks the cessation of chemical sedimentary deposition in the Animikie Basin. Numbers refer to members 1 through 7.

persistent between drill holes from O'Connor (TB0633, TB0634, TB0635, TB0636, TB0637, TB0638, TB0639, TB0640, TB0641, TB0642) and Blake (TB0218) Townships, and Cook (GF-3) and St. Louis (MGS-2, MGS-5) Counties in the Main Mesabi. It thins slightly towards the southwest from 25 m in the Gunflint range to 13 m in the Mesabi range (MGS-2). Member 4's true thickness in drill hole GF-3 is ambiguous because accurate footage markers are missing; the drill core from GF-3 was dropped by the contributing company. Member 5 thins considerably from 98 m in Blake Township (TB0218) to 6 m in Itasca County (MGS-7) in the West Mesabi. Member 6 is present only in Minnesota. It thickens from 33 m in northern Cook County (GF-3) to 153 m in Crow Wing County (18290), in the Emily district of the Cuyuna iron range. Member 6's maximum thickness is believed to be slightly greater than that recorded here. Its true thickness in the Emily district is not known as the underlying Pokegama Quartzite and overlying Virginia Formation are missing from drill core (18290). Member 7 is intersected in the West Mesabi (MGS-7, MGS-8) where it thickens from 6 m to 295 m in the Cuyuna north range (G-1).

The overlying Virginia, Rove, Rabbit Lake and Thomson Formations form a slaty, clastic sequence which fines from north to south. Their true thicknesses are vague as their tops have been erosively removed since their deposition.

5.4 Depositional cyclicity

Examination of vertical and lateral transitions of iron formation facies comprising the Gunflint, Mesabi and Cuyuna iron ranges shows that 5 changes in relative sea level governed iron formation deposition (Fig. 34): a basal, fining upwards transgressive phase extending from the underlying **Cs** facies sandstones of the Pokegama Quartzite to 6 m above the transition into the iron-bearing strata of the Biwabik iron formation from the western Mesabi; a basal, 20 to 30 m thick, coarsening upwards regressive succession; a middle, 30 to 50 m thick, fining upwards, transgressive phase; a 20 to 30 m thick, coarsening upwards, middle regressive succession; and a fining upwards, upper transgressive phase extending from the top of the middle regression into the overlying **Vs** facies slates of the Rove and Virginia Formations. The basal transgression, middle regression and upper transgression of the Gunflint (Fig. 25) are correlative with the middle transgressive, middle regressive and upper transgressive phases discussed here. The basal transgression and regression are not present in iron-bearing strata in the East Mesabi and Gunflint ranges. Cycles are not correlatable to the Cuyuna iron range as iron formation facies are too fine-grained to permit accurate identification and correlation of cycles. The presence of similar allocyclic trends has been recorded by White (1954), Morey (1983) and Morey *et al.* (1991). However, the relative stratigraphic positions noted by them differs significantly than those described in this study.

Also present are smaller coarsening upwards cycles which comprise members 5 and 6. These previously unrecognized minor trends span a vertical distance of 5 to 10 m. In member 5 they coarsen gradually from medium-grained, chert-carbonate **Gc** facies grainstones to coarse-grained, chert-carbonate **Gc** facies grainstones. In member 6 cycles are generally finer-grained than those comprising member 5 and less well developed. They coarsen from parallel and wavy bedded, **Sc** facies chemical slates to **Gm** facies grainstones. In all instances their top contact is gradational over a span of 1 m into the base of the overlying cycle.

5.5 Volcanism

Three pulses of volcaniclastic deposition (**Vs** facies) punctuated iron formation accumulation (Fig. 39). The first is a volcaniclastic horizon correlatable from the Gunflint to the Western Mesabi at the base of the upper transgression (lower volcaniclastic horizon). Its thickness varies from 6 m in the Gunflint, to a maximum of 22 m in the Main Mesabi, to about 9 m in the Western Mesabi. Its lower bounding surface is sharp with the underlying iron formation. Its upper contact is gradational over a maximum span of 10 m with the overlying iron formation. The second is a volcaniclastic horizon occupying a stratigraphic position approximately 61 m above the first (middle volcaniclastic horizon). It is present only in the Main and West Mesabi. Like the first, its basal contact is also sharp. It

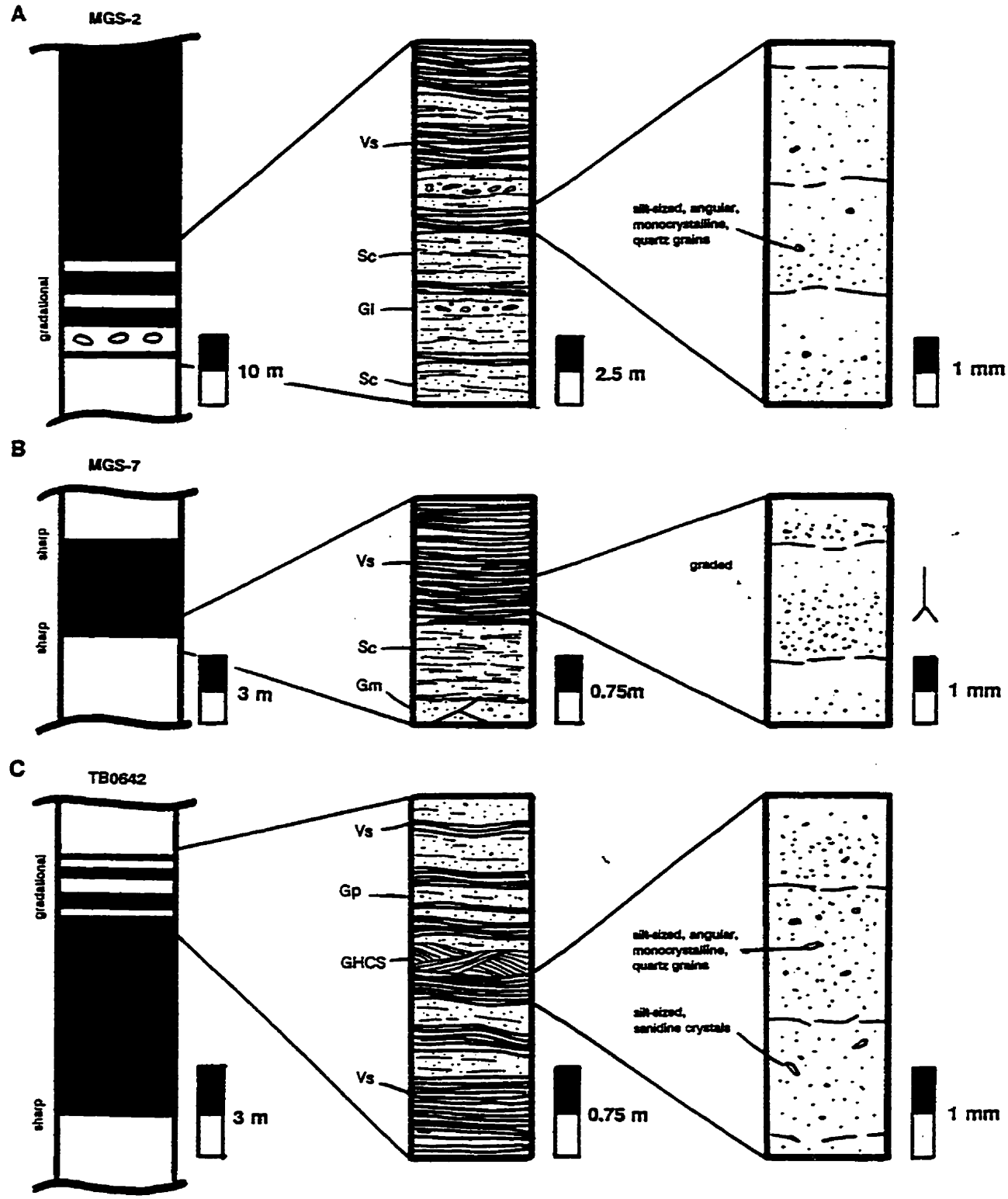

Fig. 39. Detailed facies associations at transitions in iron-bearing strata to the (A) upper volcaniclastic horizon, (B) middle volcaniclastic horizon, (C) lower volcaniclastic horizon. Facies relations indicate that the onset of the volcanic episode responsible for the upper ash horizon occurred gradationally (gradational lower boundary), that the onset and cessation of the episode which produced the middle volcaniclastic horizon occurred abruptly (sharp upper and lower boundaries), and that the start of the episode responsible for the lower horizon was abrupt (sharp lower boundary) and waned gradually over time (gradational upper boundary).

thins to the northeast and southwest from about 9 m in MGS-5 to roughly 4 m in MGS-2 and MGS-7. However, unlike the lower volcaniclastic horizon its upper contact is sharp. Accurate correlation of the lower and middle volcaniclastic horizons to the Emily district and Cuyuna north range was hindered by the frequent interbedding of **Sl** and **Sc** facies chemical slates with thinly laminated, carbonaceous layers. The third pulse forms the 120 to 140 m thick basal slaty member of the overlying Virginia and Rove Formations and the 60 m thick lower slaty member of the Rabbit Lake Formation (upper volcaniclastic horizon). Unlike the previous two volcaniclastic horizons its contact with the underlying iron-bearing strata is gradational over a span of 6 to 20 m. In the Gunflint and Mesabi iron ranges its base is characterized by **Gi** facies beds interbedded with **Sc** facies chemical slates and its upper contact is gradational into the siltstones and fine-grained sandstones comprising the upper member of the Virginia and Rove Formations. In the Cuyuna north range this volcaniclastic unit is transitional with iron formation of the middle member of the Rabbit Lake Formation. Lapilli tuffs (**Vt** facies) similar to those characterizing the base of the upper transgressive cycle in the Gunflint Formation in O'Connor Township were not observed in the Mesabi and Cuyuna iron ranges.

CHAPTER 6: GUNFLINT-MESABI-CUYUNA DEPOSITIONAL SYSTEM, PALEOGEOGRAPHIC RECONSTRUCTION

6.1 Introduction

Regional stratigraphic correlations show that vertical and lateral facies transitions within the Gunflint-Mesabi-Cuyuna depositional system are similar to those observed in many Phanerozoic, marine shelf systems. Like sediments accumulating along the margins of modern oceans, the chemical sedimentary rocks in Ontario and Minnesota also form a sedimentary wedge which fines and thickens from coarse, wave reworked, nearshore deposits of the foreshore and shoreface to parallel laminated mudstones of the outer shelf and slope break. The main morphological elements, bedforms and internal sedimentary structures along a typical shelf-to-slope profile are shown in Fig. 40. The following summary of these features is taken from Friedman *et al.* (1992), Davis (1992), and Mitchell and Reading (1986).

The depositional terrace at the margin of any marine basin accumulating sediment can be divided, from the shore seaward, into the *nearshore, shelf, slope, rise,* and *abyssal plain* (Fig. 40) (Friedman *et al.*, 1992). The *nearshore* zone is comprised of the *foreshore* and *shoreface.* The foreshore, also synonymous with beach, borders the peripheral regions of continental land masses and consists of the portion above the low tide line. It is dominated by the swash and backwash of

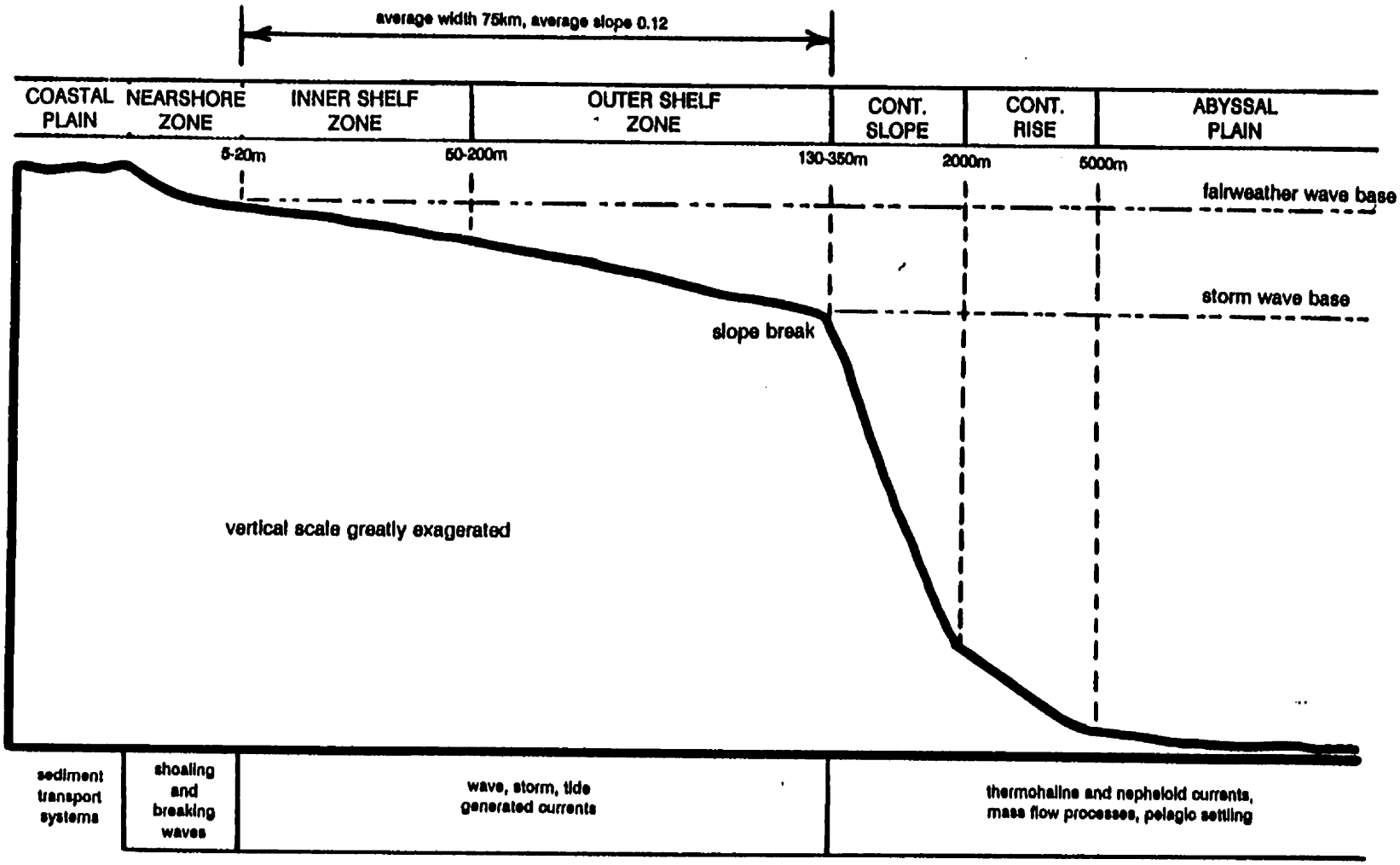

Fig. 40. Idealized profile across continental margin showing locations of coastal plain, nearshore, inner shelf, outer shelf, continental slope, continental rise, and abyssal plain, as well as sediment transport systems which distribute sediment in each of these regions. The shelf lies above storm weather wave base.

breaking waves. The *shoreface* lies below low tide level and is characterized by day-to-day sand transport above fairweather wave base. The shoreface normally has a concave-upward profile, which is in equilibrium with the waves that shape it. A detailed summary of depositional processes acting in the nearshore is given in Chapter 4 and will therefore not be repeated here.

The *shelf* is defined as the extremely flat (mean slope 0.12°) portion of the terrace above storm wave base (Rich, 1951) which is bound on its landward side by the concave upwardly sloping shoreface, and on its seaward edge by the shelf break (Fig. 40) (Friedman *et al.*, 1992). Its commonly subdivided into two zones, the *inner* and *outer shelf*. The inner shelf forms the transition from the sandy nearshore to the mud-dominated outer shelf. The change from the nearshore to the inner shelf, and the inner shelf to the outer shelf occurs between 5 and 20 m, and 50 and 200 m water depth respectively (Fig. 40) (Mitchell and Reading, 1986). The shelf break, varies in depth from 130 to more than 350 m (Friedman *et al.*, 1992). The width of the shelves surrounding the present-day continents averages 75 km; the range is from less than 0.5 to 1 300 km (Friedman *et al.*, 1992).

Shelf deposition is controlled primarily by extrinsic processes such as climate, which affects sediment run-off, organic productivity, the availability of detrital sediment, the chemistry of the ocean waters, waves, storms, tides, changes in sea-level (Mitchell and Reading, 1986), and in part by plate tectonics

(Davis, 1992). Thus the type of sediment forming on shelves depends on latitude and climate, on the facing of a shelf relative to major wind belts, and on tidal range (Mitchell and Reading, 1986). In the Paleoproterozoic geochemical factors involved with the deposition of iron formation are equally important in determining the kind of sediment which formed. They include the source of the iron and silica, transport mechanisms, and controls on precipitation (Fralick and Barrett, 1995).

Shelves that develop on the trailing edges of continents are commonly called passive continental margins and are wide and generally slope less than a degree (Davis, 1992). In contrast, leading edge or active shelves tend to be narrow and steep and have high relief (Davis, 1992). Shelves may also be classified as being either wave, tide, oceanic current, or storm dominated depending on the type of hydraulic regime governing deposition (Johnson and Baldwin, 1986). Wave-dominated shelves are controlled by seasonal fluctuations in wave and current intensity, with active sediment transport being restricted to intermittent storms. Tide-dominated shelves are swept daily by powerful currents enabling a wide range of bedforms to develop. Oceanic current-dominated shelves are characteristically narrow and are more or less constantly under the influence of powerful and persistent, unidirectional ocean currents. Storm-dominated shelves are controlled by frequent, storm-generated currents which commonly overprint other shelf regimes.

In a more general sense shelves can be categorized as being either allochthonous or autochthonous, depending on the kind of sediment accumulating on them. Allochthonous shelves receive large amounts of extrabasinal sediment from the adjacent continent. They typically form near modern deltas, near localities where fans are active at the shore, and off deserts where wind is blowing sand into the water (Friedman *et al.*, 1992). Modern examples include the siliclastic, wind-and-wave dominated Oregon-Wahington shelf, the storm-dominated northwest Atlantic shelf and the Bering Sea, the narrow, oceanic current-dominated southeast African shelf, and the tide-dominated shelf of the northeast United states (Johnson and Baldwin, 1986). Autochthonous shelves accumulate little or no extrabasinal sediment from the bordering continental land mass (Friedman *et al.*, 1992). The bottom of siliclastic, autochthonous shelves are generally composed of wave and current reworked sediment deposited by lowstand systems tracts. Those which accumulate intrabasinal carbonate sediment are called carbonate shelves. Examples of modern autochthonous shelves consists of the carbonate-rich, open, northwest Yucatan shelf, the rimmed Great Bahama Bank (Sellwood, 1986) and the siliclastic, Atlantic coast of Canada (Dalrymple *et al.*, 1995). Ancient examples include the broad, shallow Paleoproterozoic shelves on which iron formation was deposited.

The *slope*, *rise* and *abyssal plain* are below storm wave base and are consequently free from wave reworking (Fig. 40) (Rich, 1951). Deposition on the

slope and rise is dominated by muds, silts and fine sands transported by thermohaline contour-following currents and nepheloid layers (Mitchell and Reading, 1986). Thermohaline currents are oceanic bottom currents formed by the cooling and sinking of surface water at high latitudes and the slow thermohaline circulation of these polar water masses throughout the oceans (Stow, 1986). Nepheloid layers or turbid bottom waters contain large concentrations of suspended, fine sediment, and are commonly associated with the higher velocity bottom currents in many parts of the oceans (Stow, 1986). Mass flow processes such as turbidity currents, grain flows and debris flows generated from large-scale rotational sliding and slumping are also important in moving sediment from the slope to the rise (Mitchell and Reading, 1986). Abyssal plain sedimentation is dominated by pelagic settling of suspended, silt-sized particles through the oceanic water column (Stow, 1986). Suspended particulates are transported by surface currents, winds and floating ice and mix with pelagic biogenic components during settling (Stow, 1986). Waning density currents descending from the slope and rise are also important in delivering sediment to the abyssal plain.

6.2 Paleogeographic interpretation

The following discussion is subdivided into three sections. Each part deals with interpreting the lithofacies comprising, 1) the sandstone-siltstone succession

at the base of the Animikie (Pokegama Quartzite) and North Range Groups (Mahnomen Formation), 2) the overlying chemical sedimentary wedge (Gunflint, Biwabik, and Trommald iron formations), and 3) the siltstone-shale succession forming the top of the Animikie (Rove and Virginia Formations) and North Range Groups (Rabbit Lake Formation). Emphasis will be placed on interpreting the chemical sedimentary facies comprising the Gunflint, Biwabik, and Trommald iron formations as they are the focus of the current investigation. However, a brief interpretation of the facies comprising the under- and overlying clastic and volcaniclastic sequences is essential for accurately interpreting the paleogeographic evolution of Gunflint-Mesabi-Cuyuna depositional system and are therefore included in the following discussion.

Basal sandstone-siltstone succession

Ojakangas (1983, 1993) has interpreted the basal shale, middle siltstone-shale, and upper sandy members of the Pokegama Quartzite as forming in tide-dominated environments during a major, marine transgression. The presence of alternating thin beds of shale, siltstone, and sandstone, and lenticular, parallel, wavy, and flaser bedding are all characteristic of tidal sedimentation (Reinick and Singh, 1975). Similar structures in the Moodies Group of South Africa have been interpreted by Eriksson (1977) as also having formed in tidal environments by bidirectional, paleo-tidal currents with variable flow velocities (Ojakangas, 1983). The coarse sediments were apparently transported by high-energy tidal and storm

currents via bedload traction, whereas the fine sediments appear to have settled from suspension during the slack high-water stages of the tidal cycle and during calms after wave-induced turbulence (Ojakangas, 1983).

The three members which comprise the Pokegama Quartzite (Fig. 32), from bottom to top, formed in successively deeper tidal environments (Ojakangas, 1983, 1993). The basal shale member (figure) was deposited as the initial unit upon the Archean basement as the Animikie sea transgressed, and is interpreted by Ojakangas (1983, 1993) as representing deposition of suspended material during high-slack tide periods from water which moved onto supra-tidal flats by tidal currents and wave action. The rarity of desiccation features within this basal member suggests that the supratidal and intertidal zones were not well developed on the Animikie shoreline during this initial phase of clastic deposition; a situation typical of modern microtidal (tidal range <2 m) environments (Reineck and Singh, 1975). The overlying, middle siltstone-shale member, which comprises most of the Pokegama Quartzite, is interpreted as the product of an alternation of bedload and suspension depositional processes operating on intertidal, "mixed" sand-mud flats (Ojakangas, 1983, 1993). Associated interbeds of mud, silt, sand, and wavy, parallel, lenticular and flaser beds present within this member characterize the intertidal tidal zone in many modern, tide-dominated depositional systems. The parallel and planar cross-stratified beds composing the upper member are typical of deposition in the lower tidal flat environment near the low water line or shallow

subtidal environment strongly influenced by tidal currents (Ojakangas, 1983, 1993). The sands are believed to have accumulated as lower tidal sand flats or as subtidal sand shoals in water above fair weather wave base. Iron formation formed seaward, away from the land derived clastics during this early phase of deposition in the Animikie Basin (Ojakangas, 1983) (Fig. 41).

No detailed sedimentological or stratigraphic investigation of the Mahnomen Formation at the base of the North Range Group in east-central Minnesota has ever been undertaken. However, the cursory observations made during the course of this study and published descriptions (Schmidt, 1963; Morey, 1978; Marsden, 1972; Southwick *et al.*, 1988) of this unit indicate that the Mahnomen Formation is probably the distal equivalent of the Pokegama Quartzite. The intimately interbedded shale and siltstone layers which comprise the Mahnomen Formation are characteristic of deposition by waning storm generated turbidity currents (Aigner, 1985; Einsele, 1992, Davis 1992) and pelagic settling of suspended, silt-sized particles through the oceanic water column (Stow, 1986).

The thin, discontinuous conglomeratic unit at the base of the Pokegama Quartzite and the correlative Kakabeka conglomerate at the base of the Gunflint Formation were present prior to the development of the Animikie Basin, occupying small low relief depressions on the peneplained, Archean surface (Ojakangas, 1983), most of which had undergone erosion for at least 200 million years during

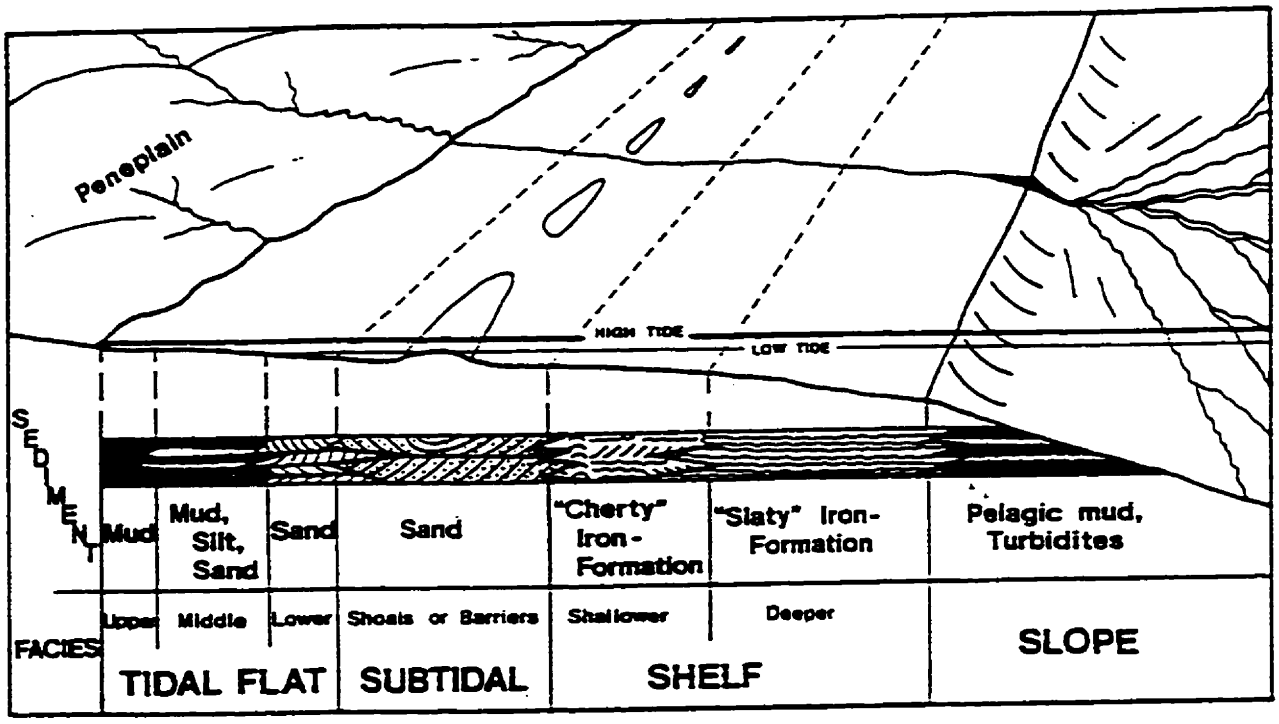

Fig. 41. Sedimentological model showing lateral relations of siliclastic facies and iron formation facies during the initial stages of iron formation accumulation the Animikie Basin. From Ojakangas (1983, 1993).

the deposition of the approximately 2.3 Ga (Symons and O'Leary, 1978) Huronian Supergroup (Sims, 1976; Young, 1983; Fralick and Miall, 1989). Evidence from the Gunflint Formation suggests that this basal matrix and clast supported conglomerate was locally reworked by wave action into crudely stratified supratidal beach deposits during encroachment of the Animikie Sea (Chapter 4).

Chemical sedimentary wedge

Stratigraphic correlations indicate that the seven members comprising the iron-bearing strata in Ontario and Minnesota are diachronous, and constitute a complete shelf sequence which thickens over a lateral distance of 450 km from 175 m in the Gunflint to approximately 295 m in the Cuyuna north range (Fig. 42). Nearshore facies consist of flaser (**Gf** facies) and wavy bedded (**Gw** facies) chert-carbonate grainstones and strand proximal stromatolites (**Ad** facies) which are transitional distally into parallel bedded (**Gp** facies) and hummocky cross stratified chert-carbonate (**GHCS** facies) grainstones. Inner shelf facies are composed entirely of massive and cross stratified chert-carbonate grainstones (**Gc** facies). Hematite-rich chert, grainstones (**Gm**) and chert-rich chemical slates (**Sc** facies) comprise facies of the middle shelf. The most distal shelfal regions are dominated by intimately interbedded magnetite- and chert-rich chemical slates (**Sl** and **Sc** facies). Facies characteristic of lower slope, rise and abyssal plain sedimentation were not observed. Vertical transitions in iron formation facies indicate that deposition of this chemical sedimentary wedge occurred during an overall marine

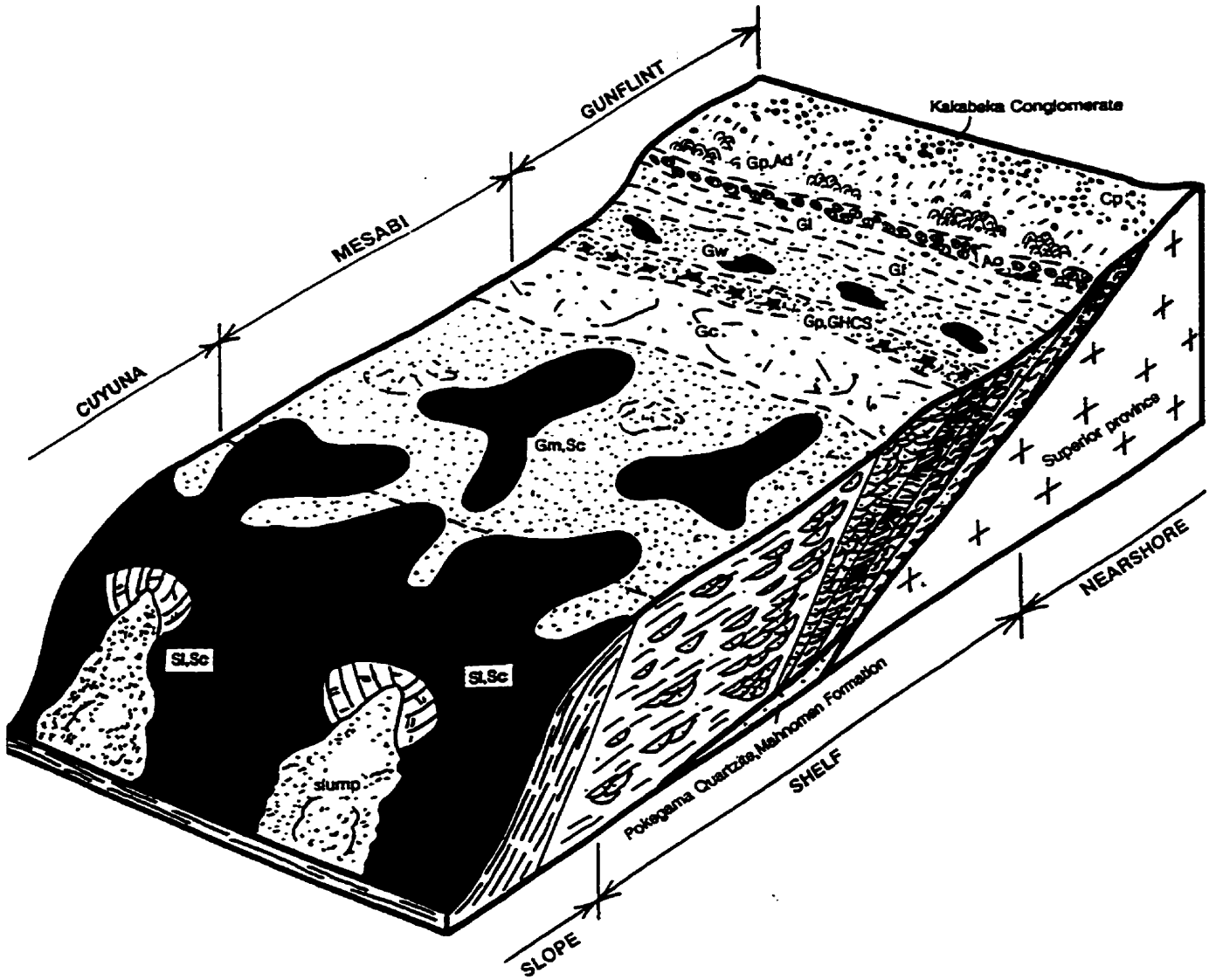

Fig. 42. Paleogeographic reconstruction of the Gunflint-Mesabi-Cuyuna depositional system. Stratigraphic correlations between iron ranges in Ontario and Minnesota indicates that iron-bearing members constitute a complete shelf sequence. Nearshore facies include Gf, Gw, Gp and GHCS facies grainstones and Ad and Ao cryptalgal facies. Inner shelf facies are composed entirely of Gc facies grainstones. Gm facies grainstones and Sc facies chemical slates characterize middle shelf facies. The distal shelf and slope break are dominated by Sl and Sc facies chemical slates. Mass flow processes produced by large-scale rotational slumping and sliding near the slope break were important in moving sediment from the slope to the rise. The Gunflint range is comprised of nearshore and inner shelf facies. The Mesabi range is dominantly composed of inner and outer shelf facies. The Cuyuna iron range is comprised exclusively of facies characteristic of the outer shelf and slope break.

transgression punctuated by two minor regressions.

The following is a detailed paleoenvironmental synthesis of chemical sedimentary facies comprising the nearshore, inner and outer shelf of the Animikie Basin. This discussion will primarily focus on interpreting vertical and lateral facies transitions present within members 6 and 7, as those comprising members 1 through 5 have already been dealt with in detail in Chapter 4.

Deposition of nearshore, iron formation facies began with member 1. This thin, parallel bedded grainstone (**Gp** facies) unit marks the onset of intertidal, chemical sedimentation on the foreshore. Like the shale-siltstone member, which characterizes the base of the Pokegama Quartzite, member 1's relative thinness and apparent lack of desiccation features also suggests that the intertidal zone was not well developed on the Animikie shore (Chapter 4). The overlying flaser (**Gf** facies) and wavy bedded (**Gw** facies) chert-carbonate grainstones of member's 2 and 3 represent subtidal sheet sand development on a shallow, storm enhanced, non-barred shoreline. They record energy transformations from the high energy surf and breaker zones of the upper shoreface through to the lower energy, storm influenced, mixed grainstone-chemical mud flats of the lower shoreface. Similar Middle and Upper Cambrian peritidal carbonate sequences from the Elbrook and Conococheague Formations in the Virginia Appalachians have been interpreted by Demicco (1985), and Koerschner and Read (1989) as representing deposition of

subtidal sand sheets in storm-influenced, nearshore settings. The parallel (**Gp** facies) and hummocky cross stratified (**GHCS** facies) grainstones of member 4 mark the progressive onlap of offshore facies over those of the lower shoreface. The fine- and medium-grained chert- and hematite-rich grainstone beds comprising this member represent episodic development of storm-generated, chemical sedimentary beds.

Deposition on the inner shelf was dominated by the development of coarse-grained, shoaling upward, chert-carbonate grainstone successions (member 5) (Fig. 42) which may be associated with offshore bar development. In Chapter 4 their genesis was shown to be the result of a unique interplay between the geochemical and physiological conditions which prevailed in the Animikie Basin during iron formation deposition. They formed near shelfal regions where iron oxide and silica gels were actively precipitating, and where currents could rework chemical precipitates into rip-up grains (Simonson and Goode, 1989) and possibly redistribute these intraclasts to form offshore bars. Similar sequences comprising the Upper Cretaceous Sussex and Shannon sandstones of the Powder River Basin in northern Wyoming (Berg, 1975; Brenner, 1978; Hobson *et al.*, 1982) have also been interpreted as representing progradation of offshore bars. The depositional model proposed for the Sussex and Shannon consists of migrating sand sheets formed by tide- and storm-generated currents. Coarse detritus is believed to have been provided to the shelf via storm-generated bypass mechanisms (storm-induced

bottom return-flow and turbidity currents) which redirected sediment from nearshore to offshore regions. The sequence that accumulates is coarsening upwards, and is suggestive of continued shoaling (Davis, 1992). Similar sandbodies are also present on the western Grand Banks of Newfoundland. There, Dalrymple *et al.* (1995) have determined that the interaction of the weak, thermohaline, Labrador Current and wave-orbital motion with directionally-variable storm currents are responsible for shaping bedforms.

Similar trends comprising member 6 are interpreted as representing offshore bar development on the middle shelf, away from areas of primary chert/carbonate grain genesis (Fig. 42). Cycles are generally finer-grained and are less well developed than those forming member 5. They coarsen from parallel and wavy laminated, chert- and magnetite-rich, slaty iron formation (**Sc** and **Sl** facies) to medium- and coarse-grained massive and cross-stratified, hematite-rich grainstones. Identical successions from the Gogebic iron range have been interpreted by Pufahl (1994) as representing progradation of offshore bar complexes near the shelf break (Fig. 43).

Alternatively, it was shown that these coarsening upwards successions may represent paracycle development (Vail *et al.*, 1977) during a punctuated rise in overall sea level. Data at the present time is not sufficient to accurately ascertain whether an allocyclic (sea level) or autocyclic (depositional) mechanism, or both,

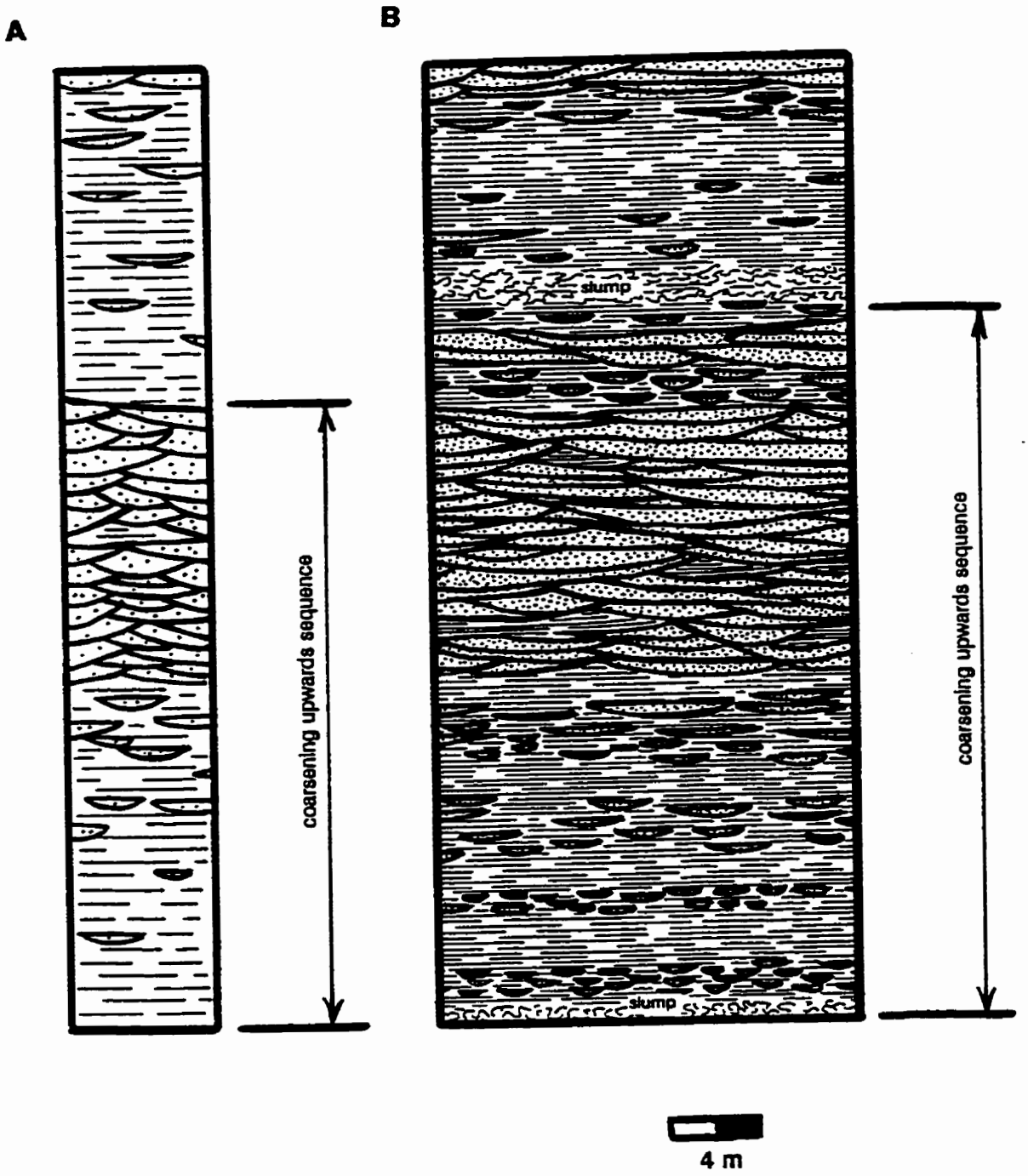

Fig. 43. Comparison of coarsening upwards sequences from Mesabi (A) and Gogebic (B) iron ranges. Cycles are similar except for the presence of slumped horizons at the top of grainstone successions in the Gogebic iron range. This may suggest that sequences from the Gogebic iron range formed closer to the slope break, where slope failure occurred, than those in the Mesabi.

governed cycle formation. However, regardless of how cycles formed stratigraphic correlations indicate that their genesis was the result of a unique interplay between the geochemical and physiological conditions which prevailed in the Animikie Basin during the time when iron formation was accumulating. Member 5 pinches laterally towards the base of the Biwabik iron formation (Fig. 34, 38) which indicates that a similar environment did not exist during deposition of the underlying Pokegama Quartzite and Mahnomen Formation. The bidirectional paleocurrent data (Fig. 35) from cherty grainstones in the Main Mesabi (Ojakangas, 1983) suggests that northwest-southeast flowing tide, and possibly storm generated currents interacted to redistribute sediment on the middle shelf.

The monotonously interbedded packages of magnetite-rich **Sl** and **Sc** facies chemical slates of member 7 characterize deposition of iron formation on the outer shelf (Fig. 42). Like the Middle Member of the Baby Formation of the northern Labrador Trough (Fralick and Barrett, 1995) the predominance of chemical slates, the lack of wave or tide deposits, and the rare presence of medium- and coarse-grained chert grainstones (**Gm** facies) suggests that deposition of member 7 took place below storm wave base on the most distal shelfal regions or upper slope. The rare, physically graded, **Sl** facies chemical slates may have been deposited from low-density turbidity currents similar to those attributed to comparable laminations comprising the Baby Formation (Fralick and Barrett, 1995). The massive chert grainstone beds described by Schmidt (1963) were probably moved

by grainflow processes which operated on the upper slope. The cross stratified hematite-rich chert grainstones (**Gm** facies) observed at the top of the Merritt drill hole from the Cuyuna north range may have been moved into the area by storm-induced bottom return flow and/or turbidity currents originating on the inner shelf, where grain production took place. This places member 7 on the outer shelf but close enough to areas affected by tide- or storm-generated currents to receive shelf sediments during unusually high-velocity flow events.

The iron formation breccias described by Schmidt (1963) are probably slump scars produced by slumping and sliding on the upper slope. The best evidence for this comes from Schmidt's (1963) description of the large, lenticular fragment of **Vs** facies slate whose contacts with the under and overlying **Sl** and **Sc** facies iron formation are characterized by brecciated iron formation and slabs of slaty iron formation 30 cm in length. Similar features within the Cambro-Ordivician, continental margin assemblages in the Appalachian region in the northeast United States have been interpreted by Friedman *et al.* (1992) as slump blocks which formed as a consequence of slope failure on the upper slope. Their presence in the chemical sedimentary wedge is important because they indicate that mass flows processes generated by large-scale rotational slumping and sliding near the slope break were important in moving sediment from the slope to the rise.

Five changes in relative sea level controlled iron formation deposition in

Ontario and Minnesota (Fig. 34). The lowest of these, the basal transgression and regression, exists only in the iron-bearing strata at the base of the Biwabik iron formation in the Western Mesabi. Consequently, they are interpreted as recording a cycle of relative sea level change which governed iron formation accumulation during a time prior to the deposition of the eastern Biwabik and Gunflint iron formations. Stratigraphic relations suggest that correlative cycles may be present in the Pokegama Quartzite at the base of the Biwabik iron formation in the East Mesabi. If correct these observations support Ojakangas' (1983, 1993) model that accumulation of chemical sediments occurred seaward away from land derived clastics during this initial phase of iron formation accumulation (Fig. 41). They also give credence to the diachronous nature of iron-bearing members. The presence of iron formation facies characteristic of the middle shelf and the absence of nearshore iron-bearing facies (Figs. 34 and 38) near the base of the chemical sedimentary wedge at the same stratigraphic position as the lower transgressive-regressive cycle further substantiates that iron formation deposition initially occurred away from land derived clastics accumulating in the nearshore.

The middle transgression marks the encroachment of the Animikie Sea into northeastern Minnesota and Ontario, and is responsible for the progressive onlap of the chemical sedimentary rocks comprising the Main and East Mesabi, and Gunflint ranges over the Superior province. Vertical changes in iron formation facies suggests that the middle regression only briefly affected iron formation

accumulation. In the Gunflint its peak is marked by the development of strand proximal stromatolites in member 3. The upper transgression is a major transgressive marine event which governed the accumulation of iron formation to the top of the Gunflint, Mesabi, and Cuyuna iron ranges.

The existence of minor mafic flows and tuffaceous horizons in the Gunflint (Goodwin, 1956, 1960; Hassler and Simonson, 1989; Kissin and Fralick, 1994; Fralick and Barrett, 1995), and the presence of three volcaniclastic horizons in the Gunflint and Mesabi iron ranges indicate that the region was volcanically active during basin formation and subsidence. Lithofacies transitions between iron formation and volcaniclastic (**Vs**) facies indicate that initial burst of volcanism, the lower volcaniclastic horizon, and resedimentation of this material occurred swiftly and waned gradually allowing a slow return to a chemical sedimentary dominated depositional system (Fig. 39). Facies transitions within the middle volcaniclastic horizon, in the Mesabi iron range (Fig. 39), indicate that both commencement and cessation of this volcanic pulse and resedimentation of clastics derived from it was abrupt. The third pulse, which comprises the basal member of the Rove, Virginia and Rabbit Lake Formations, occurred gradually, and marks the end of chemical sedimentary deposition within the Animikie Basin (Fig. 39).

The presence of a complete shelf sequence arouses serious concern regarding the validity of the foreland model. If iron formation deposition was to

have occurred in a migrating peripheral foreland basin, accumulation of chemical sediments would be restricted to the outer shelf (Hoffman, 1987), as erosive processes operating on the peripheral bulge (Fig. 44) (Quinlon and Beaumont, 1984; Ojakangas, 1995) would continually shed clastics into nearshore areas preventing iron formation deposition (Fralick and Barrett, 1995). Consequently, the chemical sediments which accumulated would only be characterized by facies of the distal shelf. The observed lateral and vertical facies trends within correlative members are to the contrary, a complete shelf sequence is present, not just the distal portion (Fig. 42).

Upper shale-siltstone succession

Morey (1967, 1969), Lucente and Morey (1983), and Morey and Ojakangas (1970), have interpreted the Rove, Virginia, and Thompson Formation, respectively, as being deposited in moderately deep quiet water, by southward flowing turbidity currents moving down a regional paleoslope perpendicular to the inferred shoreline. Lucente and Morey (1983) concluded that the sedimentological attributes of the Virginia Formation resemble thickening and coarsening upward turbidite sequences associated with the lower and mid-fan parts of a prograding submarine fan complex. In this model the upward transition from the lower slaty member of the Rove, Virginia, and Rabbit Lake Formations to the upper siltstone-sandstone member represents the transition from pelagic sedimentation on a basin plain to sparse thin-bedded turbidite deposition on the outer part of the mid fan area

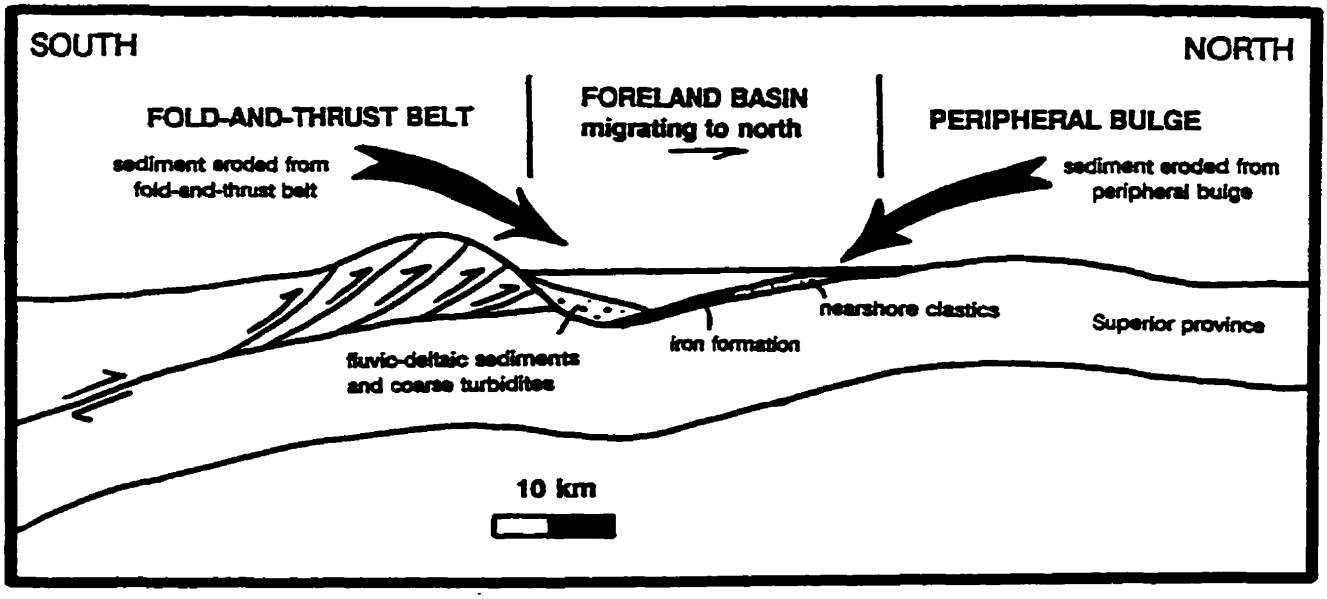

Fig. 44. Schematic cross section depicting deposition of iron formation in migrating peripheral foreland basin. In this model accumulation chemical sediments would be restricted to the outer shelf as erosive processes operating on the peripheral bulge would continually shed clastics into nearshore areas preventing deposition of iron formation. Lateral and vertical facies transitions within correlative iron-bearing members are to the contrary, a complete shelf sequence is present, not just the distal portion. Paleocurrent data also contradicts the foreland model. Orientations of cross-bedded units in the Thomson Formation indicate that deposition of this clastic unit was by dominantly north-to-south flowing currents not south-to-north as would be expected if its source was from an orogenic terrane situated to the south. Modified from Ojakangas (1995).

(Lucente and Morey, 1983). However, if this scenario is correct the lower slaty members should be diachronous with the underlying iron-bearing members, indicating a gradual shifting of environments from iron formation accumulation on the shelf to clastically dominated deposition on the slope and rise. Stratigraphic data are to the contrary, they indicate the lower member of the Rove, Virginia, and Rabbit Lake Formations truncates time-transgressive bounding surfaces between iron-bearing units (Figs. 34 and 38). Also, if this model is correct the area of the Mesabi range must be located toward the edge of the depositional basin (Lucente and Morey, 1983), a criteria not supported by lithofacies associations comprising the Biwabik iron formation.

An alternative interpretation is that the lower slaty members of the Rove, Virginia and Rabbit Lake Formations are a volcaniclastic horizon marking a volcanic episode that rapidly brought deposition of iron formation to an end, and the upper members represent turbidite deposition from southward flowing currents once this pulse of volcanism ceased. This explanation is useful in that it can readily explain why the lower member truncates diachronous iron formation members. In this model the middle iron-bearing member of the Rabbit Lake Formation is interpreted as representing the return of chemical sedimentary deposition on the distal shelf immediately following the cessation of volcanism. Its upper member records the termination of iron formation accumulation on the outer shelf by progradation of clastics from the north. The **Gi** facies chert-carbonate grainstone beds

characterizing transitional facies from the underlying iron-bearing strata of the Gunflint, Biwabik, and Trommald iron formation to the lower slaty members of the Rove, Virginia, and Rabbit Lake Formations (Figs. 34 and 38) are interpreted as representing redeposition of volcaniclastics from suspension clouds generated by either storms or tectonism.

Recently, Southwick *et al.* (1988), and Southwick and Morey (1990) have reinterpreted the rhythmically interbedded shales, siltstones, and sandstones comprising the Thomson and Virginia Formations as having the sedimentary characteristics of orogenic turbidites deposited in a migrating peripheral foreland basin which developed penecontemporaneously with the evolving Penokean orogeny to the south (Chapter 1). However, this model is not supported by sedimentological data. Orientations of 201 cross bedded units from the Thomson Formation (Fig. 37) (Morey and Ojakangas, 1970) indicate that deposition of this clastic unit was by dominantly north-to-south flowing currents, not south-to-north as would be expected if its source was from an orogenic terrane situated to the south (Fig. 44). Nevertheless, Southwick *et al.* (1988) contend that this contravening data can be reconciled if the basin had a bathometric form of a deep trench or elongate trough that trended essentially east-west, more or less parallel to the tectonic highland. With this basinal configuration the east-west trending sole marks (Fig. 37) would be produced by axial flowing density currents along the southern margin of the Animikie Basin. The south flowing currents, implied from

the cross bedding data, would then represent deposition from waning currents derived from a regime which prevailed on the north slope (Southwick *et al.*, 1988). However, even with this basinal configuration, it would be expected that sediments accumulating in such close proximity to a southern fold-and-thrust belt would be deposited by dominantly south-to-north flowing paleocurrents, indicating their derivation from the tectonic front, not the other way around. Sediments deposited in a peripheral foreland basin should also be coarser-grained than those comprising the Thomson and Virginia Formations; there is an apparent lack of coarse turbiditic, deltaic and fluvial sediments adjacent to the fold-thrust belt. In the most impressive present-day peripheral foreland basin, the Indo-Gangetic trough south of the seismically active Himalayas (Parkash *et al.*, 1980), sediment eroded from the rising mountains is deposited in the basin as alluvial fans, transverse to the tectonic axis. Adjacent to the Arabian Gulf, another modern foreland (Mitchell and Reading, 1986), the clastic sedimentary fill is primarily fluvio-deltaic.

CHAPTER 7: CONCLUSIONS

The iron-bearing rocks in Ontario and Minnesota form a chemical sedimentary wedge which fines and thickens from coarse, wave reworked, nearshore deposits of the Gunflint Formation to offshore, parallel-laminated, chemical mudstones of the Trommald iron formation in east-central Minnesota. Lateral and vertical facies transitions are directly comparable to those observed in modern shallow marine clastic and carbonate depositional systems. They record energy transformations from deep water, offshore waves to nearshore, shoaling waves under fairweather and storm conditions. Paleocurrent data suggests deposition of chemical sedimentary rocks occurred on a southward facing paleoslope.

Nearshore chemical sedimentary rocks consist of successions of strand-proximal stromatolites, flaser and wavy bedded chert-carbonate grainstones, and parallel bedded and hummocky cross stratified hematite-rich cherty grainstones deposited on a non-barred, microtidal, storm-enhanced shoreline with little clastic influx. Deposition on the inner shelf was dominated by accumulation of coarse-grained, shoaling upwards, chert-carbonate grainstone successions, possibly associated with offshore bar development. Their genesis is believed to have been the result of a unique interplay between the chemical and physiological conditions which prevailed in the Animikie Basin during iron formation deposition. They

formed in proximal offshore areas where iron oxide and silica gel were actively precipitating, and where currents could rework chemical precipitates into rip-up grains and redistribute them. The shoaling upwards successions replace a mud dominated offshore, which is so characteristic of modern shallow-marine depositional systems.

Distally, coarsening upwards sequences become finer-grained and less well developed. They coarsen from parallel laminated, magnetite-rich chemical slates to medium-grained, massive and cross stratified, chert-carbonate grainstones, and are interpreted as recording progradation of offshore bar complexes on the middle shelf below fairweather wave base, away from areas of high primary grain genesis. These successions may also represent paracycle development during an overall rise in relative sea level.

Monotonously interbedded parallel and wavy bedded chemical slates characterize deposition of iron formation on the outer shelf and slope-break. The presence of rare, massive and cross stratified, chert-carbonate grainstones and graded, magnetite-rich slaty laminations indicates that storm-generated turbidity currents originating on the inner shelf, where grain production took place, were an important mechanism for moving sediment onto the distal shelf. The existence of iron formation breccia (Schmidt, 1963) in the Cuyuna north range suggests that mass flow processes generated by large-scale rotational slumping and sliding on

the distal shelf were important in moving sediment from the slope to the rise.

Sedimentological and stratigraphic data do not provide definitive answers to the question of plate tectonic setting of the Animikie Basin. However, paleogeographic reconstructions based on vertical and lateral facies transitions present within the Gunflint, Biwabik, and Trommald iron formations, and clastic units above and below iron-bearing strata indicate that it is doubtful deposition of the Animikie Group occurred within a migrating peripheral foreland basin. There is an apparent lack of coarse turbiditic, deltaic, and fluvial sediments, adjacent to the fold thrust belt, and paleocurrent data from clastic and chemical sedimentary rocks are opposite to what should be observed if deposition took place in a foreland basin. Also, if iron formation was to have accumulated in a foreland setting it should be restricted to the distal shelf as weathering of the peripheral bulge would shed clastics into nearshore regions effectively preventing deposition of iron formation. Facies transitions within iron-bearing members indicate the contrary, a complete shelf sequence, not just the distal portion is present.

Although data is insufficient to reconstruct the tectonic evolution of the Animikie Basin in detail, some general inferences regarding the depositional history of the Paleoproterozoic strata in Ontario and Minnesota can be made. Sedimentation within the basin began with an overall marine transgression onto the southern margin of the peneplained Superior province and deposition of the

Pokegama Quartzite and Mahnomen Formation. The Pokegama Quartzite accumulated in nearshore, tidally influenced settings while the Mahnomen Formation was deposited simultaneously in more distal shelf regions by pelagic settling and waning turbidity currents. This phase of clastic deposition was probably associated with the early history of basin development. Through time, the continuing erosion of the source terrain resulted in a reduction of clastic supply to the basin, to a point where iron formation began to accumulate on the shelf, away from the land-derived clastics still accumulating in the nearshore. Once the highland was reduced to near base level iron formation was then able to accumulate in the nearshore, and directly onlap the Superior province.

Deposition of iron formation occurred during an overall transgressive marine event punctuated by two minor regressions. Lateral facies transitions within iron-bearing units record a complete shelf sequence which fines and thickens from coarse, wave reworked nearshore deposits to parallel-laminated chemical mudstones of the distal shelf. The existence of minor mafic flows and tuffaceous horizons in the Gunflint, and the presence of three volcaniclastic horizons in the Gunflint and Mesabi iron ranges indicate that the region was volcanically active during subsidence in this phase of basin development. The thickest volcaniclastic horizon forms the base of the Rove, Virginia, and Rabbit Lake Formations, and marks the transition from chemical to clastic sedimentation. This volcanic episode stopped iron formation genesis by choking the depositional system with

volcaniclastics. As relative sea level continued to rise deposition within the Animikie Basin was dominated by accumulation of clastics derived from the north by southward flowing turbidity currents.

REFERENCES

Ainger, T., 1985, Storm Depositional Systems *in* Friedman, H.J., Neugebauer, AND Seilacher, A., eds., Lecture Notes Earth Sciences, 3: Springer-Verlag, Berlin, 174 p.

Awrawik, S.M., 1976, Gunflint stromatolites: microsfossils distribution in relation to stromatolite morphology, *in* Walter, M.R., ed., Stromatolites: Elsevier, Amsterdam, p. 311-320.

Barghoorn, E.S., 1971, The oldest fossils: Scientific American, v. 224, p. 30-42

Barghoorn, E.S., AND Tyler, S.A.,1965a, Microorganisms of middle Precambrian age from the Animikie Series, Ontario, Canada, *in* Current Aspects of Exobiology: California Institute of Technology, Jet Propulsion Laboratory, Pasedena, p. 93-118.

Barghoorn, E.S., AND Tyler, S.A., 1965b, Microorganisms from the Gunflint chert: Science, v. 147, p. 563-577.

Barovich, K.M., Patchett, P.J., Peterman, Z.E., AND Sims, P.K., 1989, Nd isotopes and the origin of 1.9-1.7 Ga Penokean continental crust of the Lake Superior region: Geological Society of America Bulletin, v. 101, p. 333-338.

Bath, G.D., Schwartz, G.M., AND Gilbert, F.P., 1964, Aeromagnetic and geologic map of east-central Minnesota: United States Geological Survey Geophysical Investigations Map GP-474, scale 1:250 000.

Bath, G.D., Schwartz, G.M., AND Gilbert, F.P., 1965, Aeromagnetic and geologic map of west-central Minnesota: United States Geological Survey Geophysical Investigations Map GP-473, scale 1:250 000.

Beck, K.J., 1987, Implications for Early Proterozoic tectonics and the origin of continental flood basalts, based on combined trace element and neodymium/strontium isotopic studies of mafic igneous rocks of the Penokean Lake Superior belt, Minnesota, Wisconsin and Michigan: Unpublished Ph.D. thesis, University of Minnesota, Minneapolis, 262 p.

Beck, W., AND Murthy, V.R., 1982, Rb-Sr and Sm-Nd isotopic studies of Proterozoic mafic dikes in northeastern Minnesota: Proceedings of the Lake Superior Institute on Lake Superior Geology, v. 28, p. 5.

Beltrame, R.J., Holtzman, R.C., AND Wahl, T.E., 1981, Manganese resources of the Cuyuna range, east-central Minnesota: Minnesota Geological Survey, Report of Investigations 24, 22p.

Berg, R.R., 1975, Depositional Environment of Upper Cretaceous Sussex Sandstone, House Creek Field, Wyoming: The American Association of Petroleum Geologists Bulletin, v. 59, p. 2099-2110.

Borchert, H., 1960, Genesis of marine sedimentary iron ore: Institute of Mining and Metallurgy Transactions, v. 69, p. 261-279.

Bourgeois, J., 1980, A transgressive shelf sequence exhibiting hummocky stratification: the Cape Sebastian Sandstone (Upper Cretaceous), southwestern Oregon: Journal of Sedimentary Petrology, v. 50, p. 681-702.

Brenner, R.L., 1978, Sussex Sandstone of Wyoming-Examples of Cretaceous Offshore Sedimentation: The American Association of Petroleum Geologists Bulletin, v.62, p.181-200.

Broderick, T.M., 1919, Detail stratigraphy of the Biwabik iron-bearing formation, East Mesabi District, Minnesota: Economic Geology, v. 14, p. 441-457.

Broderick, T.M., 1920, Economic geology and stratigraphy of the Gunflint iron district, Minnesota: Economic Geology, v. 15, p. 422-452.

Cambray, F.W., 1978, Plate tectonics as a model for the environment of deposition and deformation of the early Proterozoic (Precambrian X) of northern Michigan: Geological Association of America Abstracts with Programs, v. 10, p. 376.

Cameron, E.M., 1983, Genesis of Proterozoic iron-formation: Sulphur isotope evidence: Geochemica et Cosmochemica Acta, v. 47, p. 1069- 1074.

Card, K.D., 1990, A review of the Superior Province of the Canadian Shield, a product of Archean accretion: Precambrian Research, v. 48, p. 99-156.

Carrigan, W.J., AND Cameron, E.M., 1991, Petrological and stable isotope studies of carbonate and sulfide minerals from the Gunflint Formation, Ontario: evidence for the origin of early Proterozoic iron-formation: Precambrian Research, v. 52, p. 347-380.

Chandler, V.W., 1983a, Aeromagnetic map of Minnesota, St. Louis County: Minnesota Geological Survey Aeromagnetic Map Series A-2, scale 1:250 000.

Chandler, V.W., 1983b, Aeromagnetic map of Minnesota, Carlton an Pine Counties: Minnesota Geological Survey Aeromagnetic Series A-3, scale 1:250 000.

Chandler, V.W., 1983c, Aeromagnetic map of Minnesota, east-central region: Minnesota Geological Survey Aeromagnetic Map Series A-4, scale 1:250 000.

Chandler, V.W., 1985, Aeromagnetic map of Minnesota, central region: Minnesota Geological Survey Aeromagnetic Map Series A-5, scale 1:250 000.

Chandler, V.W., AND Malek, K.C., 1991, Moving-window Poisson analysis of gravity and magnetic data from the Penokean orogen, east-central Minnesota: Geophysics, v. 56, p. 123-132.

Clifton, H.E., Hunter, R.E., AND Phillips, R.L., 1971, Depositional structures and processes in the non-barred, high energy nearshore: Journal of Sedimentary Petrology, v. 41, p. 651-670.

Cloud, P., 1973, Paleoecological significance of the banded iron-formation: Economic Geology, v. 68, p. 1135-1143.

Dalrymple, R.W., LeGresley, E.M., Fadar, G.B.J., AND Petrie, B.D., 1992, The western Grand Banks of Newfoundland: Transgressive Holocene sedimentation under the combined influence of waves and currents: Marine Geology, v. 105, p. 95-118.

Davis, R.A., 1992, Depositional Systems, An Introduction to Sedimentology and Stratigraphy, Second Edition: Prentice Hall, Englewood Cliffs, 604 p.

Demicco, R.V., 1983, Wavy and lenticular-bedded carbonate ribbon rocks of the Upper Cambrian Conococheague Limestone, Central Appalachians: Journal of Sedimentary Petrology, v. 53, p. 1121-1132.

Dott, R.H., AND Bourgeois, J., 1982, Hummocky stratification: significance of its variable bedding sequences: Geological Society of America Bulletin, v. 93, p. 663-680.

Drever, J.I., 1974, Geochemical model for the origins of Precambrian banded iron formations: Geological Society of America Bulletin, v. 85, p. 1099-1106.

Edhorn, A., 1973, Further investigations of fossils from the Animikie, Thunder Bay, Ontario: Proceedings Geological Association of Canada, v. 14, p. 37-66.

Einsele, G.E., 1992, Sedimentary Basins, Evolution, Facies, and Sediment Budget: Springer-Verlag, Berlin, 628 p.

Eriksson, K.A., 1977, Tidal deposits from the Archean Moddies Group, Barberton Mountain Land, South Africa: Sedimentary Geology, v. 18, p. 257-281.

Faure, G., AND Kovach J., 1969, The age of the Gunflint Iron Formation of the Animikie Series in Ontario, Canada: Geological Society of America Bulletin, v. 80, p. 1725-1736.

Faure, G., 1986, Principles of Isotope Geology: John Wiley and Sons, New York, 589 p.

Floran, R.J., AND Papike, J.J., 1975, Petrology of the low grade rocks of the Gunflint iron formation, Ontario-Minnesota: Geological Society of America Bulletin, v. 86, p. 1169-1190.

Fralick, P.W., 1988, Microbial bioherms, Lower Proterozoic Gunflint Formation, Thunder Bay, Ontario, *in* Geldsetzer, H.H.J., James, N.P., and Tebbutt, G.E., eds., Reefs. Canada and Adjacent Areas: Memoirs of the Canadian Society of Petroleum Geologists, Calgary, 13, p. 24-29.

Fralick, P.W., AND Miall, 1989, Sedimentology of the Lower Huronian Supergroup (Early Proterozoic), Elliot Lake area, Ontario, Canada: Sedimentary Geology, v. 63, p. 127-153.

Fralick, P.W., AND Barrett, T.J., 1995, Depositional controls on iron formation associations in Canada: Special Publications of the International Association of Sedimentologists, v. 22, p. 137-156.

Franklin, J.M., 1978, Rubidium-strontium age determination of the Rove Formation Shale, *in* Wanless, R.K., and Loveridge, W.D., eds., Rubidium-Strontium isochron age studies, Report 2: Geological Survey of Canada Paper 77-14, p. 35-39

French, B.M., 1968. Progressive contact metamorphism of the Biwabik iron-formation, Mesabi range: Minnesota Geological Survey, Bulletin 45, 103 p.

Friedman, G.M., Sanders, J.E., AND Kopaska-Merkel, D.C., 1992, Priciples of Sedimentary Deposits, Stratigraphy and Sedimentology: Macmillan, New York, 717 p.

Gibbs, A.K., Payne, B., Setzer, T., Brown, L.D., Oliver, J.E., AND Kaufman, S., 1984, Seismic-reflection study of the Precambrian crust of central Minnesota: Geological Society of America Bulletin, v. 95, p. 280-294.

Gill, J.E., 1924, Gunflint iron-bearing formation, Ontario, *in* Summary Report: Geological Survey of Canada, Part C, p. 28-88.

Gill, J.E., 1927, Origin of the Gunflint Iron-bearing Formation: Economic Geology, v. 22, p. 687-728.

Ginsburg, R.N., 1960, Ancient analogues of recent stromatolites: International Geological Congress, Part 22, p. 26-35.

Goldich, S.S., Nier, A.O., Baadsgaard, H., Hoffman, J.H., AND Krueger, H.W., 1961, The Precambrian geology and geochronology of Minnesota: Minnesota Geological Survey Bulletin 41, 193 p.

Goodwin, A.M., 1956, Facies relations in the Gunflint Iron Formation: Economic Geology, v. 51, p. 565-595.

Goodwin, A.M., 1960, Gunflint Iron Formation of the Whitefish Lake Area: Ontario Department of Mines, v. 69, p. 41-63.

Gregg, W.J., 1993, Structural geology of the parautochthonous and allochthonous terranes of the Penokean orogeny in Upper Michigan - Comparisons with northern Appalachian tectonics: United States Geological Survey Bulletin 1904-Q, 28 p.

Grout, F.F., AND Broderick, T.M., 1919 Organic structures in the Biwabik iron-bearing formation of the Huronian in Minnesota: American Journal of Science, v. 48, p. 199-205.

Grout, F.F., AND Wolff, J.F., 1955, The Geology of the Cuyuna District, Minnesota, a progress report: Minnesota Geological Survey, Bulletin 36, 144 p.

Gruner, J.W., 1922a, The origin of sedimentary iron formations: the Biwabik Formation of the Mesabi Range: Economic Geology, v. 17, p. 407-460.

Gruner, J.W., 1922b, Paragenesis of the Martite ore bodies and magnetites of the Mesabi range: Economic Geology, v. 17, p. 1-14.

Gruner, J.W., 1924, Contributions to the geologyof the Mesabi range with special reference to the magnetites of iron-bearing formation west of Mesaba: Minnesota Geological Survey, Bulletin 19, 71 p.

Gruner, J.W., 1930, Hydrothermal oxidation and leaching experiments, their bearing on the origin of Lake Superior hematite-limonite ores: Economic Geology, v. 25, p. 697-719, 837-867.

Gruner, J.W., 1936, The structure and composition of greenalite: American Mineralogist, v. 20, p. 475-483.

Gruner, J.W., 1937a, Hydrothermal leaching of iron ores of the Lake Superior type - a modified theory: Economic Geology, v. 32, p. 121-130.

Gruner, J.W., 1937b, Composition and structure of stilpnomelane: American Mineralogist, v. 22, p. 855-860.

Gruner, J.W., 1944, The composition and structure of minnesotaite, a common iron silicate in iron-formations: American Mineralogist, v. 29, p. 363-372.

Gruner, J.W., 1946, The Mineralogy and Geology of the Taconites and Iron Ores of the Mesabi Range, Minnesota: Office of the Commissioner Iron Range Resources and Rehabilitation, St. Paul, 127 p.

Guel, J.J.C., 1970, Geology of Crooks Township, Jarvis and Prince Locations: Ontario Department of Mines and Northern Affairs, GR 87, 52 p.

Guel, J.J.C., 1973, Geology of Crooks Township, Jarvis and Prince Locations, and offshore islands, district of Thunder Bay: Ontario Dision of Mines, GR102, 46 p.

Hanson, G.N., 1975, $^{40}Ar/^{39}Ar$ spectrum ages on Logan intrusions, a lower Keweenawan flow and mafic dikes in northeastern Minnesota-northwestern Ontario: Canadian Journal of Earth Sciences , v. 12, p. 821-835.

Hamblin, A.P., AND Wailker, R.G., 1979, Storm dominated shallow marine deposits: the Fernie-Kootenay (Jurassic) transition, southern Rocky Mountains: Canadian Journal of Earth Sciences , v. 16, p. 1637-1690.

Harder, E.C., AND Johnston, A.W., 1918: Preliminary report on the geology of east-central Minnesota, including the Cuyuna iron-ore district: Minnesota Geological Survey, Bulletin 15, 178 p.

Hassler, S.W., AND Simonson, B.M., 1989, Deposition and alteration of volcaniclastic strata in two large, Early Proterozoic iron formations in Canada: Canadian Journal of Earth Sciences, v. 26, p. 1574-1585.

Hemming, S.R., 1994, Pb isotope studies of sedimentary rocks and detrital components for provenance analysis, Unpublished PhD thesis, State University of New York, Stoney Brook, p. 212.

Hemming, S.R., McLennan, S.C., Hanson, G.N., Krogstad, E.K., AND Mezger, K., 1990, Pb isotope systematics in quartz, EOS, v. 71, p. 654-655.

Hemming, S.R., McLennan, S.C., AND Hanson, G.N., 1992, Provenance of the Animikie Group, NE Minnesota, based on Nd and Pb isotopes: Proceedings of the Institute on Lake Superior Geology, v. 38, p. 35.

Hemming, S.R., Hanson, G.B., McLennan, S.M., Southwick, D.L., AND Morey, G.B., 1993, Nd isotopic constraints on the provenance of Early Proterozoic sediments and the location of tectonic boundaries in Central Minnesota (abstract): Proceedings of the Institute on Lake Superior Geology, v. 39, p. 40-41.

Hemming, S.R., McLennan, S.M., AND Hanson, G.N., 1995, Geochemical and Nd/Pb isotopic evidence for the provenance of the Early Proterozoic Virginia Formation, Minnesota. Implications for tectonic setting of the Animikie Basin: Journal of Geology, v. 103, p. 147-168.

Hobson, J.P., Fowler, M.L., AND Beaumont, E.A., 1982, Depositional and Statistical Exploration Models, Upper Cretaceous Offshore Sandstone Complex, Sussex Member, House Creek Field, Wyoming: The American Association of Petroleum Geologists Bulletin, v. 66, p. 689-707.

Hofmann, H.J., 1969, Stromatolites from the Proterozoic Animikie and Sibley Groups, Ontario: Geological Survey of Canada, paper 68-69, 77 p.

Hoffman, P., 1976, Stromatolite morphologies in Shark Bay, Western Australia,*in* Walter, M.R., ed., Stromatlites: Elsevier, Amsterdam, p. 261-272.

Hoffman, P.F., 1987, Early Proterozoic foredeeps, foredeep magmatism and Superior-type iron-formations of the Canadian shield, *in* Kröner, A., ed., Proterozoic lithospheric evolution: American Geophysical Union Series, v. 17, p. 85-98.

Hoffman, P.F., 1988, United plates of America, the birth of a craton-Early Proterozoic assembly and growth of Laurentia: Annual Reviews of Earth and Planetary Sciences, v. 16, p. 543-603.

Hoffman, P.F., 1989, Precambrian geology and tectonic history of North America, *in* Bally, A.W., AND Palmer, A.R., eds., The Geology of North America; An Overview: Geological Society of America, Boulder, p. 447-512.

Hurley, P.M., Fairbairn, H.W., Pinson, W.H., AND Howler, J., 1962, Unmetamorphosed minerals in the Gunflint Formation used to test the age of the Animikie: Journal of Geology, v. 70, p. 489-492.

Ingall, E.D., 1888, Mines and mining on Lake Superior, Part I, *in* Annual Report: Geological and Natural History Survey of Canada, Report H, v. 3, p. 1-131.

James, H.L., 1954, Sedimentary facies of iron formation: Economic Geology, v. 49, p. 235-293.

James, N.P., AND Kendall, A.C., 1992, Intoduction to Carbonate and Evaporite Facies Models, *in* Walker, R.G., AND James, N.P., eds., Facies Models Response to Sea Level Change: Geological Association of Canada, Stittsville, p. 265-275.

Johnson, H.D., AND Baldwin, C.T., 1986, Shallow siliclastic seas, *in* Reading, H.G., ed., Sedimentary Facies and Environments, Second Edition: Blackwell, Oxford, p. 229-252.

King, E.R., AND Zietz, I., 1971, Aeromagnetic study of the Midcontinental gravity high central United States: Geological Society of America Bulletin, v. 82, p. 2187-2208.

Kissin, S.A., AND Fralick, P.W., 1994, Early Proterozoic volcanics of the Animikie Group, Ontario and Michigan, and their tectonic significance: Proceedings from the Institute on Lake Superior Geology, v. 40, p. 18-19.

Klasner, J.S., Ojakangas, R.W., Schulz, K.J., AND Laberge, G.L., 1991, Nature and style of deformation in the foreland of the Penokean orogen, Michigan: United States Geological Survey Bulletin 1904-K, 22 p.

Koerschner, W.F., AND Read, J.F., 1989, Field and modelling studies of Cambrian carbonate cycles, Virginia Appalachians: Journal of Sedimentary Petrology, v. 59, p. 654-687.

Krenz, K.A., AND Ervin, C.P., 1977, Simple Bouguer gravity map of Minnesota, Duluth sheet: Minnesota Geological Survey Miscellaneous Map M-37, scale 1:250 000.

Kronberg, B.I., AND Fralick, P.W., 1992, Geochemical alteration of felsic Archean rocks by Gunflint Formation-derived fluids, Quetico-Superior region, northwest Ontario: Canadian Journal of Earth Sciences, v. 29, p. 2610-2616.

Lawton, D.C., Spratt, D.A, AND Hopkins, J.C., 1994, Tectonic wedging beneath the Rocky Mountain foreland basin, Alberta, Canada: Geology, v. 22, p. 519-522.

Logan, B.W., Rezak, R., AND Ginsburg, R.N., 1964, Classification and environmental significance of algal stromatolites: Journal of Geology, v. 72, p. 68-83.

Lougheed, M.S., 1983, Origin of Precambrian iron-formations in the Lake Superior region: Geological Society of America Bulletin, v. 94, p. 325-340.

Lucente, M.E., AND Morey, G.B., 1983, Stratigraphy and sedimentology of the Lower Proterozoic Virginia Formation, Northern Minnesota: Minnesota Geological Survey, Report of Investigations 28, 28 p.

Marsden, R.W., 1972, Cuyuna district, *in* Sims, P.K., AND Morey, G.B., eds., Geology of Minnesota: A centennial volume: Minnesota Geological Survey, p. 227-239.

McGinnis, L.D., Carlson, D.R., Pederson, R., AND Schafersman, J.S., 1977, Simple Bouguer gravity map of Minnesota, Stillwater sheet: Minnesota Geological Survey Miscellaneous Map M-35, scale 1:250 000.

McGinnis, L.D., Jackson, J.K., AND Ervin, C.P., 1978, Simple Bouguer gravity map of Minnesota, Brainerd sheet: Minnesota Geological Survey Miscellaneous Map M-40, scale 1:250 000.

Miall, A.D., 1984, Principles of Sedimentary Basin Analysis: Springer-Verlagm New York, 490 p.

Mitchell, A.H.G., AND Reading, H.G., 1986, Sedimentation and Tectonics, *in* Sedimentary Environments and Facies, Second Edition: Blackwell, Oxford, p. 471-519.

Moorhouse, W.W., 1960, Gunflint Iron Range in the Vicinity of Port Arthur: Ontario Department of Mines, v. 69, p. 1-40.

Morey, G.B., 1967, Stratigraphy and sedimentology of the middle Precambrian Rove Formation in northeastern Minnesota: Journal of Sedimentary Petrology, v. 37, p. 1154-1162.

Morey, G.B., 1969, The Geology of the Middle Precambrian Rove Formation in northeastern Minnesota: Minnesota Geological Survey, SP-7, 62 p.

Morey, G.B., 1978, Lower and middle Precambrian stratigraphic nomenclature for east-central Minnesota: Minnesota Geological Survey, Report of Investigations 21, 52 p.

Morey, G.B., 1983, Animikie Basin, Lake Superior Region, U.S.A., *in* Trendall, A.F. AND Morris, R.C., eds., Iron-Formation: Facts and Problems: Elsevier, Amsterdam, p. 13-67.

Morey, G.B., 1990, Geology and manganese resources of the Cuyuna iron range, east-central Minnesota: Minnesota Geological Survey, Information Circular 32, 28 p.

Morey, G.B., 1992, Chemical composition of the Eastern Biwabik iron range (Early Proterozoic), Mesabi Range, Minnesota: Economic Geology, v. 87, p. 1649-1658.

Morey, G.B., 1993, Geology of the Mesabi Range, *in* Geology and taconite mines of the Mesabi Range: Proceedings of the Institute on Lake Superior Geology, v. 39, Part 2-Field Trips, p. 2-18.

Morey, G.B., AND Ojakangas, R.W., 1970, Sedimentology of the middle Precambrian Thomson Formation, east-central Minnesota: Minnesota Geological Survey, Report of Investigations 13, 32 p.

Morey, G.B., Olsen, B.M. AND Southwick, D.L., 1981, Geologic map of Minnesota, bedrock geology: Minnesota Geological Survey, scale 1:250 000.

Morey, G.B., AND Van Schmus, W.R., 1988, Correlation of Precambrian Rocks of the Lake Superior Region, United States: United States Geological Survey Professional Paper 1241-F, 31 p.

Morey, G.B., Southwick, D.L., AND Schottler, S.P., 1991 Manganiferous zones in Early Proterozoic iron formation in the Emily district, Cuyuna range, east-central Minnesota: Minnesota Geological Survey, Report of Investigations 39, 42 p.

Morey, G.B. AND Southwick, D.L., 1993, Stratigraphic and Sedimentological Factors Controlling Epigenetic Manganese Deposits in Iron-Formation of the Emily District, Cuyuna Iron Range, East-Central Minnesota: Economic Geology, v. 88, p. 104-122.

Morris, R.C., 1993, Genetic modelling for banded iron formation of the Hamersley Group, Pilbara Craton, Western Australia: Precambrian Research, v. 60, p. 243-286.

Morton, R.A., 1988, Neashore responses to great storms: Geological Society of America Special Paper 229, p. 7-22.

Nummedal, D., 1991, Shallow storm sedimentation: the oceanographic perspective, *in* Eisele, G.E., Ricken, W., AND Seilacher, A., eds., Cycles and events in stratification: Springer-Verlag, New York, p. 227-248.

Ojakangas, R.W., 1983, Tidal deposits in the Early Proterozoic basin of the Lake Superior region-The Palms and Pokegama Formations: Evidence for subtidal-shelf deposition of Superior-type banded iron-formation, *in* Medaris, L.G., ed., Early Proterozoic Geology of the Great Lakes Region: Gelogical Society of America Memoir 160, p. 49-66.

Ojakangas, R.W., 1993, Pokegama Quartzite, *in* Geology and taconite mines of the Mesabi Range: Proceedings of the Institute on Lake Superior Geology, v. 39, Part 2-Field Trips, p. 19-21.

Ojakangas, R.W., 1995, Sedimentology and Provenance of the Early Proterozoic Michigamme Formation and Goodrich Quartzite, Northern Michigan-Regional Stratigraphic Implications and Suggested Correlations: United States Geological Survey Bulletin 1904-R, 31 p.

Parkash, B., Sharma, R.P., AND Roy, A.K., (1980), The Siwalik Group (molasse)-sediments shed by collision of continental plates: Sedimentary Geology, v. 25, p. 127-159.

Peterman, Z.E., 1966, Rb-Sr dating of middle Precambrian metasedimentary rocks of Minnesota: Geological Society of America Bulletin, v. 77, p. 1031-1044.

Pratt, B.R., James, N.P., AND Cowan, C.A., 1992, Peritidal Carbonates, *in* Walker, R.G., AND James, N.P., eds., Facies Models Response to Sea Level Change: Geological Association of Canada, Stittsville, p. 303-322.

Pufahl, P.K., AND Fralick, P.W., 1994, Depositional controls on shallow water iron formation accumulation, Gogebic range, Wisconsin: Proceedings of the Institute on Lake Superior Geology, v. 40, p. 58-59.

Pufahl, P.K., AND Fralick, P.W., 1995, Paleogeographic reconstruction of the Gunflint-Mesabi-Cuyuna depositional system: a basin analysis approach: Proceedings of the Institute on Lake Superior Geology, v. 41, p. 59-60.

Quinlon, G.M., AND Beaumont, 1984, Appalachian thrusting, lithospheric flexure, and the Paleozoic stratigraphy of the eastern interior of North America: Canadian Journal of Earth Sciences, v. 21, p. 973-996.

Randazzo, A.F., AND Markun, C.D., 1980, Sedimentary structures in the Gunflint iron formation, Schreiber Beach, Ontario: Precambrian Research, v. 12, p. 287-310.

Reineck, H.E., AND Singh, I.B., 1972, Genesis of laminated sand and graded rhythmites in storm-sand layers of shelf mud: Sedimentology, v.18, p.123-128.

Reineck, H.E., and Singh, I.B., 1975, Depositional Sedimentary Environments: Springer-Verlag, New York, 439 p.

Rich, J.L., 1951, Three critical environments of deposition and criteria for recognition of rocks deposited in each of them: Geological Society of America Bulletin, v. 62, p. 1-20.

Schmidt, R.G., 1963, Geology and ore deposits of the Cuyuna north range, Minnesota: United States Geological Survey, professional paper 407, 96 p.

Schreiber, H.C., 1986, Arid shorelines and evaporites, *in* Reading, H.G., ed., Sedimentary Environments and Facies, Second Edition: Blackwell, Oxford, p. 189-228.

Seeling, A., 1978, The Shannon Sandstone, a further look at the environment of deposition at Heldt Draw field, Wyoming: The Mountain Geologist, v. 15, p. 133-144.

Sellwood, B.W., 1986, Shallow-marine Carbonate Environments, *in* Reading, H.G., ed., Sedimentary Environments and Facies, Second Edition: Blackwell, Oxford, p. 283-342.

Shegelski, R.J., 1982, The Gunflint Formation in the Thunder Bay Area, *in* Franklin, J.M., McIlwaine, W.H., Shegelski, R.J., Mitchell, R.H. and Platt, R.G., eds., Geological Association of Canada, Mineralogical association of Canada joint annual meeting, Winnipeg Manitoba, Field Trip Guidebook, Proterozoic Geology of the Northern Lake Superior Area, p. 15-31.

Silver, L.P., 1906, The Animikie iron range, *in* Annual Report: Ontario Bureau of Mines, v. 15, p. 156-172.

Silver, L.T., AND Green, J.C., 1972, Time constraints for Keweenawan igneous activity: Geological Society of America Abstracts with Programs, v. 4., p. 665-666.

Simonson, B.M., 1985, Sedimentological constraints on the origins of Precambrian iron-formations: Geological Society of America Bulletin, v. 96, p. 244-252.

Simonson, B.M., 1987, Early silica cementation and subsequent diagenesis in arenites from four Early Proterozoic iron formations of North America: Journal of Sedimentary Petrology, v. 57, p. 494-511.

Simonson, B.M, AND Goode, A.D.T., 1989, First discovery of ferruginous chert arenites in the early Precambrian Hamersely Group of Western Australia: Geology, v. 17, p. 269-272.

Sims, P.K., 1976, Precambrian tectonics and mineral deposits, Lake Superior region: Economic Geology, v. 71, p . 1092-1127.

Sims, P.K., 1991, Precambrian geology of the Lake Superior region -- An overview, *in* Ojakangas, R.W., ed., Precambrian geology of the southern Canadian Shield and the eastern Baltic Shield: Minnesota Geological Survey, Information Circular 34, p. 1-8.

Sims, P.K., Card, K.D., Morey, G.B., AND Peterman, Z.E., 1980, The Great Lakes tectonic zone - a major crustal structure in central North America: Geological Society of America Bulletin, v. 91, p. 690-698.

Sims, P.K., Van Schmus, W.R., Schulz, K.J., AND Peterman, Z.E., 1989, Tectonostratigraphic evolution of the Early Proterozoic Wisconsin magmatic terranes of the Penokean orogen: Canadian Journal of Earth Sciences, v. 26, p. 2145-2158.

Smith, W.N., 1905, Loon Lake iron bearing district, *in* Annual Report: Ontario Bureau of Mines, v. 14, p. 254-260.

Southwick, D.L, AND Day, W.C., 1983, Geology and petrology of Proterozoic mafic dikes, north-central Minnesota and western Ontario: Canadian Journal of Earth Sciences, v. 20, p. 622-638.

Southwick, D.L., Morey, G.B., AND McSwiggen, P., 1988, Geological map (scale 1:250 000) of the Penokean Orogen, central and east-central Minnesota, and accompanying text: Minnesota Geological Survey, Report of Investigations RI-37.

Southwick, D.L., AND Morey, G.B., 1991, Tectonic Imbrication and Foredeep Development in the Penokean Orogen, East-Central Minnesota - An Interpretation Based on Regional Geophysics and the Results of Test-Drilling: United States Geological Survey Bulletin 1904-C, 17 p.

Spearing, D.R., 1976, Shallow marine sands, *in* Depositional Environments as Interpreted from Primary Sedimentary Structures and Stratification Sequences: SEPM Short Course 2, p. 103-132.

Spurr, J.E., 1894, The iron-bearing rocks of the Mesabi range in Minnesota: Geological and Natural History Survey of Minnesota, Bulletin 10, 268 p.

Stille, P., AND Clauer, N., 1986, Sm-Nd isochron-age and provenance of the argillites of the Gunflint Formation in Ontario, Canada: Geochemica et Cosmochemica Acta, v. 50, p. 1141-1146.

Stow, D.A.V., 1986, Deep Clastic Seas, *in* Reading, H.G., ed., Sedimentary Environments and Facies, Second Edition: Blackwell, Oxford, p. 399-444.

Symons, D.T.A, AND O'Leary, R.J., 1978, Huronian polar wander and paleomagnetism of the Thessalon volcanics: Canadian Journal of Earth Sciences, v. 15, p. 1141-1150.

Tanton, T.L., 1923, Iron formation at Gravel Lake, Thunder Bay District, Ontario, *in* Summary Report: Geological Survey of Canada, Part C, p. 1-75.

Tanton, T.L., 1931, Fort William and Port Arthu, and Thunder Cap Map Areas, Thunder Bay District, Ontario: Geological Survey of Canada Memoir 167

Tillman, R.W., AND Martinsen, R.S., 1984, The Shannon shelf-ridge sandstone complex, Salt Creek anticline area, Powder River basin, Wyoming, *in* Tillman, R.W., AND Siemers, C.T., eds., Siliclastic shelf sediments: Society of Economic Paleontologists and Mineralogists, Special Publication 34, p. 85-142.

Trendall, A.F., 1968, Three great basins of Precambrian banded iron formation deposition: a systematic comparison: Geological Society of America Bulletin, v. 79, p. 1527-1544.

Tyler, S.A., Barghoorn, E.S., 1954, Occurrence of structurally preserved plants in Precambrian rocks of the Canadian shield: Science v. 199, p. 606-608.

Vail, P.R., Mitchum, J.R., AND Thompson, S., 1977, Seismic Stratigraphy and Global Changes of Sea Level, Part 3: Relative Changes of Sea Level from Coastal Onlap, *in* Payton, C.E., ed., Seismic Stratigraphy-applications to hydrocarbon exploration: American Society of Petroleum Geologists, Tulsa, p. 63-97.

Van Schmus, W.R., 1976, Early and middle Proterozoic history of the Great Lakes area, North America: Philosophical Transactions of the Royal Society of London Series A, v. 280, p. 605-628.

Van Schmus, W.R., AND Bickford, M.E., 1981, Proterozoic chronology and evolution of the Midcontinent region, North America, *in* Kröner, A., ed., Precambrian plate tectonics, Developments in Precambrian geology: Elsevier, New York, p. 261-296.

Van Schmus, W.R., AND Hinze, W.J., 1985, The Midcontinent rift system: Annual Reviews of Earth and Planetary Sciences, v. 13, p. 345-383.

Van Hise, C.R., AND Leith, C.K., 1911, The geology of the Lake Superior region: United States Geological Survey Monograph 52, 641 p.

Walker, R.G., 1984, Shelf and Shallow Marine Sands *in* Walker, R.G., ed., Facies Models Second Edition: Geological Association of Canada, Stittsville, p.141-170.

Walker, R.G., AND Plint, A.G., 1992, Wave and Storm-Dominated Shallow Marine Systems, *in* Walker, R.G., AND James, N.P., eds., Facies Models Response to Sea Level Change: Geological Association of Canada, Stittsville, p. 219-238.

Wanless, R.K. AND Lovebridge, W.D., 1978, Rubidium-strontium isotopic age studies, Report 2, (Canadian Shield): Geological Survey of Canada Paper 77-14, 70 p.

White, D.A, 1954, The stratigraphy and structure of the Mesabi range, Minnesoata: Minnesota Geological Survey, Bulletin 38, 92 p.

Wold, R.J., AND Hinze, W.J., 1982, Geology and tectonics of the Lake Superior basin: Geological Society of America Memoir 156, 280 p.

Wolff, E.M., 1915, Ore bodies of the Mesabi range: Engineering Mining Journal, v. 100, p. 89-94, 135-139, 178-185, 219-224.

Wolff, E.M., 1917, Recent Geological developments on the Mesabi iron range, Minnesota: American Institute of Mining Engineers, Transactions, v. 56, p. 142-169.

Woyski, M.S., 1949, Intrusions of central Minnesota: Geological Society of America Bulletin, v. 62, p. 999-1016.

Young, G.M., 1983, Tectono-sedimentary history of early Proterozoic rocks of the northern Great Lakes region, *in* Medaris, L.G., ed., Early Proterozoic Geology of the Great Lakes Region: Geological Society of America Memoir 160, p. 15-32.

Zapffe, C., 1925, Stratigraphy and correlation of the Cuyuna iron ore district, Minnesota: Lake Superior Mining Institute Proceedings, v. 25, p. 219-227.

IMAGE EVALUATION
TEST TARGET (QA-3)

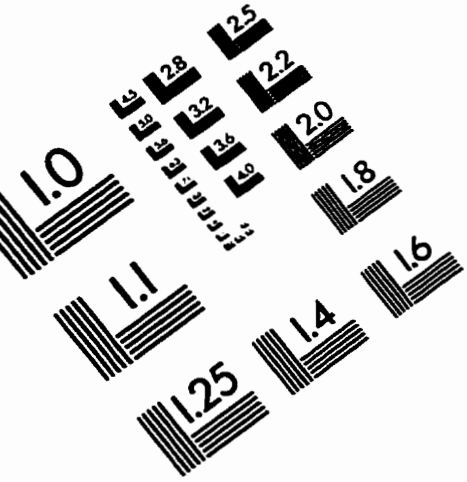

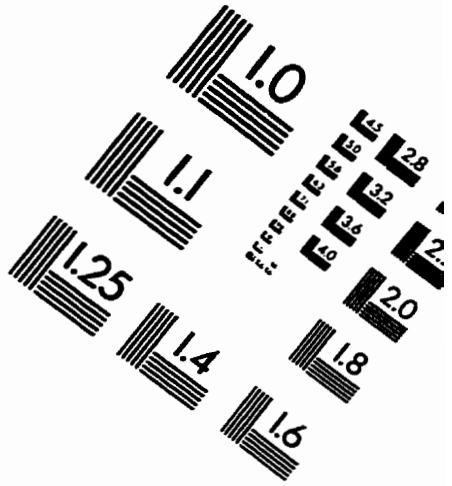

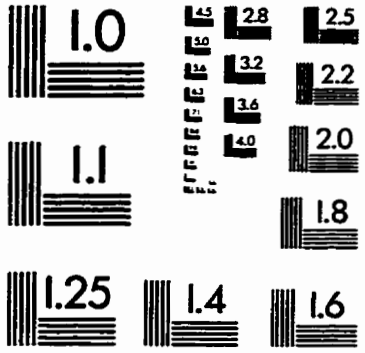

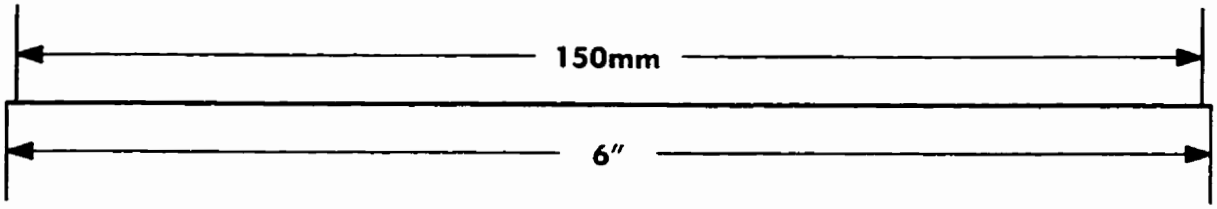

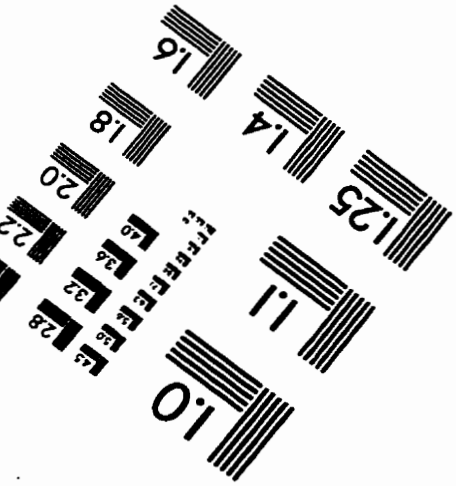

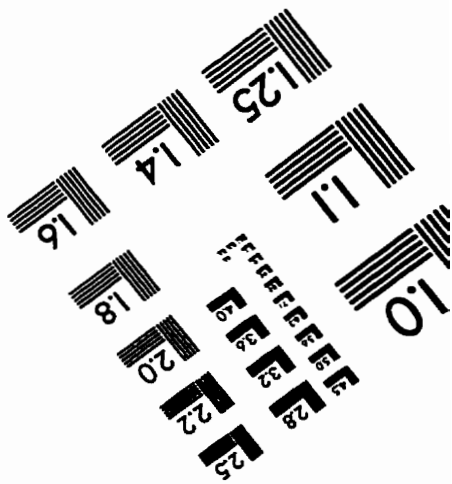

APPLIED IMAGE, Inc
1653 East Main Street
Rochester, NY 14609 USA
Phone: 716/482-0300
Fax: 716/288-5989